University of Tuscia
Department for Agriculture and Forest Sciences (DAFNE)

Ph.D. Course
Plant and Animal Sciences (XXXVII)

New survey to investigate biotic and abiotic factors involved in the outbreak of Kiwifruit Vine Decline Syndrome (KVDS) in the Latium Region

Scientific-disciplinary sector
Plant pathology - **AGRI/05B**

Supervisor
Prof. Giorgio M. Balestra

Ph.D. candidate
Antonella Cardacino

Ph.D. Coordinator
Prof.ssa Roberta Bernini

A.Y. 2024/2025

Dedicated to my mother, to her absence that is so present.
Wherever she is, with her beautiful smile.

With all my love

"If I can see further than anyone else,
it is only because I am standing on the shoulder(s) of giants."

Sir Isaac Newton (1675),
and… a bit more of a half-drunk Mancunian in 1999

Summary

Chapter 1

Introduction

1.1 The genus *Actinidia*

The genus *Actinidia* belongs to the Actinidiaceae family. According to Li et al. (2007a), it comprises 54 species and 21 varieties, totalling approximately 75 taxa. Commercial cultivation primarily focuses on *A. chinensis* var. *chinensis* and *A. chinensis* var. *deliciosa* (A. Chevalier). The genus *Actinidia* exhibits a wide geographic distribution across eastern Asia, ranging from equatorial (tropical) to cold temperate regions as far north as 50° latitude (Liang, 1983; Ferguson, 1990a). The vast majority of *Actinidia* taxa are endemic to China, concentrated in the mountainous and hilly regions of south-central and southwest China. *Actinidia chinensis* var. *deliciosa* is primarily distributed in western mainland China, whereas *A. chinensis* is more prevalent further east (Liang, 1975; Ferguson, 1990a,b,c; Li et al., 2007c). In regions where their distributions overlap, *A. chinensis* var. *deliciosa* typically occupies higher altitudes. Despite China being the center of origin for the genus and possessing the richest natural resources, serious domestication efforts within the country were limited until successful cultivation had been established elsewhere. The process of kiwifruit domestication and commercial cultivation began in New Zealand in 1904 when Isabel Fraser, a New Zealand schoolteacher visiting Yichang, Hubei Province, obtained seeds of *A. chinensis* var. *deliciosa* and transported them back to New Zealand (Huang, 2016). Plants derived from these original seeds were fruiting by 1910, likely representing the first fruiting of *A. chinensis* var. *deliciosa* outside China. While numerous European naturalists and plant hunters introduced *Actinidia* species from China to Europe and North America during the late 19th and early 20th centuries, all subsequent significant New Zealand cultivars of *A. chinensis* var. *deliciosa*, including 'Hayward,' 'Bruno,' 'Allison,' 'Monty,' 'Abbott,' and 'Gracie,' can be traced back to the seeds introduced by Isabel Fraser (Ferguson, 2004, 2005; Ferguson and Bollard, 1990).

1.1.1 Morphological traits of *Actinidia chinensis* var. *deliciosa*

Plants of this species exhibit a robust, vigorous growth habit, characteristic of large, deciduous vines. One-year-old shoots are green and covered with short, coarse, gray-brown hairs (Figure 1.1, panel A). Two-year-old stems are reddish-brown, glabrous, with white, round to ovate lenticels. Leaves are papery to thick-papery, nearly round or occasionally oblong (Figure 1.1, panel B). The upper leaf surface is dark green, glabrous or puberulent, with a nearly entire margin that is green and adorned with small, spine-like awns. The lower leaf surface is light green and densely covered with pale yellow stellate hairs.

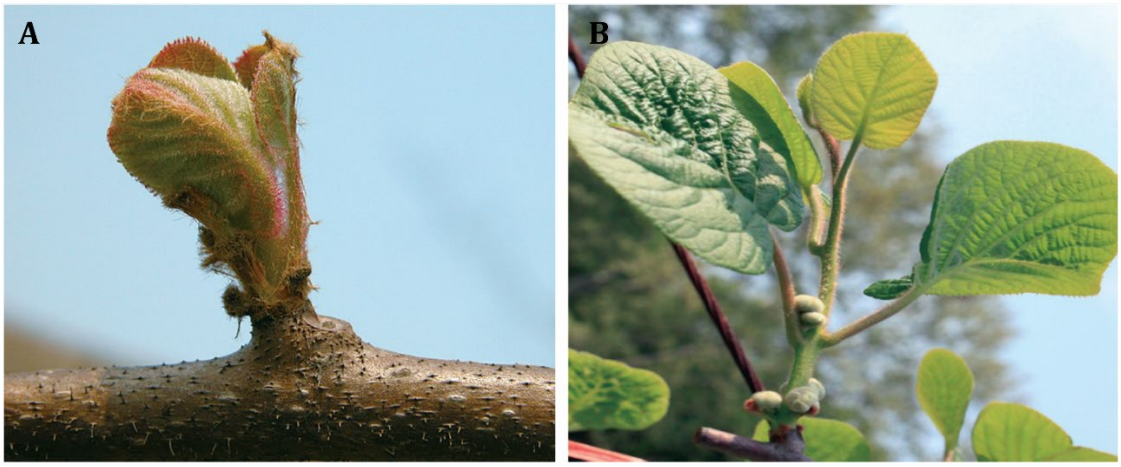

Figure 1.1 - Stem, emerging shoot (A), and leaves (B) of *Actinidia chinensis* var. *deliciosa* (Huang, 2016)

Pistillate flowers (Figure 1.2, panel A) are predominantly single, with a calyx comprising five to six elliptical or obovate sepals densely covered with light brown tomentum. These flowers are approximately 5.5 cm in diameter, initially white, and subsequently turn yellow to apricot-yellow within a day. They possess six to seven petals, white filaments, yellow, sagittate anthers, and a short cylindrical ovary covered with white to light brown pubescence. Staminate flowers (Figure 1.2, panel B) occur in cyme inflorescences, typically with two to three flowers. The calyx consists of four to six sepals, predominantly six, which are light brown and covered by pale brown tomentum. These flowers are initially white, turning yellow after one day, and are smaller than pistillate flowers. They possess four to six petals, yellow,

sagittate anthers, and a vestigial, tiny cone-shaped ovary covered by light brown tomentum.

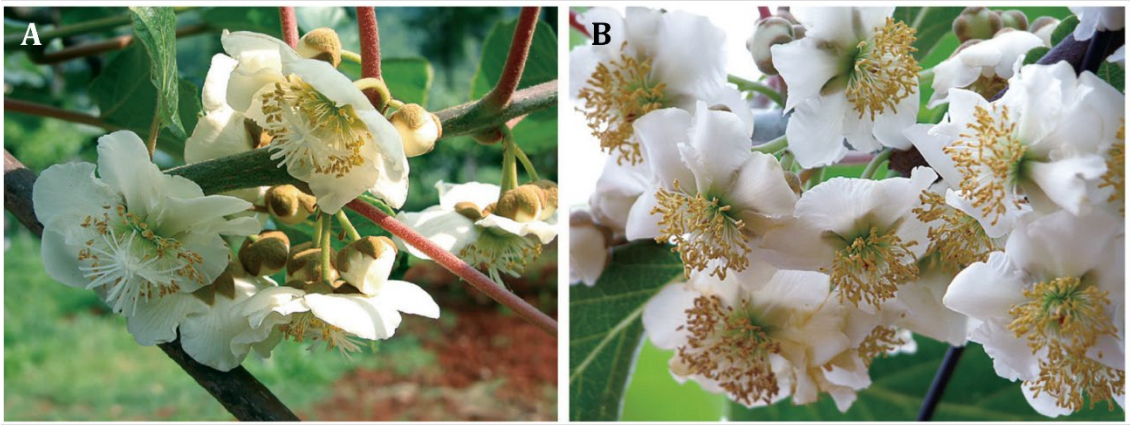

Figure 1.2- Pistillate flowers (A) and staminate flowers (B) of *Actinidia chinensis* var. *deliciosa* (Huang, 2016)

The fruit is predominantly ellipsoid, cylindrical, or ovoid, with a green to brown skin densely covered with long yellow-brown hispid hairs. The pericarp is bright green and contains a small, round, creamy white core (Figure 1.3, panel A). In some instances, red pigments may be observed in the inner pericarp surrounding the core. Numerous dark purple to black seeds, elliptical with concave furrows, are present within the fruit (Figure 1.3, panel B). Fruit ripening occurs between October and November, yielding a sweet-acid flavour, juicy texture, and fine quality.

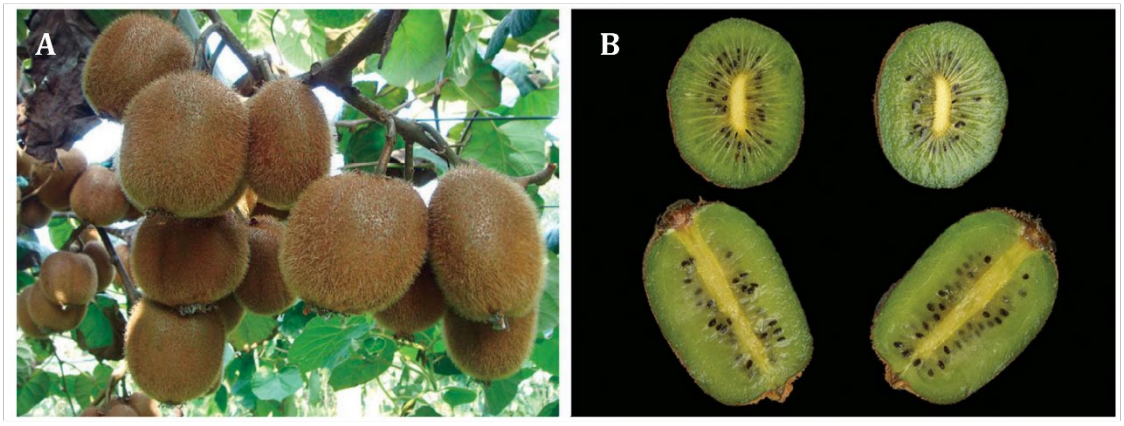

Figure 1.3 - Fruits of *Actinidia chinensis* var. *deliciosa* (Huang, 2016)

Actinidia chinensis var. *deliciosa* exhibits a range of ploidy levels, including tetraploids, pentaploids, and hexaploids. This ploidy variation exhibits geographic distribution patterns, with hexaploids predominantly found in the western Yun-Gui Plateau and tetraploids coexisting with other ploidy levels in the middle Yun-Gui Plateau and the Wuling-Xuefeng Mountains (Figure 1.4) (Li et al., 2010; Wang et al., 2020). Polyploidization has likely enhanced their adaptability to environmental changes, enabling them to expand their range during different climatic periods (Wang et al., 2020; Liu et al., 2023).

Figure 1.4 - Natural range of *Actinidia chinensis* var. *deliciosa*, adapted from Huang (2016)

1.2 The evolution of kiwifruit cultivation: from amateur enthusiasts to global market leader

As already mentioned, *A. chinensis* var. *deliciosa* was introduced to New Zealand in 1904. Initially, plant exchanges and sales primarily occurred between nurserymen and amateur plant enthusiasts. By 1917, New Zealand nurseries began offering *A. chinensis* var. *deliciosa* seedlings to the public, and by 1924, the plant had garnered significant public interest and widespread promotion. Grafting emerged as a viable propagation method between 1922 and 1926. All *Actinidia* species exhibit functional dioecism, necessitating pollination from a male vine for fruit production. While female flowers exhibit a morphology superficially resembling male flowers, they are functionally male-sterile, producing non-viable pollen. This observation initially confounded growers who encountered a lack of fruit set despite the presence of seemingly intact female flowers. Given the unreliability of sex determination based solely on floral morphology, grafting onto seedling rootstocks became the established propagation method within the industry.

The establishment of the first commercial *A. chinensis* var. *deliciosa* orchard occurred in Wanganui, New Zealand, in the early 1930s. This initial orchard, comprising only 14 plants, yielded high-quality fruit. The successful marketing of fruit from this orchard to other New Zealand towns stimulated further plantings, particularly in the Bay of Plenty. However, these early orchards remained relatively small, typically less than one hectare in size. Despite consistent high fruit prices, kiwifruit cultivation remained on a small scale for several decades. This period witnessed the development of crucial growing and management techniques, as well as postharvest storage procedures (Ferguson, 2013). As production began to exceed domestic demand, trial shipments were sent to Britain in 1952 and Australia in 1954. In 1959, the exporting firm Turners & Growers proposed the name "kiwifruit," inspired by the kiwi, a native New Zealand bird. This new brand was extensively promoted in Western markets and quickly gained widespread acceptance, both commercially and in scientific literature. Until the early 1970s, kiwifruit production in New Zealand primarily served the domestic market. However, after 1975, exports rapidly surpassed domestic consumption. By 1980, over 80% of the fruit produced was exported. This surge in demand fuelled rapid expansion of plantings and necessitated more intensive management practices and technological

advancements. Commercial kiwifruit cultivation began in other countries during this period, including the United States (first commercial crops in 1965), Italy (1966), France (1967), and Japan (around 1977) (Ferguson and Bollard, 1990). Further expansion of commercial production occurred in Chile (South America) and Iran (Middle East) during the 1980s (Huang, 2016).

Global kiwifruit production has significantly expanded over the past decade. China has consistently held the position of the leading producer, contributing a substantial portion of the worldwide supply (FAOSTAT, 2024). This growth is attributed to factors such as the expansion of cultivated areas and the introduction of new, high-yielding varieties (Ferguson, 2013). Furthermore, the industry has witnessed a strong emphasis on innovation, with a focus on developing cultivars that exhibit enhanced flavour, extended shelf-life, and improved resistance to diseases (Nazir et al., 2024). This ongoing innovation, coupled with a growing global demand driven by the fruit's nutritional value (Richardson et al., 2018), has fostered a dynamic and evolving market for kiwifruit worldwide.

1.2.1 Kiwifruit cultivation in Italy

The Italian kiwifruit industry was established in the late 1960s and rapidly achieved global prominence in the 1990s. The establishment of new kiwifruit orchards was strongly influenced by the relative profitability of competing crops. In Latina (Lazio), for example, kiwifruit cultivation gained traction as a more profitable alternative to table grapes, which experienced declining yields in the 1970s and 1980s (Testolin and Ferguson, 2009). On the other hand, the Lazio region, located on the west coast of central Italy along the Tyrrhenian Sea, offered ideal conditions for kiwifruit cultivation. This region offered a favourable combination of factors: a long growing season (8-9 months), high levels of solar radiation, and sufficient winter chilling to meet the requirements of the crop without the need for artificial dormancy treatments. In addition, the availability of suitable agricultural land within the region further supports its suitability for kiwifruit production (Testolin and Ferguson, 2009).

Initially dominated by the 'Hayward' cultivar, the industry has since diversified to include several new cultivars, including yellow-fleshed varieties (Testolin and Ferguson, 2009; Testolin, 2015). With an annual production exceeding 435,696 tons, Italy is a major global player in kiwifruit cultivation, contributing 15% to global demand (ISTAT, 2024). As a leading producer and exporter, Italy ranks second only to China in production volume and exhibits strong export competitiveness alongside New Zealand (Testolin and Ferguson, 2009). The primary market for Italian kiwifruit is within Europe, in contrast to New Zealand's focus on global export markets (D'Evoli et al., 2015). Kiwifruit grown in Italy, particularly in the Lazio region, is known for its high nutritional value, particularly for its significant content of ascorbic acid and other antioxidants (Giangrieco et al., 2016).

1.3 Kiwifruit Vine Decline Syndrome: a threat to the Italian kiwifruit industry

Over the past decade, Italian kiwifruit production has experienced a significant decline, primarily attributed to the emergence of Kiwifruit Vine Decline Syndrome (KVDS), a novel and complex disease. Between 2020 and 2023, Italian kiwifruit production experienced a significant decline, decreasing from 534,000 tons to 391,000 tons. Concurrently, the cultivated area contracted from 26,690 hectares to 25,116 hectares (ISTAT, 2024). The initial symptoms of KVDS were documented in 2012 within aged orchards located in the Veneto region of northern Italy (Tacconi et al., 2014). These initial observations included a rapid decline of the plants, particularly evident in the canopy, manifesting as leaf curling, twig wilting, and desiccation (Figure 1.5). However, the most prominent symptoms were observed in the root system, characterized by browning, cortex detachment, the presence of rotting areas, and the loss of feeding roots (Figure 1.6) (Donati et al., 2020). Several agronomic and microbiological studies have investigated the potential causative factors of Kiwifruit Vine Decline Syndrome (KVDS). Emerging evidence strongly suggests that abiotic stressors, including waterlogging, elevated soil temperatures, the use of contaminated irrigation water, and heat stress, significantly contribute to the syndrome's dissemination (Reid et al., 1991; Tacconi et al., 2015; Savian et al., 2019; Bardi et al., 2020).

Subsequent microbiological investigations have highlighted the involvement of various plant pathogens.

Figure 1.5 - *Actinidia* plants exhibiting visible canopy symptoms in response to KVDS (A) compared with plants showing no evidence of the syndrome (B). Leaf curling predominantly occurs during the summer months (C)

KVDS is therefore recognized as a multifaceted syndrome with multiple contributing factors. A diverse array of microorganisms, including oomycetes (*Phytophthora* spp., *Pythium* spp., *Phytopythium* spp.), fungi (*Desarmillaria* spp., *Ilyonectria* spp., *Fusarium* spp., *Cylindrocarpon* spp.), and to a lesser extent, bacteria, have been implicated in the syndrome's spread (Tacconi et al., 2015; Donati et al., 2020; Prencipe et al., 2020; Savian et al., 2022; Prencipe et al., 2023; Mian et al., 2023). While the role of bacteria remains relatively understudied, two *Clostridium* species (*C. bifermentans* and *C. subterminale*) have been associated with the syndrome (Spigaglia et al., 2020). However, Donati et al. (2020) reported the absence of pathogenic bacteria in root samples from KVDS-affected plants, highlighting the need for further investigation into the bacterial component of this complex disease. The interplay between soil organisms, abiotic stressors, and plants emerges as a pivotal factor in the emergence and progression of KVDS. While some studies suggest a link between KVDS and microbial dysbiosis, recent findings have yielded conflicting results. Guaschino et al. (2024) demonstrated that stochastic processes

primarily drive the assembly of rhizosphere bacterial, fungal, and oomycete communities, regardless of plant health status. In contrast, Mosca et al. (2024) observed a marginal shift towards stochastic processes in the assembly of the bacterial root microbiome, but not in fungal and oomycete communities. These findings suggest that KVDS may have a limited impact on the diversity and structure of the plant rhizosphere and root microbiomes, implying that microbial dysbiosis may not be the primary driver of the syndrome.

Figure 1.6 – *Actinidia* roots showing KVDS symptoms (Ermacora et al., 2020)

1.4 Multifactorial stress combination: a complex challenge requiring multifaceted approaches

Climate change and environmental pollution impose a complex array of abiotic and biotic stressors upon plant systems (Zandalinas et al., 2021). Studies have shown that an escalation in the number of co-occurring multifactorial stress factors results in a significant deterioration of plant growth and survival (Coolen et al., 2016; Rillg et al., 2019; Zandalinas et al., 2021). Concomitantly, there is a decline in the biodiversity of the plant microbiome, upon which plant health is critically reliant. This emerging paradigm of stress combination underscores that while individual stressors may exert relatively minor impacts on plant growth and survival, the

cumulative influence of multifactorial stress combinations can be profoundly detrimental. This observation demonstrates that negative synergistic interactions among different stress factors can significantly diminish plant yield and agricultural productivity (Figure 1.7) (Pascual et al., 2022). Furthermore, multifactorial stress combinations can significantly impact the plant microbiome, which plays a pivotal role in plant development, reproduction, and survival (Rilling et al., 2021).

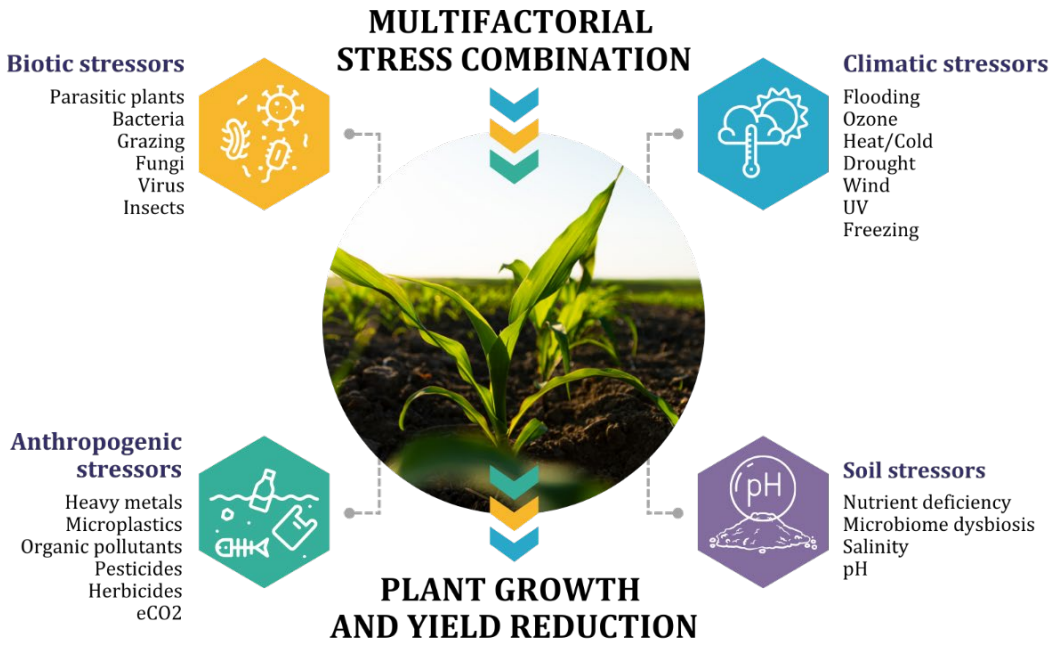

Figure 1.7 – Schematic representation of multifactorial stress combinations. Multifactorial stress combination occurs when three or more stresses impact a plant or a crop simultaneously or sequentially (adapted from Zadalinas et al., 2024)

Plant responses to combinatorial stress are not simply additive but rather exhibit unique and complex patterns that cannot be predicted simply by considering the individual responses to each constituent stressor. In certain instances, the response to a specific stressor within a combination may prevail over others (Zhou et al., 2017; Sewelam et al., 2020), while in other instances, the overall effect may be additive (Rizhsky et al., 2004; Zadalinas et al., 2020). Multifactorial stress combinations (MFSC) have been demonstrated to exert a detrimental effect on various physiological and metabolic processes, including photosynthesis and the accumulation of osmo-protectants. These adverse effects are further associated

with significant reductions in plant growth rate, height, biomass, and ultimately, yield (Zadalinas et al., 2024). Agroecosystems, and agricultural production systems in general, are more susceptible to adverse effects under MFSC conditions. Agroecosystems, often characterized by a reliance on monoculture, exhibit heightened vulnerability to pathogen and insect infestations, which can lead to devastating crop losses and significant yield reductions (Zandalinas and Mittler, 2022). How can MFSC contribute to this vulnerability? Basically, MFSCs can compromise plant vigor and diminish overall resilience to biotic stressors, thereby exacerbating the severity of insect and pathogen outbreaks under prevailing climatic conditions. Furthermore, shifts in climatic patterns, encompassing rising temperatures and alterations in precipitation regimes across diverse geographical regions, have the potential to foster the proliferation of pathogens and insects (Zadalinas et al., 2024). This phenomenon can result in augmented initial inoculum levels and, consequently, the triggering of widespread outbreaks.

Recent advancements in genomic technology have led to significant progress in the field of plant disease ecology (Crandall et al., 2020). The integration of various omics approaches, including genomics, transcriptomics, proteomics, and metabolomics, along with histological methods, has emerged as a crucial strategy for elucidating the response mechanisms of plants to stress combinations (Jing et al., 2024). These technologies have profoundly transformed our understanding of plant disease ecology, facilitating a more comprehensive and integrated approach to understanding pathogenesis and its underlying mechanisms. Consequently, this enhanced understanding has led to the development of more effective disease management strategies. The significance of these *-omics* approaches is especially pronounced in the context of rapid environmental change, where both biotic and abiotic stressors pose a growing threat to plant health. The capacity to adapt to and mitigate these stressors is imperative for preserving the resilience of terrestrial ecosystems and maintaining sustainable agricultural systems. Despite its nascent state, this integrative framework holds considerable promise for propelling the study of microbial plant disease ecology.

1.5 References

Bardi, L. (2020). Early kiwifruit decline: A soil-borne disease syndrome or a climate change effect on plant–soil relations? *Frontiers in Agronomy, 2*. https://doi.org/10.3389/fagro.2020.00003

Coolen, S., Proietti, S., Hickman, R., Davila Olivas, N. H., Huang, P. P., van Verk, M. C., van Pelt, J. A., Wittenberg, A. H. J., de Vos, M., Prins, M., van Loon, J. J. A., Aarts, M. G. M., Dicke, M., Pieterse, C. M. J., & van Wees, S. C. M. (2016). Transcriptome dynamics of *Arabidopsis* during sequential biotic and abiotic stresses. *The Plant Journal, 86*(2), 249–267. https://doi.org/10.1111/tpj.13167

Crandall, S. G., Gold, K. M., Jiménez-Gasco, M. del M., Filgueiras, C., & Willett, D. S. (2020). A multi-omics approach to solving problems in plant disease ecology. *PLOS ONE, 15*(9), e0237975. https://doi.org/10.1371/journal.pone.0237975

D'Evoli, L., Moscatello, S., Lucarini, M., Aguzzi, A., Gabrielli, P., Proietti, S., Battistelli, A., Famiani, F., Böhm, V., & Lombardi-Boccia, G. (2015). Nutritional traits and antioxidant capacity of kiwifruit (*Actinidia deliciosa* Planch., cv. Hayward) grown in Italy. *Journal of Food Composition and Analysis, 37*, 25–29. https://doi.org/10.1016/j.jfca.2014.06.012

Donati, I., Cellini, A., Sangiorgio, D., Caldera, E., Sorrenti, G., & Spinelli, F. (2020). Pathogens associated with kiwifruit vine decline in Italy. *Agriculture, 10*(4), 119. https://doi.org/10.3390/agriculture10040119

Ermacora, P., Cipriani, G., Savian, F., Testolin, R., & Tosi, L. (2020). Morìa del kiwi, capire le cause per mettere in atto i rimedi. *Rivista di Frutticoltura e Ortofloricoltura.*

Ferguson, A. R. (1984). Kiwifruit: A botanical review. In J. Janick (Ed.), *Horticultural Reviews* (Vol. 6, pp. 1–64). https://doi.org/10.1002/9781118060797.ch1

Ferguson, A. R. (1990a). Biology of the genus *Actinidia*. In I. J. Warrington & G. C. Weston (Eds.), *Kiwifruit: Botany, production and uses* (pp. 29–51). https://doi.org/10.1079/9781800620933.0003

Ferguson, A. R. (1990b). Botanical nomenclature: *Actinidia chinensis, Actinidia deliciosa,* and *Actinidia setosa*. In *Kiwifruit science and management* (pp. 36–57). New Zealand Society for Horticultural Science, Ray Richards, Auckland, New Zealand.

Ferguson, A. R. (1990c). The kiwifruit in China. In *Kiwifruit: Science and management* (pp. 155–164). New Zealand Society for Horticultural Science, Ray Richards Publisher, Auckland, New Zealand.

Ferguson, A. R. (2003). Le cultivar di *Actinidia*—una prospettiva dalla Nuova Zelanda. *Actinidia, la novità frutticola del XX secolo. Convegno Nazionale della Società Orticola Italiana, 21*, 51–67.

Ferguson, A. R. (2004). 1904—The year that kiwifruit (*Actinidia deliciosa*) came to New Zealand. *New Zealand Journal of Crop and Horticultural Science, 32*(1), 3–27. https://doi.org/10.1080/01140671.2004.9514276

Ferguson, A. R. (2005). Why were kiwifruit initially successful only in New Zealand? *Acta Horticulturae, 694*, 223–227. https://doi.org/10.17660/ActaHortic.2005.694.36

Ferguson, A. R. (2013). Kiwifruit: The wild and the cultivated plants. *Advances in Food and Nutrition Research, 68*, 15–32. https://doi.org/10.1016/B978-0-12-394294-4.00002-X

Ferguson, A. R., & Bollard, E. G. (1990). Domestication of the kiwifruit. In *Kiwifruit: Science and management* (pp. 165–246).

Giangrieco, I., Proietti, S., Moscatello, S., Tuppo, L., Battistelli, A., La Cara, F., Tamburrini, M., Famiani, F., & Ciardiello, M. (2016). Influence of geographical location of orchards on green kiwifruit bioactive components. *Journal of Agricultural and Food Chemistry, 64*(48), 9172–9179. https://doi.org/10.1021/acs.jafc.6b03930

Guaschino, M., Garello, M., Nari, L., Zhimo, Y. V., Droby, S., & Spadaro, D. (2024). Soil, rhizosphere, and root microbiome in kiwifruit vine decline, an emerging multifactorial disease. *Frontiers in Microbiology, 15*. https://doi.org/10.3389/fmicb.2024.1330865

Huang, H. (2016). *Kiwifruit: The genus Actinidia.* Academic Press.

Jing, Z., Liu, N., Zhang, Z., & Hou, X. (2024). Research progress on plant responses to stress combinations in the context of climate change. *Plants, 13*(4), 469. https://doi.org/10.3390/plants13040469

Li, D., Liu, Y., Zhong, C., & Huang, H. (2010). Morphological and cytotype variation of wild kiwifruit (*Actinidia chinensis* complex) along an altitudinal and longitudinal gradient in central-west China. *Botanical Journal of the Linnean Society, 164*, 72–83. https://doi.org/10.1111/j.1095-8339.2010.01073.x

Liang, C. F. (1983). On the distribution of *Actinidia*. *Guihaia, 3*(4), 229–248.

Liu, Y., Zhou, Y., Cheng, F., Zhou, R., Yang, Y., Wang, Y., Zhang, X., Soltis, D., Xiao, N., Quan, Z., & Li, J. (2023). Chromosome-level genome of putative autohexaploid *Actinidia deliciosa* provides insights into polyploidisation and evolution. *The Plant Journal.* https://doi.org/10.1111/tpj.16592

Mian, G., Cipriani, G., Firrao, G., Martini, M., & Ermacora, P. (2023). Genetic diversity of *Actinidia* spp. shapes the oomycete pattern associated with kiwifruit vine decline syndrome (KVDS). *Scientific Reports, 13*, Article 43754. https://doi.org/10.1038/s41598-023-43754-y

Mosca, S., Aci, M. M., Procopio, G., Vadalà, V., Vizzari, G., Francomano, E., Mohamed, N. Z., Li Destri Nicosia, M. G., Agosteo, G. E., Spadaro, D., Schena, L., & Malacrinò, A. (2024). Integrated analyses of the plant and soil microbiome identify *Phytopythium vexans* as agent of the kiwifruit vine decline syndrome. *Plant and Soil*. https://doi.org/10.1007/s11104-024-06891-5

Nazir, M. F., Lou, J., Wang, Y., Zou, S., & Huang, H. (2024). Kiwifruit in the omics age: Advances in genomics, breeding, and beyond. *Plants, 13*(15), Article 2156. https://doi.org/10.3390/plants13152156

Pascual, L. S., Segarra-Medina, C., Gómez-Cadenas, A., López-Climent, M. F., Vives-Peris, V., & Zandalinas, S. I. (2022). Climate change-associated multifactorial stress combination: A present challenge for our ecosystems. *Journal of Plant Physiology, 276*, Article 153764. https://doi.org/10.1016/j.jplph.2022.153764

Prencipe, S., Savian, F., Nari, L., Ermacora, P., Spadaro, D., & Martini, M. (2020). First report of *Phytopythium vexans* causing decline syndrome of *Actinidia deliciosa* 'Hayward' in Italy. *Plant Disease, 104*(6), 1868. https://doi.org/10.1094/PDIS-10-19-2101-PDN

Prencipe, S., Schiavon, G., Rosati, M., Nari, L., Schena, L., & Spadaro, D. (2023). Characterization of *Phytopythium* species involved in the establishment and development of kiwifruit vine decline syndrome. *Microorganisms, 11*(1), Article 216. https://doi.org/10.3390/microorganisms11010216

Reid, J. B., Tate, K. G., Brown, N. S., & Cheah, L. H. (1991). Effects of flooding and alluvium deposition on kiwifruit (*Actinidia deliciosa*): I. Early vine decline. *New Zealand Journal of Crop and Horticultural Science, 19*(3), 247–257. https://doi.org/10.1080/01140671.1991.10421808

Richardson, D. P., Ansell, J., & Drummond, L. N. (2018). The nutritional and health attributes of kiwifruit: A review. *European Journal of Nutrition, 57*(8), 2659–2676. https://doi.org/10.1007/s00394-018-1627-z

Rillig, M. C., Ryo, M., Lehmann, A., Aguilar-Trigueros, C. A., Buchert, S., Wulf, A., Iwasaki, A., Roy, J., & Yang, G. (2019). The role of multiple global change factors in driving soil functions and microbial biodiversity. *Science, 366*(6467), 886–890. https://doi.org/10.1126/science.aay2832

Rillig, M. C., Lehmann, A., Orr, J. A., & Waldman, W. R. (2021). Mechanisms underpinning nonadditivity of global change factor effects in the plant–soil system. *New Phytologist, 232*(4), 1535–1539. https://doi.org/10.1111/nph.17714

Rizhsky, L., Liang, H., Shuman, J., Shulaev, V., Davletova, S., & Mittler, R. (2004). When defense pathways collide: The response of *Arabidopsis* to a combination of drought and heat stress. *Plant Physiology, 134*(4), 1683–1696. https://doi.org/10.1104/pp.103.033431

Savian, F., Marroni, F., Ermacora, P., Firrao, G., & Martini, M. (2022). A metabarcoding approach to investigate fungal and oomycete communities associated with kiwifruit vine decline syndrome in Italy. *Phytobiomes Journal, 6*(4), 290–304. https://doi.org/10.1094/PBIOMES-03-22-0019-R

Savian, F., Musetti, R., Sandrin, N., Ermacora, P., & Martini, M. (2019). Etiological studies over kiwifruit decline reveal the involvement of both flooding and biotic factors. In *Proceedings of the abstracts of presentations at the XXV Congress of the Italian Phytopathological Society (SIPaV)* (pp. 811–848). *Journal of Plant Pathology, 101*(4), 811–848.

Spigaglia, P., Barbanti, F., Marocchi, F., Mastroleo, M., Baretta, M., Ferrante, P., Caboni, E., Lucioli, S., & Scortichini, M. (2020). *Clostridium bifermentans* and *C. subterminale* are associated with kiwifruit vine decline, known as moria, in Italy. *Plant Pathology, 69*(4), 765–774. https://doi.org/10.1111/ppa.13161

Tacconi, G., Giacopini, A., & Tosi, L. (2014). La moria del kiwi nel veronese. *Kiwi Informa, 4*(6), 5–23.

Tacconi, G., Paltrinieri, S., Mejia, J. F., Fuentealba, S. P., Bertaccini, A., Tosi, L., Giacopini, A., Mazzucchi, U., Favaron, F., Sella, L., & Bertaiola, F. (2015). Vine decline in kiwifruit: Climate change and effect on water

Testolin, R. (2015). Kiwifruit (*Actinidia* spp.) in Italy: The history of the industry, international scientific cooperation and recent advances in genetics and breeding. *Acta Horticulturae, 1096*, 47–61. https://doi.org/10.17660/ACTAHORTIC.2015.1096.2

Testolin, R., & Ferguson, A. (2009). Kiwifruit (*Actinidia* spp.) production and marketing in Italy. *New Zealand Journal of Crop and Horticultural Science, 37*(1), 1–32. https://doi.org/10.1080/01140670909510246

Wang, Z., Zhong, C., Li, D., Yan, C., Yao, X., & Li, Z. (2020). Cytotype distribution and chloroplast phylogeography of the *Actinidia chinensis* complex. *BMC Plant Biology, 21*, Article 99. https://doi.org/10.1186/s12870-021-03099-y

Zandalinas, S. I., Fritschi, F. B., & Mittler, R. (2020). Signal transduction networks during stress combination. *Journal of Experimental Botany, 71*(5), 1734–1741. https://doi.org/10.1093/jxb/erz486

Zandalinas, S. I., Peláez-Vico, M. Á., Sinha, R., Pascual, L. S., & Mittler, R. (2024). The impact of multifactorial stress combination on plants, crops, and ecosystems: How should we prepare for what comes next? *The Plant Journal, 117*(6), 1800–1814. https://doi.org/10.1111/tpj.16557

Zandalinas, S. I., Sengupta, S., Fritschi, F. B., Azad, R. K., Nechushtai, R., & Mittler, R. (2021). The impact of multifactorial stress combination on plant growth and survival. *New Phytologist, 230*(3), 1034–1048. https://doi.org/10.1111/nph.17232

Zhou, R., Yu, X., Ottosen, C. O., Rosenqvist, E., Zhao, L., Wang, Y., Yu, W., Zhao, T., & Wu, Z. (2017). Drought stress had a predominant effect over heat stress on three tomato cultivars subjected to combined stress. *BMC Plant Biology, 17*(1), Article 97. https://doi.org/10.1186/s12870-017-0974-x

Zhou, Z., Wang, C., & Luo, Y. (2020). Meta-analysis of the impacts of global change factors on soil microbial diversity and functionality. *Nature Communications, 11*, Article 3072. https://doi.org/10.1038/s41467-020-16881-7

Chapter 2

Seasonal dynamics of kiwifruit microbiome: A case study in a KVDS-affected orchard

Antonella Cardacino [1], Silvia Turco[1], Giorgio Mariano Balestra[1]

[1] *Department of Agriculture and Forest Sciences, University of Tuscia, Via S. Camillo de Lellis snc, Viterbo, Italy*

Published on: *Microbiological Research*, 1 January 2025
doi: https://doi.org/10.1016/j.micres.2024.128044

Abstract

Over the past decade, Italian kiwifruit orchards and overall production have faced a significant threat from Kiwifruit Vine Decline Syndrome (KVDS). Despite the insights gained from metagenomics studies into the microbial communities associated with the disease, unanswered questions still remain. In this study, the evolution of bacterial, fungal, and oomycetes communities in soil and root endosphere at three different time points during the vegetative season was investigated for the first time in a KVDS-affected orchard in the Lazio Region. The fungal and oomycetes genera previously associated with the syndrome, including *Fusarium, Ilyonectria, Thelonectria, Phytophthora, Pythium* and *Globisporangium*, were identified in both groups. In contrast, the characterization of bacterial communities revealed the first instance of the presence of the genus *Ralstonia* in soil and root samples. The microbiome composition shifts between KVDS-affected and asymptomatic plants were significant as evidenced by the results, particularly after the temperature increase. This temperature change coincided with the onset of severe disease symptoms and may indicate a key role in the progression of KVDS.

Keywords: metagenomics, microbiome, microbial communities, metabarcoding, KVDS

2.1 Introduction

Actinidia chinensis var. *deliciosa* is a deciduous vine belonging to the family *Actinidiaceae*, renowned for producing the commercially popular kiwifruit. Native to the temperate forests of China, later expanded to New Zealand in the early 20th century. Today, with an overall harvested production of 435,696 tons per year, Italy is one of the largest global kiwifruit producers, accounting for 15% of the world's demand (ISTAT, 2024). However, since 2012 the annual production has been strongly reduced due to the spread of a novel and complex disease known as Kiwifruit Vine Decline Syndrome (KVDS) (Tacconi et al., 2015). Italian kiwifruit production underwent a notable decline from 521,000 tons in 2020 to 391,000 tons in 2023, with a corresponding decrease in cultivated area from 26,690 hectares to 25,116 hectares in 2023 (ISTAT, 2024).

Typical KVDS symptoms are related to the damaged root system, characterized by browning, cortical layer detachment, and loss of feeding roots (Tacconi et al., 2014). Root cortical layers exhibited hypertrophy, followed by phloem detachment from the central cylinder, resulting in the breakdown of the cortex (Donati et al., 2020). KVDS-affected plants exhibit severe canopy symptoms, including leaf wilting, overall plant decline, and a tendency to collapse, especially during the summer months. (Savian et al., 2020). As a consequence of root damage, canopy symptoms typically spread later, when the overall plant fitness is severely compromised. Since 2012, initial observations of KVDS in North Italy (Veneto and Friuli Venezia Giulia) indicated a potential plant response to a particularly wet season and anomalous temperature trends (Tacconi et al., 2014). Nevertheless, analogous symptoms were subsequently documented in other regions dedicated to the cultivation of kiwifruit, including Piedmont, Emilia-Romagna, Latium, and Calabria. Approximately 34.5% of Italian kiwifruit orchards have been affected by this syndrome (Ermacora and Saro, 2020).

Several agronomic and microbiological studies have been conducted to investigate the potential causative factors of KVDS. It has become evident that abiotic stressors, including waterlogging (Tacconi et al., 2015; Tosi et al., 2015; Sorrenti et al., 2016), elevated soil temperature, the use of contaminated irrigation water, and heat stress, play a significant role in the dissemination of the syndrome (Reid et al., 1991; Savian

et al., 2019; Bardi et al., 2020). Tacconi et al. (2015) initially proposed the involvement of biotic stressors, a hypothesis that has since been corroborated by other authors (Donati et al., 2020; Spigaglia et al., 2020; Prencipe et al., 2020). Several microbiological studies have highlighted the involvement of the plant microbiota in the multifaced KVDS syndrome spread. Several soil-borne pathogens have been associated with the syndrome, including oomycetes such as *Phytophthora* spp., *Pythium* spp. and *Phytopythium* spp., along with fungi from the genera *Desarmillaria*, *Ilyonectria*, *Fusarium* and *Cylindrocarpon* (Tacconi et al., 2015; Donati et al., 2020; Savian et al., 2022; Prencipe et al., 2023, Mian et al., 2023). However, the characterization of bacterial communities remains relatively understudied. To date, only two species of *Clostridium* (*C. bifermentas* and *C. subterminale*) have been associated with the syndrome (Spigaglia et al., 2020) while Donati et al., (2020) reported that no pathogenic bacteria have been isolated from roots of KVDS-affected plants.

This study aims to characterize the bacterial, fungal, and oomycetes communities inhabiting the rhizosphere of plants affected by the syndrome, in comparison with asymptomatic samples. Root and soil samples were collected at three different time points throughout the season: during vegetative renewal in May, during flowering in June, and at fruit set in July. To the best of our knowledge, this is a pivotal comprehensive investigation of microbial composition and biodiversity within the same field conducted over a single year.

2.2 Material and methods

2.2.1 Experimental site

Samples were collected from *Actinidia chinensis* var. *deliciosa* "BO-ERICA®" plants cultivated in an orchard located in Cisterna di Latina (Lazio Region, Center Italy, 41°33'34.0344''N, 12°47'32.7948''E). The orchard is planted on soil with high clay content and a low percentage of organic matter, which are known to adversely affect the composition of microbial communities, as well as the structural properties and fertility of the soil (Khanghahi et al., 2019; Dincă et al., 2022). More detailed physical and chemical soil analyses are reported in Table S2.1. Despite the soil's

homogeneous composition, the plantation can be divided into two distinct areas: Area A, characterized by a higher prevalence of KVDS-affected plants, and Area B, where the majority of the plants, at the time of sampling and in the following monitoring activities, exhibit no symptoms on the canopy and roots that can be attributed to KVDS and are thus called asymptomatic (Figure S2.1).

2.2.2 Soil and root sampling

In 2022, nine asymptomatic and nine KVDS-symptomatic plants were chosen for the study according to a symptomatology scale shown in Figure S2.2. Sampling was carried out at three different time points starting at the end of the vegetative renewal in May, at the end of flowering in June, and at the fruit set in July. From each plant, three soil cores (about 300 grams) were drilled using a hand auger at a depth of 30-35 cm, homogenized, and pooled to form a composite sample per vine. At the same time, three root samples from three adjacent plants were collected and pooled together to create a bulk. Thus, three bulk of KVDS soil samples and three bulk of asymptomatic soil samples, together with three bulk of KVDS root samples and three bulk of asymptomatic roots were collected at each of the three time points, for a total of 36 samples.

Soil samples were dried at room temperature and sifted through 4 mm and 2 mm sieves, placed into sterile tubes, and stored at -20°C until DNA extraction. Roots were placed in sterile tubes, washed the first time with 0.8% NaCl, and vortexed for one minute. The washing solution was discarded, and the roots were washed again with 1% sodium hypochlorite and 0.01% Tween 80, rinsed in sterile water, transferred to new sterile tubes, and stored at -20 °C until DNA extraction.

2.2.3 DNA extraction from soil

For DNA extraction from soil, an optimized protocol from Zhou et al. (1996), Yeates et al. (1998) and Burgmann et al. (2001) was followed. Briefly, 5 gr aliquots of soil were mixed with 13.5 mL of extraction buffer [100 mM Tris-HCl (pH 8.0), 100 mM sodium EDTA (pH 8.0), 100 mM sodium phosphate (pH 8.0), 1.5 M NaCl, 1% CTAB]

and 100 µl of proteinase K (10 mg/mL) in 50 mL tubes and incubated for 40 min at 37 °C by shaking at 225 rpm. 1.5 mL of SDS (20%) was added and the tubes were incubated in a water bath at 65 °C for 2 hours and inverted every 20 minutes. After incubation, samples were centrifuged at 6,500 g for 30 minutes at RT and the supernatant was transferred into new sterile tubes. The pellets were further incubated twice with 4.5 ml of extraction buffer and 500 µl of SDS (20%), vortexed for 10 sec, kept at 65 °C for 15 min, and centrifuged as above. Supernatants were mixed with an equal volume of chloroform/isoamyl alcohol (24:1, vol/vol), followed by a centrifugation step at 7,500 g for 30 min at 4 °C. The aqueous phase was recovered, and 0.6 volume of isopropanol was added and incubated for 1 hour at room temperature. After centrifugation at 9.000 g for 20 min at 4 °C, the pellet was washed with 70% cold ethanol, centrifuged, and resuspended in 500 µl of nuclease-free water. DNA concentration was measured with Qubit™ dsDNA BR Assay Kit.

2.2.4 DNA extraction from roots

Root samples were grinded with mortar and pestle in liquid nitrogen, transferred in 50 mL sterile tubes, and incubated with 5 mL of lysis buffer [CTAB 2% (w/v), PVP40 2% (w/v), Tris-HCl (pH 8) 100 mM, EDTA 25 mM, NaCl 2M] at 60°C for 30 min, inverting every 10 min. From this solution, 1 mL was transferred into 2 mL tubes and mixed with one volume of chloroform/isoamyl alcohol (24:1) and the tubes were centrifuged at 7,000 g for 10 min at 4°C. After repeating the previous step, the supernatant was transferred into a new tube, and 1/10 volume of sodium acetate was added. The tubes were incubated at -20°C for 90 min and then centrifuged at 9,000 g for 20 minutes at 4°C. The supernatant was discarded, and the pellet was washed with 70% of cold ethanol and centrifuged for 15 min at 4°C. After discarding the supernatant, the pellet was dried at room temperature under the hood and then eluted in 50 µl of nuclease-free water. DNA concentration was measured with Qubit™ dsDNA BR Assay Kit.

2.2.5 Amplification of 16S and ITS and sequencing

Amplification, library preparation and Illumina NovaSeq sequencing were carried out by Novogene (Cambridge, UK). Briefly, all PCR reactions were carried out with 15 µL of Phusion® High - Fidelity PCR Master Mix (New England Biolabs), 0.2 µM of forward and reverse primers, and 10 ng of template DNA. Thermal cycling consisted of initial denaturation at 98 °C for 1 min, followed by 30 cycles of denaturation at 98°C for 10 s, annealing at 50°C for 30 s, and elongation at 72°C for 30 s and 72°C for 5 min. For bacteria, primers 799F (5'-AACMGGATTAGATACCCKG–3') and 1193R (5'-ACGTCATCCCCACCTTCC-3') were selected for sequencing of the hypervariable V5-V7 bacterial 16S rRNA region. For fungi and oomycetes, primers ITS5-1737F (5'-GGAAGTAAAAGTCGTAACAAGG-3') and ITS2-2043R (5'-GCTGCGTTCTTCATCGATGC-3') of ITS1 fungal Internal Transcribed Spacer (ITS) gene were used. Sequencing libraries were generated, and indexes were added. The library was checked with Qubit™ and real-time PCR for quantification and bioanalyzer for size distribution detection. Quantified libraries were pooled and sequenced on Illumina platforms, according to effective library concentration and data amount required.

2.2.6 Bioinformatic analysis

The microbiome characterization was performed following the Quantitative Insight into Microbial Ecology 2 (QIIME2 v.2023.2.0, Bolyen et al., 2019) pipeline, as previously adjusted by Turco et al., (2024a). The raw merged reads (R1 and R2) were demultiplexed, chimeras were removed, and denoised with the Divisive Amplicon Denoising Algorithm (DADA2), to get the feature table with the Amplicon Sequence Variants (ASVs) and the representative sequences in FASTA format.

Fungal taxonomic classification of the ASVs was performed using the classify-consensus-blast algorithm and an *in-house* database built with the rescript QIIME2 plugin using the *Actinidia chinensis* sequences (taxID 3625), the NCBI Fungi RefSeq ITS project (PRJNA177353), and the oomycetes sequences present in the International Nucleotide Sequence Databases (www.insdc.org). Bacterial taxonomic classification of the obtained ASVs was performed using the *classify-consensus-blast*

algorithm towards the SILVA 138 database (Quast et al., 2013). A phylogenetic tree was built on the bacterial representative sequences using MAFFT and FastTree implemented within the QIIME2 pipeline.

After removal of host-related sequences, including chloroplast and mitochondria, uncharacterized and uncultured sequences as well as low-frequency ASVs according to Bokulich et al. (2013), the four main input files (feature table, taxonomy, representative sequences, and phylogenetic tree) were imported within the R environment v.4.2.3 and further processed with the *phyloseq* package v1.42.0 (McMurdie and Holmes, 2013). The rarefaction curves were obtained with the *vegan* R package v. 2.6 (Dixon, 2003), diversity within samples (alpha diversity) was evaluated with Shannon and Simpson indexes, while richness was evaluated with Chao1 and ACE indexes. Differences in alpha diversity among factors were determined using a Kruskal-Wallis test. The dissimilarity between the samples (beta diversity) was evaluated through Non-metric Multidimensional Scaling (NMDS) and Principal Coordinate Analysis (PCoA) plots based on the Bray-Curtis index. Statistical testing of beta diversity was performed with the permutational multivariate analysis of variance (PERMANOVA, 1,000 permutations). Relative microbial abundance was plotted for the 30 most abundant genera, with the least abundant collapsed as "<1%". Bacterial ASVs functional classification was performed using *picrust2* plugin within QIIME2, the *ggpicrust2* R package (Douglas et al., 2020; Yang et al., 2023) using DESeq2 for the differential analysis, KEGG Orthology (KO) for pathway annotation and a P value set at 0.05. Functional guilds of the identified fungal ASVs were assigned using the *fungaltraits* v.0.0.3 package within the R environment v.4.2.3. This package leverages information from both the FunGuild and FunFun databases for functional guild assignment (Turco et al., 2024a).

2.3 Results

2.3.1 Amplicon sequencing and denoising results

A total of 6.03 M reads were obtained from the Illumina sequencing. After applying DADA2 filtering and denoising, 41,400 reads were assigned to Amplicon Sequence Variants (ASVs). The average of ASVs per sample was 2,612, with a range from 1,790 to 3,518 for the 16S sequencing and 845 ASVs for the ITS, with a range from 559 to 1,178 per sample (Table S2.2). After removal of chloroplast, mitochondria, uncultured and unassigned ASVs, 572 bacterial taxa, 218 fungal taxa and 111 oomycetes taxa were imported within R as a *phyloseq* object and further processed.

2.3.2 Microbial communities' richness and diversity

The bacterial community richness, expressed by Chao1 and ACE indexes, resulted to be comparable between the two groups, asymptomatic and KVDS samples (Figure 2.1, panel A), as well as between soil and root samples (Figure S2.3, panel A). Conversely, during the vegetative stages, the richness was higher during flowering (second stage) and at fruit set (third stage), compared to the vegetative renewal (first stage), which exhibited the lowest value (Figure 2.2, panel A). No statistically significant differences were identified. A similar trend was observed for the alpha within-sample bacterial diversity, expressed by Shannon and Simpson indexes, with a similar heterogeneity between asymptomatic and KVDS plants, even though with slightly higher variability in the asymptomatic ones (Figure 2.1, panel A). At the matrix level roots samples exhibited a higher diversity than soil samples (Figure S2.3, panel A). Among the three time points, the diversity was the highest during the flowering stage, followed by the fruit set stage and the vegetative renewal, which exhibited the lowest diversity (Figure 2.2, panel A). As previously, no statistically significant differences were identified.

In contrast to the bacterial communities, the fungal richness was higher in the KVDS samples, especially for the Chao1 index (Figure 2.1, panel B). Notably, significant differences were observed among sample types, with the soil exhibiting the highest Chao1 and ACE values (Figure S2.3, panel B). Indices related to the vegetative stages demonstrated a decline in richness during the fruit set compared to the other stages

(Figure 2.2, panel B). No statistically significant differences were identified. Asymptomatic samples exhibited a lower within-sample diversity compared to the KVDS ones (Figure 2.1, panel B), but no statistically significant differences were identified. Instead, significant differences were observed between soil and root samples regarding the Chao1 and ACE indexes, with soil samples displaying a higher richness (Figure S2.3, panel B).

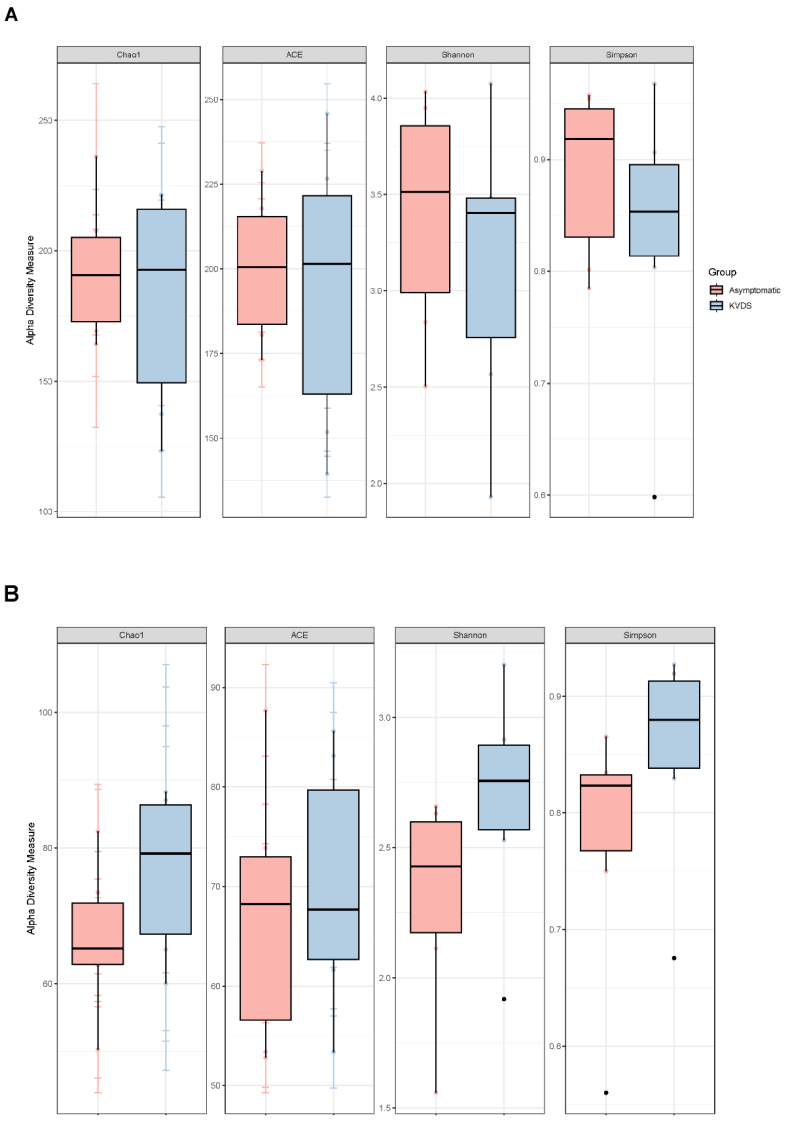

Figure 2.1 - Alpha-diversity of bacterial (A) and fungal (B) communities in asymptomatic (pink) and KVDS (light blue) samples. Alpha diversity metrics summarize the structure of the microbial community concerning its richness (Chao1 and ACE indexes), and within-sample diversity expressed by Shannon and Simpson indexes. No significant differences were observed in both communities for all indexes.

During the vegetative season, both communities exhibited a decline in diversity, with values decreasing from their highest point during vegetative renewal to a lower level during fruit set (Figure 2.2, panel B).

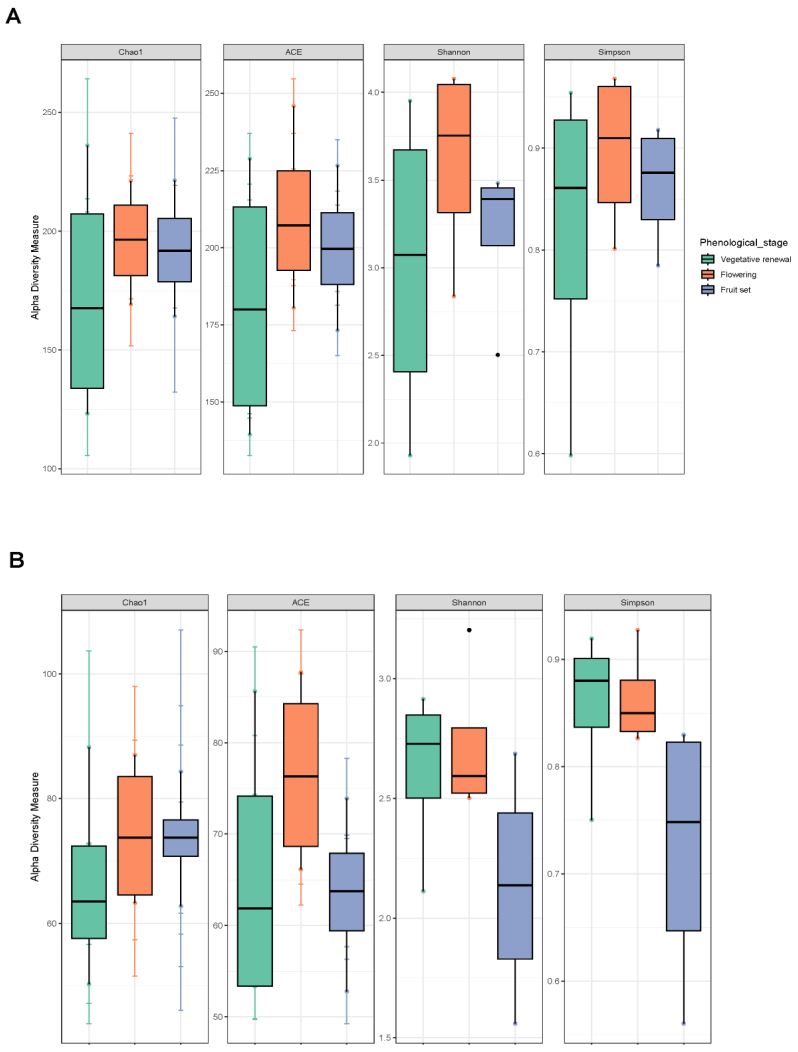

Figure 2.2 - Alpha-diversity of bacterial (A) and fungal (B) communities during the vegetative season: vegetative renewal (green), flowering (orange), and fruit set (purple). No significant differences were observed in both communities for all indexes.

2.3.3 Microbial communities' dissimilarities

The beta diversity between the samples was evaluated through NMDS and PCoA analysis based on Bray-Curtis distance (Figure 2.3). Significant differences were observed in the community structures and compositions, particularly concerning

the sample type (i.e., differences between roots and soil) and phenological stage (i.e., vegetative renewal, flowering, and fruit set).

For the bacterial communities, there was a clear microbiota distinction for the samples collected during the three vegetative stages, in both soil and roots (Figure 2.3, panels A and B). The PERMANOVA supported the NMDS results, indicating a significant association between community similarity and sample type (R^2 = 0.178; $P < 0.05$) and phenological stage (R^2 = 0.258; $P < 0.05$) (Table S2.3).

Concerning fungal communities, the phenological stages have also exerted an influence on the structure of these communities (Figure 2.3, panels C and D). The data were corroborated by the results of the PERMANOVA, which demonstrated a significant effect of phenological stage (R^2 = 0.379; $P < 0.01$) on fungal communities (Table S2.4). No effects related to different variables were observed in oomycete communities (Figure 2.3, panels E and F). The PERMANOVA analysis corroborated the NMDS results, indicating that no significant differences were observed across all categories (Table S2.5).

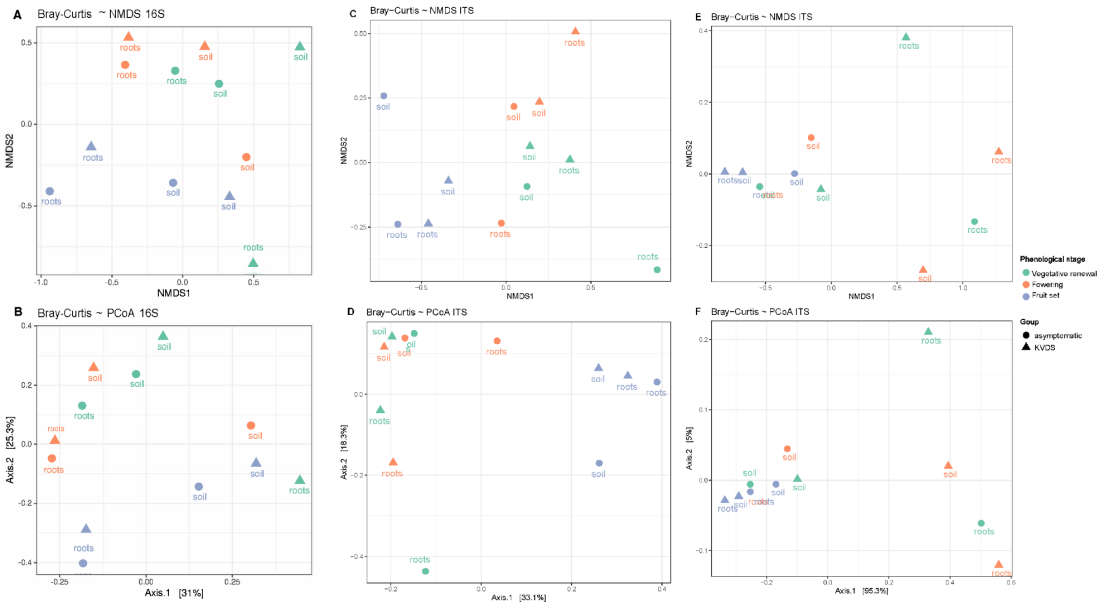

Figure 2.3 - Non-metric Multidimensional Scaling (NMDS) and Principal Coordinate Analysis (PCoA) plots based on Bray-Curtis similarity of ASV-based bacterial (A-B), fungal (C-D) and oomycete (E-F) communities structure in asymptomatic (circle) and KVDS (triangle) samples in different phenological stages (green = vegetative renewal, orange = flowering, blue = fruit set).

2.3.4 Soil and roots bacterial communities

Overall, at the phylum level, the bacterial communities were predominantly composed of Proteobacteria (50%), followed by Actinobacteriota (35%), Firmicutes (10%), and Bacteroidota (5%). The most abundant genera were *Ralstonia*, *Pseudomonas*, *Streptomyces*, *Methylobacterium*, *Bacillus*, and TRA3-20. Interestingly, the microbiome composition changes during the vegetative season in both KVDS and asymptomatic samples (Figure 2.4).

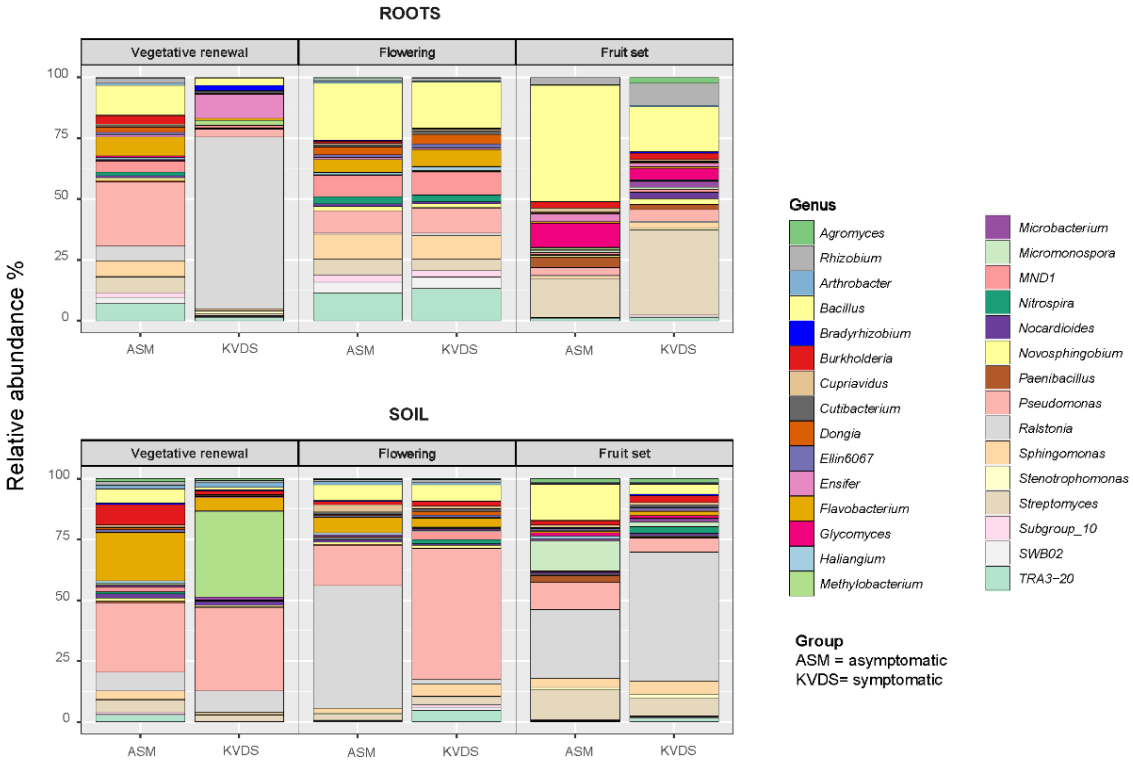

Figure 2.4 - Taxonomy plots showing the relative abundance of the top 30 genera of bacterial communities in roots and soil of asymptomatic and KVDS samples during the vegetative season.

At the end of vegetative renewal, *Ralstonia* spp. was the most abundant genus in KVDS root samples (64%), followed by *Ensifer* spp. (9%), *Pseudomonas* spp. (2.8%), and *Bacillus* spp. (2.7%). It is noteworthy that the relative abundance of *Bacillus* spp. increased significantly during the flowering time-point (10%). Additionally, bacteria belonging to the *Nitrosomonadaceae* family (7%), as well as the genera *Pseudomonas* spp. (5.4%) and *Sphingomonas* spp. (5%), were present. During the

fruit set, the most common genera were *Streptomyces* spp. (25.5%), *Bacillus* spp. (13.4%), and *Rhizobium* spp. (6.6%).

In asymptomatic root samples, *Pseudomonas* spp. (17.4%), *Bacillus* spp. (8%), and *Flavobacterium* spp. (5%) were the most abundant genera found during the first vegetative stage. Furthermore, at the time-points of flowering and fruit set, *Bacillus* spp. was the most common genus, accounting for 13% and 43% respectively. Other notable bacteria at the flowering time-point were from the *Nitrosomonadaceae* family (6.5%), as well as *Sphingomonas* spp. (5.9%) and *Pseudomonas* spp. (5%) genera. Fruit set samples exhibit a distinct abundance of *Streptomyces* spp. (14%) and *Glycomyces* spp. (9%) genera.

The relative abundance of the soil microbiome differed from that of the root samples. Here, at the end of vegetative renewal, KVDS samples showed a high abundance of *Methylobacterium* spp. (30%) and *Pseudomonas* spp. (30%), followed by *Ralstonia* spp. (7.5%), and *Flavobacterium* spp. (4.6%). In asymptomatic samples, *Pseudomonas* spp. was the most abundant genus (21%), followed by *Flavobacterium* spp. (14.4%), *Burkholderia* (6.2%), *Ralstonia* spp. (5.7%), and *Bacillus* spp. (4%). During flowering in the asymptomatic samples, there was a significant increase in the relative abundance of *Ralstonia* spp. (41%), compared to KVDS samples (1.3%). Asymptomatic samples also exhibited a high relative abundance of *Pseudomonas* spp. (13%), and *Bacillus* spp. (5%). The most abundant genus found in KVDS samples was *Pseudomonas* (37.5%), followed by *Bacillus* spp. (4.7%), *Sphingomonas* spp. (3.4%), TRA3-20 (3.2%), and *Flavobacterium* spp. (2.6%).

Ralstonia spp. was the most abundant genus in KVDS samples at the last time point – fruit set - with a percentage of 36.3%, followed by *Streptomyces* spp. and *Pseudomonas* spp. (5.2% and 4% respectively). Furthermore, the microbiome consists of *Sphingomonas* spp. (3.7%), and *Bacillus* spp. (2.7%). Asymptomatic samples exhibited a higher number of abundant genera compared to KVDS samples. The *Ralstonia* genus was the most abundant even in asymptomatic samples, accounting for 20.3%. Additionally, *Bacillus* spp. (10.7%), *Micromonospora* (9%), *Streptomyces* spp. (8.7%), *Pseudomonas* spp. (8.1%), and *Sphingomonas* spp. (2.7%) were also abundant.

The distribution of bacterial members within the different groups (asymptomatic and KVDS) and sample types (roots and soil) was deeply investigated and represented by a Venn diagram (Figure S5). A core of 279 ASVs (48.8% of the total) was reported between soil and root samples in both groups. The root core microbiota consisted of 33 ASVs (5.8%), predominantly represented by *Nitrosomonas*, *Solimonas*, *Clostridium*, *Exiguobacterium*, *Luteimonas*, and *Terrisporobacter*. The KVDS root sample showed a total of 12 unique ASVs (*Actinomyces, Bacteroides, Polyangium, Coprococcus, Xanthobacter, Ciceribacter, Eubacterium, Luedemannella, Agathobacter, Lachnospiraceae*, and two genera belonging to the *Sphingobacteriales* and *Lachonospirlaes* orders). *Halobacillus, Anaerococcus*, and *Caenimonas* were the most representative of the 9 unique ASVs of asymptomatic root samples. *Haemophilus, Mogibacterium, Psuchoroglaciecola, Pirellula, Kytococcus, Acetitomaculum, Aurantimonas, Thermoactinomyces,* and *Fusobacterium* were the most representative genera of soil core microbiota (60; 10.5%). *Friedmanniella, Rhodobacter, Martelella*, and AD3 were found in KVDS soil, but not in the asymptomatic ones.

2.3.5 Functional analysis of bacterial communities

In silico functional analysis of the most significantly abundant bacterial communities was performed with *picrust2* through a KEGG annotation (Figure S2.7). In total, 30 metabolic functions were identified and correlated with ASVs relative abundance values. The results showed that the highest relative abundance of ASVs related to KVDS samples belonged to a family of transcription factors (DtxR) associated with the management of manganese transport, followed by enzymes involved in cysteine and methionine metabolism, specifically (2R)-3-sulfolactate dehydrogenase (NADP+), and methane metabolism, particularly the subunit alpha and beta of malate-CoA ligase. Two families of transporters, the MFS and the ABC families, were identified as the most abundant. These families contain proteins related to the transport of quinolones, galactorates, and drugs.

2.3.6 Soil and roots fungal and oomycete communities

The soil and roots fungal communities were predominantly composed of Ascomycota (69.2%), Basidiomycota (23.8%), and Mucoromycota (5.5%). The most prevalent fungal genera in KVDS samples were identified as *Fusarium, Starmerella, Ilyonectria/Thelonectria*, *Neurospora,* and *Mortierella*, (Figure 5). Notable changes in the fungal community profile occurred during the vegetative season, with the soil compartment exhibiting a higher prevalence of different genera than the root endosphere (Figure 2.5).

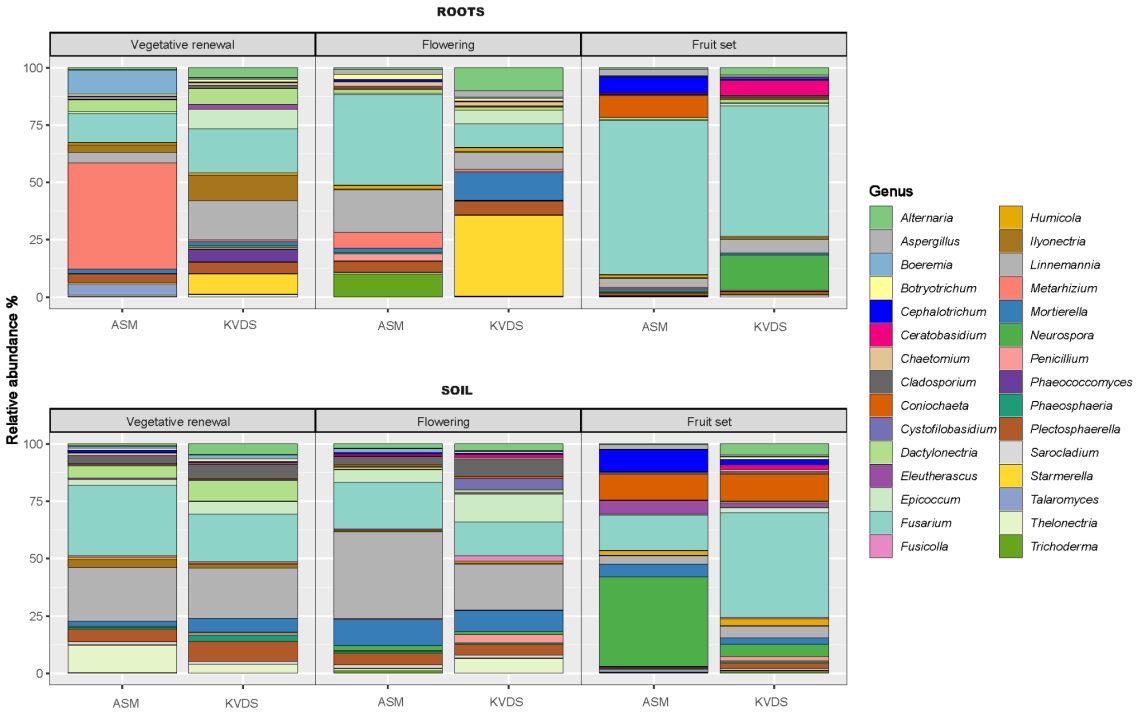

Figure 2.5 - Taxonomy plots showing the relative abundance of top 30 genera of fungal communities in roots and soil of asymptomatic and KVDS samples during the vegetative season

During the vegetative renewal, the most abundant genera in KVDS root samples were *Fusarium* spp. (19.1%), *Linnemannia* spp. (17,2%), *Ilyonectria* spp. (11%), and *Starmerella* spp. (9%), followed by *Epicoccum* spp. (8.5%), *Dactylonectria* spp. (6.7%), *Plectosphaerella* spp. (5%) and *Alternaria* spp. (4.2%). *Starmerella* was the most prevalent genus in the flowering stage, accounting for 35.3% of the total, followed by *Mortirella* spp. (12.3%), *Fusarium* spp. (10.2%) and *Alternaria* spp. (9%). A remarkable increase of *Fusarium* abundance up to 56.7% was observed

during the fruit set, followed by *Neurospora* (15.4%) and *Ceratobasidum* (6.6%) (Figure 2.5).

In asymptomatic roots, during the first vegetative stage, the most abundant fungal genus was *Metarhizium* spp., accounting for 46.1% followed by *Fusarium* spp. (12.5%), *Boeremia* spp. (10.6%), and Dactylonectria spp. (5.1%). During the flowering stage, the most abundant genus was *Fusarium* spp. (39.4%), followed by *Linnemannia* spp. (18.5%), *Trichoderma* spp. (10.1%), *Metarhizium* spp. (6.7%), and *Plectosphaerella* spp. (4.7%). As for the KVDS root samples, the population of *Fusarium* spp. showed a notable increase up to 67% in the asymptomatic ones during the fruit set. Moreover, *Coniochaeta* spp. (9.6%) and *Cephalotrichum* spp. (7%) were present at this time point. Both asymptomatic and KVDS soil samples exhibited a comparable composition in the fungal genera, even though the percentages differed between groups and during the vegetative season. *Fusarium* spp. was present at all time points, with a percentage of 45.5% in KVDS samples during the fruit set and 20.2% in asymptomatic samples during flowering. At this time-point the presence of *Linnemannia* spp. was detected and accounted for 37.7% in asymptomatic samples. *Neurospora* was the most abundant in asymptomatic samples during the fruit set (39%), followed by *Coniochaeta* (11%), which was also present in KVDS samples (11.8%).

When looking at the distribution of fungal community members across the various groups (asymptomatic and KVDS) and sample types (roots and soil), a core of 112 ASVs (representing 51.6% of the total) was identified (Figure S2.6). The soil core microbiota was composed of 16 ASVs (7.4% of the total), representing the following fungal genera: *Debaryomyces, Elsinoë, Symmetrospora, Ramicandelaber, Termitomyces, Absidia, Sporocadus, Atractiella, Darksidea, Remersonia, Gongronella, Stagonospora, Entomocorticium,Lepiota, Chlamydocillium, and Botryosphaeria*. Two unique ASVs (*Lobariella* and *Montagnula*) were identified in asymptomatic soil samples, while no unique ASVs were observed in the KVDS samples. A total of 4 ASVs (*Pyricularia, Stachybotrys, Clavulina, and Clonostachys*) were identified in the root microbiota, and no unique ASVs were observed in the KVDS root samples. Conversely, only 3 unique ASVs (*Synnemellisia, Pseudoarthrographis, and Scedosporium*) were detected in the asymptomatic root.

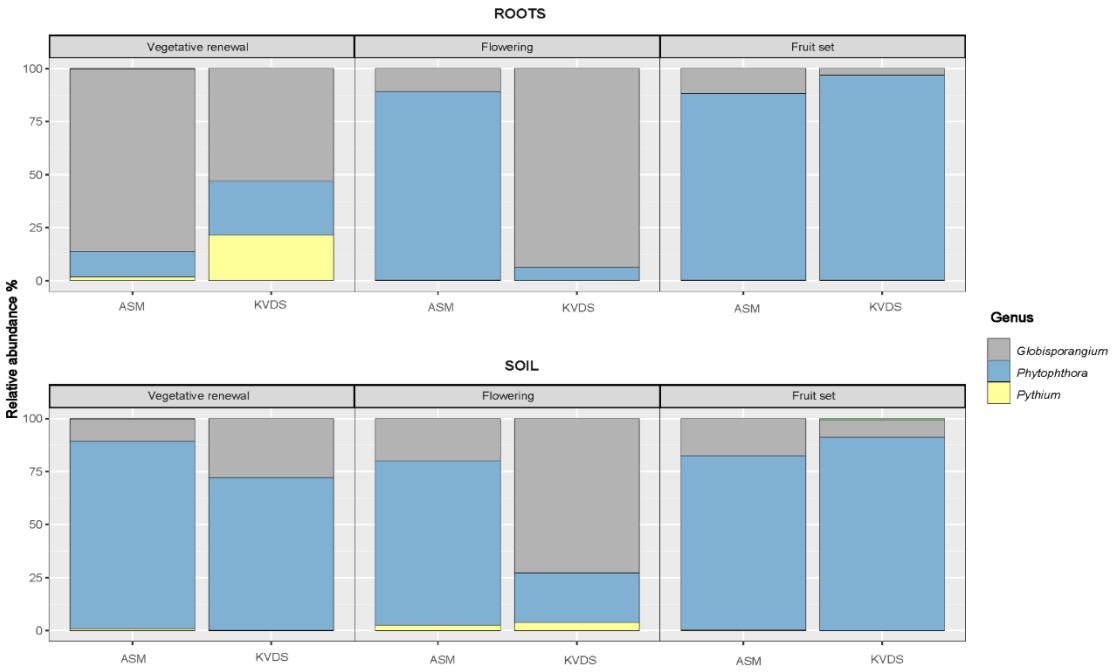

Figure 2.6 - Taxonomy plots showing the relative abundance of oomycetes communities in roots and soil of asymptomatic and KVDS samples during the vegetative season

The oomycete community was represented by three main genera: *Globisporangium*, *Phytophthora* and *Pythium*. During the flowering stage, in KVDS samples, the most abundant genus was *Globisporangium*, showing higher abundance in roots (93.7%) than soil (72.6%). Overall, the abundance of *Phytophthora* was higher in soil samples than in root samples at all time points, in both groups (asymptomatic and KVDS). The highest prevalence was observed in KVDS samples during the fruit set phase, with a percentage of 96.6% in roots and 91.1% in soil, respectively. The genus *Pythium* was present in root samples (ASM, 1.7%; KVDS, 21.4%) during the vegetative renewal phase, as well as in soil samples (ASM, 2.5%; KVDS, 4%) during the flowering phase (Figure 2.6).

2.3.7 *In silico* analysis of the fungal functional groups

The functional potential of the identified fungal taxa was assessed using FunGuild, revealing a predominance of plant pathogens belonging to the *Ascomycota* phylum (Figure S2.8). The largest group of fungal genera, including *Aspergillus*, *Alternaria*, *Epicoccum*, *Fusarium*, *Ilyonectria*, *Cladosporium*, and *Phaeosphaeria*, have been

identified as plant pathogens. Some of these fungal taxa have also been classified as endophytes (*Epicoccum, Ilyonectria, Cladosporium, Neurospora, Trichoderm*a) or wood saprophytes (*Aspergillus, Alternaria, Fusarium*, and *Chaetomium*). *Mortierella* and *Gilbertella* were the two genera of the phylum Zygomycota classified as a saprotroph and plant pathogen, respectively. The Basidiomycota phylum comprises two genera, *Ceratobasidium* and *Cotinarius*, which are classified as ectomycorrhizal.

2.4 Discussion

The increasing focus on microbiological studies in plant pathology emphasizes the crucial role of plant microbiota in sustaining plant health and fitness. In land plants, roots are the primary site for interactions with microbes in the soil, which represents the largest reservoir of microbial diversity known (Reinhold-Hurek et al., 2015). The so-called endorhizosphere is a complex and dynamic environmental niche, recruited and established through several factors that contribute to its structure and composition, such as pH, nutrient availability, and organic matter, chemical molecules (de Luna et al., 2005; Priya et al., 2021; Pantigoso et al., 2022). This recruitment is also influenced by the plant genotype and directly involved in conferring resistance/tolerance to plant diseases (Berendsen et al., 2012; Du et al., 2024). Perturbation of microbial homeostasis leads to dysbiosis and may have a negative impact on plant fitness (Du et al., 2024). Recent insights into the spread and occurrence of KVDS in Italy suggest that microbial dysbiosis may be a significant driver of the disease. However, it is clear that other factors also contribute to the dissemination and progression of the syndrome. Previous research has characterized the microbial communities associated with KVDS, identifying distinct niches, particularly involving fungi and oomycetes, present across all affected regions (Savian et al., 2021; 2022; Mian et al., 2023; Prencipe et al., 2023; Guaschino et al., 2024; Mosca et al., 2024). The role of bacterial communities in the etiology of the syndrome remains unclear, and to date, they have not been definitively linked to the disease in the same way as fungi and oomycetes.

In this study, the bacterial, fungal, and oomycete microbiomes were characterized in plants exhibiting KVDS symptoms, in comparison to asymptomatic plants, across three different stages of the vegetative season. Our findings suggest that the root

microbiome undergoes greater variation throughout the vegetative season than the soil microbiome. This is likely due to the influence of the plant on the rhizosphere environment, which varies according to the physiological stage and health of the plant. It is established that plants play a role in reshaping the microbial communities that inhabit the soil (Santoyo, 2022), and root activities modify microbial activity and the physicochemical properties of the surrounding soil or rhizosphere (Shi et al., 2015).

Overall, *Ralstonia*, *Pseudomonas*, and *Bacillus* were the most prevalent bacterial genera in the core root microbiota. Understanding the dynamics of these bacterial populations throughout the vegetative season is crucial, especially during stages when plants are more vulnerable to syndrome-induced damage.

The *Ralstonia* genus, particularly abundant in KVDS-affected root samples during the vegetative renewal, includes gram-negative bacteria belonging to the Burkholderiaceae family, which currently consists of six species: *R. insidiosa, R. mannitolilytica, R. pickettii, R. pseudosolanacearum, R. solanacearum*, and *R. syzygii*. These bacteria typically colonize diverse environments. *R. pseudosolanacearum, R. solanacearum*, and *R. syzygii* have been identified as plant pathogens (Safni et al. 2014), as forming *Ralstonia solanacearum* Species Complex, or RSSC. Over 310 species of plants belonging to 42 plant families are infected by *Ralstonia* (Genin, 2010; Genin and Denny, 2011; Paudel et al., 2020). *Ralstonia* typically colonises the root xylem tissues and infects the roots of both susceptible and resistant plants through small wounds following a rapid migration to the stem tissues (Wang et al., 2023). Exopolysaccharide, a substance produced by *Ralstonia*, causes blockage in the xylem that leads to the appearance of wilting in plants (Ingel et al., 2021). Bacteria move from plant roots to soil when plants wilt (Wang et al., 2023). To date, no correlation has been established between this genus and kiwifruit diseases. While the potential link between *Ralstonia* and KVDS is intriguing, further investigation is needed to clarify this association, especially considering the limitations in species-level identification using 16S sequencing (Johnson et al., 2019).

The *Pseudomonas* genus, detected in both symptomatic and asymptomatic roots, includes species with a longstanding association with *Actinidia*, like *Pseudomonas*

syringae pv. *syringae*, causal agent of floral bud necrosis (Balestra and Varvaro, 1997), *Pseudomonas virdiflava*, responsible of kiwifruit bacterial blight (Balestra and Varvaro, 1998) and *Pseudomonas syringae* pv. *actinidiae*, the causative agent of the kiwifruit bacterial canker (Balestra et al., 2009; Mazzaglia et al., 2021; Turco et al., 2024). On the other hand, plant-associated *Pseudomonas* species may act as plant growth promoters with a beneficial role, like the nitrogen-fixing species *Pseudomonas stutzeri*, or *Pseudomonas fluorescens* with biocontrol activity (Mehmood et al., 2023).

Known for its plant growth-promoting activity, as well as for antibacterial and antifungal compound production (Saxena et al., 2020; Poveda et al., 2021), the *Bacillus* genus, consistently present in both groups, showed a higher prevalence in asymptomatic roots during flowering and fruit set. This occurrence may be attributed to plant physiology and temperature increase. Indeed, several studies have demonstrated the capacity of certain *Bacillus* species to enhance crop development under conditions of heat stress (Abd El-Daim et al., 2014; Mukhtar et al., 2020).

The relationship between soil bacteria and kiwifruit plants exhibiting decline symptoms was investigated by Manici et al. (2022), demonstrating the impact of orchard age on bacterial communities. Older orchards showed a significant decline in beneficial genera such as *Pseudomonas* and *Bacillus* compared to adult orchards. Overall, the reduced and modified bacterial communities in older orchards may contribute to the diminished soil health and plant growth. Our findings indicate a notable increase in dynamic activity within root bacterial communities during the vegetative season. This could be attributed to the plant's ability to modulate and reshape the microbiome in response to fluctuating climate parameters, such as temperature and humidity, as well as its interaction with fungal communities.

On the other hand, fungal communities exhibited a markedly disparate pattern compared to the bacterial ones, particularly those of the soil, which showed greater dynamism and variability throughout the season.

The fungal genus *Fusarium* was the most prevalent and abundant taxon in all samples, especially in KVDS-affected roots. This genus encompasses several pathogens known to cause root rot diseases across a wide range of plants. *Fusarium*

solani, for instance, is a pathogen that attacks several plant species, including olive, soybean, pea, bean, and certain cucurbits. Infected plants often exhibit various symptoms, including a generalized decline, wilting, and root necrosis (Kurt et al., 2020). The fungus's ability to penetrate cell walls and destroy vacuoles at the root level causes damage to the plant. Another soil-borne pathogen is *Fusarium oxysporum* which causes vascular damage and root rot in more than 120 economically important plant species. Both *F. solani* and *F. oxysporum* have been previously isolated from *Actinidia* roots exhibiting symptoms of KVDS (Savian et al., 2020; D'Ippolito et al., 2022).

The *Ilyonectria* and *Thelonectria* genera were identified in both the soil and root samples from the KVDS and asymptomatic samples. These genera are typically included in the *Cylindrocarpon*-like family, encompassing various fungi that cause disease and result in plant decline (Lawrence et al., 2019). This family has been observed to affect many species, including apple, cherry, grapevine, kiwifruit, peach, and walnut. *Ilyonectria* species were isolated from roots exhibiting symptoms of KVDS (D'Ippolito et al., 2022) and were identified in the roots' endosphere compartment through a metabarcoding approach (Savian et al., 2022).

The oomycetes community was predominantly represented by *Phytophthora* and *Globisporangium*. The genus *Phytophthora* comprises a group of oomycete pathogens that are known to cause severe diseases in a wide range of crops, leading to significant agricultural losses on a global scale. Different *Phytophthora* species represent a significant threat to kiwifruit, causing root and crown rot leading to vine decline and plant collapse (Akilli et al., 2011; Kurbetli and Ozan, 2013; Li et al., 2022). Previous studies have demonstrated a correlation between the presence of *Phytophthora* spp. and KVDS (Donati et al., 2020; Prencipe et al., 2020; Savian et al., 2022). Additionally, *Pythium* spp. and *Phytopythium* spp. have been frequently isolated from affected plants. The second most prevalent genus identified was *Globisporangium*, which includes pathogens known to cause root rot in kiwifruit. In particular, the species *Globisporangium intermedium* was identified as the predominant microorganism isolated from symptomatic kiwifruit plants (Türkkan et al., 2022). Mian et al. (2023) reported the presence of *Globisporangium* spp. in Actinidia genotypes resistant to KVDS, especially in the root endosphere. The

authors noted a high presence of *Pythium* clade F (*Globisporangium intermedium*) counteracted the presence of *Phytophthora* sp., suggesting that it may compete with the recruitment of the latter species, explaining the onset of KVDS symptoms in susceptible genotypes. The involvement of specific oomycete populations in the emergence of KVDS-related symptoms is becoming increasingly evident. In this study, although to a much lesser extent than in other studies, the characterization of the oomycete community corroborates previous findings in areas where KVDS is present.

Overall, a comparative analysis of the microbiome composition in asymptomatic and KVDS-showing plants revealed a state of dysbiosis that occurred during the vegetative season. Specifically, during the peak periods of KVDS symptom development in summer, alterations in microbiota and microbiome network can influence the health status of plants susceptible to pathogen attacks. The identification of known genera previously associated with KVDS further supports the observations made in other studies. Nevertheless, the relationship between bacterial communities and KVDS-related fungal and oomycete communities in establishing conditions of biocontrol, antagonism, and/or promoting the onset of symptoms remains understudied. A more comprehensive examination of microbiome evolution can enhance our understanding of syndrome spread, especially during critical phases. It became increasingly evident that the interaction between soil microorganisms, abiotic stressors, and plants is a pivotal factor in the emergence and progression of the syndrome.

The relationship between KVDS and dysbiosis remains inconclusive, as recent studies have yielded conflicting results. Guaschino et al. (2024) demonstrate that stochastic processes primarily drive the assembly of rhizosphere bacterial, fungal, and oomycete communities, regardless of plant health status. In contrast, Mosca et al. (2024) observed a marginal shift from deterministic to stochastic processes in the assembly of the bacterial root microbiome. However, this shift was not evident in the fungal and oomycete communities. These findings suggest that KVDS may have a limited impact on the diversity and structure of the plant rhizosphere and root microbiomes, indicating that microbial dysbiosis may not be the sole cause of KVDS.

Last but not least, it would be interesting to explore the contribution of soil composition to the KVDS syndrome. Some soils possess a natural ability to prevent the establishment of pathogens or to inhibit their pathogenic activities, referred to as soil suppressiveness (Baker and Cook, 1974). On the other hand, soils that promote disease development are known as conducive soils, as the abiotic and biotic factors are favorable for pathogen infections (Gómez Expósito et al., 2017, Shlatter et al., 2017).

All these considerations emphasize the need for further investigations to understand the influence of soil composition and kiwifruit plant microbiome on KVDS establishment and spread.

2.5 References

Abd El-Daim, I. A., Bejai, S., & Meijer, J. (2014). Improved heat stress tolerance of wheat seedlings by bacterial seed treatment. *Plant and Soil, 379*(1–2), 337–350. https://doi.org/10.1007/s11104-014-2063-3

Akilli, S., Serçe, Ç. U., Katircioğlu, Y. Z., Karakaya, A., & Maden, S. (2011). Involvement of *Phytophthora citrophthora* in kiwifruit decline in Turkey. *Journal of Phytopathology, 159*(7–8), 579–581. https://doi.org/10.1111/j.1439-0434.2011.01798.x

Baker, K., & Cook, R. J. (1974). *Biological control of plant pathogens*. W. H. Freeman and Company.

Balestra, G. M., & Varvaro, L. (1997). *Pseudomonas syringae* pv. *syringae* causal agent of disease on floral buds of *Actinidia deliciosa* (A. Chev) Liang et Ferguson in Italy. *Journal of Phytopathology, 145*, 375–378.

Balestra, G. M., & Varvaro, L. (1998). Seasonal fluctuations in kiwifruit phyllosphere and ice nucleation activity of *Pseudomonas viridiflava*. *Journal of Plant Pathology, 80*(1), 151–156.

Balestra, G. M., Mazzaglia, A., Quattrucci, A., Renzi, M., & Rossetti, A. (2009). Current status of bacterial canker spread on kiwifruit in Italy. *Australasian Plant Disease Notes, 4*, 34–36. https://doi.org/10.1071/DN09014

Bardi, L. (2020). Early kiwifruit decline: A soil-borne disease syndrome or a climate change effect on plant–soil relations? *Frontiers in Agronomy, 2*. https://doi.org/10.3389/fagro.2020.00003

Berendsen, R. L., Pieterse, C. M. J., & Bakker, P. A. H. M. (2012). The rhizosphere microbiome and plant health. *Trends in Plant Science*. https://doi.org/10.1016/j.tplants.2012.04.001

Bokulich, N. A., Subramanian, S., Faith, J. J., Gevers, D., Gordon, J. I., Knight, R., Mills, D. A., & Caporaso, J. G. (2013). Quality-filtering vastly improves diversity estimates from Illumina amplicon sequencing. *Nature Methods, 10*(1), 57–59. https://doi.org/10.1038/nmeth.2276

Bolyen, E., Rideout, J. R., Dillon, M. R., et al. (2019). Reproducible, interactive, scalable, and extensible microbiome data science using QIIME 2. *Nature Biotechnology, 37*, 852–857. https://doi.org/10.1038/s41587-019-0209-9

Burgmann, H., Pesaro, M., Widmer, F., & Zeyer, J. (2001). A strategy for optimizing quality and quantity of DNA extracted from soil. *Journal of Microbiological Methods, 45*(1), 7–20. https://doi.org/10.1016/s0167-7012(01)00213-5

D'Ippolito, I., Mang, S. M., Elshafie, H. S., Camele, I., Scillitani, G., Mastrodonato, M., Sofo, A., Mininni, A. N., & Xylogiannis, E. (2022). Morpho-anatomical and microbiological analysis of kiwifruit roots with KVDS symptoms. *Acta Horticulturae, 1332*, 131–135. https://doi.org/10.17660/ActaHortic.2022.1332.18

Damm, U., Fourie, P. H., & Crous, P. W. (2010). *Coniochaeta* (*Lecythophora*), *Collophora* gen. nov. and *Phaeomoniella* species associated with wood necroses of *Prunus* trees. *Persoonia: Molecular Phylogeny and Evolution of Fungi, 24*, 60–80. https://doi.org/10.3767/003158510X500705

Du, Y., Han, X., & Tsuda, K. (2024). Microbiome-mediated plant disease resistance: Recent advances and future directions. *Journal of General Plant Pathology*. https://doi.org/10.1007/s10327-024-01204-1

de Luna, L. Z., Stubbs, T. L., Kennedy, A. C., & Kremer, R. J. (2005). Deleterious bacteria in the rhizosphere. In R. W. Zobel & S. F. Wright (Eds.), *Roots and soil management: Interactions between roots and the soil* (Chapter 13). https://doi.org/10.2134/agronmonogr48.c13

Dincă, L. C., Grenni, P., Onet, C., & Onet, A. (2022). Fertilization and soil microbial community: A review. *Applied Sciences (Switzerland)*. https://doi.org/10.3390/app12031198

Dixon, P. (2003). VEGAN, a package of R functions for community ecology. *Journal of Vegetation Science, 14*, 927–930. https://doi.org/10.1111/j.1654-1103.2003.tb02228.x

Donati, I., Cellini, A., Sangiorgio, D., Caldera, E., Sorrenti, G., & Spinelli, F. (2020). Pathogens associated with kiwifruit vine decline in Italy. *Agriculture (Switzerland), 10*. https://doi.org/10.3390/agriculture10040119

Douglas, G. M., Maffei, V. J., Zaneveld, J. R., Yurgel, S. N., Brown, J. R., Taylor, C. M., Huttenhower, C., & Langille, M. G. I. (2020). PICRUSt2 for prediction of metagenome functions. *Nature Biotechnology*. https://doi.org/10.1038/s41587-020-0548-6

Ermacora, P., & Saro, S. (2020). La moria del kiwi in Friuli-Venezia Giulia. *Bolletino ERSA*.

Genin, S. (2010). Molecular traits controlling host range and adaptation to plants in *Ralstonia solanacearum*. *New Phytologist, 187*, 920–928. https://doi.org/10.1111/j.1469-8137.2010.03397.x

Genin, S., & Denny, T. P. (2011). Pathogenomics of the *Ralstonia solanacearum* species complex. *Annual Review of Phytopathology, 50*, 67–89. https://doi.org/10.1146/annurev-phyto-081211-173000

Gómez Expósito, R., de Bruijn, I., Postma, J., & Raaijmakers, J. M. (2017). Current insights into the role of rhizosphere bacteria in disease-suppressive soils. *Frontiers in Microbiology*. https://doi.org/10.3389/fmicb.2017.02529

Guaschino, M., Garello, M., Nari, L., Zhimo, Y. V., Droby, S., & Spadaro, D. (2024). Soil, rhizosphere, and root microbiome in kiwifruit vine decline, an emerging multifactorial disease. *Frontiers in Microbiology, 15*. https://doi.org/10.3389/fmicb.2024.1330865

Ingel, B., Caldwell, D., Duong, F., Parkinson, D., McCulloh, K., & Iyer-Pascuzzi, A. S. (2021). Revisiting the source of wilt symptoms: X-ray microcomputed tomography provides direct evidence that *Ralstonia* biomass clogs xylem vessels. *PhytoFrontiers, 2*(1), 41–51. https://doi.org/10.1094/PHYTOFR-06-21-0041-R

ISTAT. (2024). Retrieved from http://dati.istat.it/Index.aspx?QueryId=33705# [Access on October 2024]

Johnson, J. S., Spakowicz, D. J., Hong, B. Y., Petersen, L. M., Demkowicz, P., Chen, L., Leopold, S. R., Hanson, B. M., Agresta, H. O., Gerstein, M., Sodergren, E., & Weinstock, G. M. (2019). Evaluation of 16S rRNA gene sequencing for species and strain-level microbiome analysis. *Nature Communications, 10*(1), 5029. https://doi.org/10.1038/s41467-019-13036-1

Khanghahi, M. Y., Murgese, P., Strafella, S., & Crecchio, C. (2019). Soil biological fertility and bacterial community response to land use intensity: A case study in the Mediterranean area. *Diversity, 11*(11), 211. https://doi.org/10.3390/d11110211

Kurbetli, I., & Ozan, S. (2013). Occurrence of *Phytophthora* root and stem rot of kiwifruit in Turkey. *Journal of Phytopathology, 161*(11–12), 887–889. https://doi.org/10.1111/jph.12145

Kurt, Ş., Uysal, A., Soylu, E. M., Kara, M., & Soylu, S. (2020). Characterization and pathogenicity of *Fusarium solani* associated with dry root rot of citrus in the eastern Mediterranean region of Turkey. *Journal of General Plant Pathology, 86*(4), 326–332. https://doi.org/10.1007/s10327-020-00922-6

Lawrence, D. P., Nouri, M. T., & Trouillas, F. P. (2019). Taxonomy and multi-locus phylogeny of *Cylindrocarpon*-like species associated with diseased roots of grapevine and other fruit and nut crops in California. *Fungal Systematics and Evolution, 4*, 59–75. https://doi.org/10.3114/fuse.2019.04.06

Li, M., Guo, Q., Liang, M., Zhao, Q., Lin, T., Gao, H., Hieno, A., Kageyama, K., Zhang, X., Cui, L., Yan, Y., & Qiang, Y. (2022). Population dynamics, effective soil factors, and LAMP detection systems for *Phytophthora* species associated with kiwifruit diseases in China. *Plant Disease, 106*(3), 846–853. https://doi.org/10.1094/PDIS-04-21-0852-RE

Manici, L. M., Saccà, M. L., Scotti, C., & Caputo, F. (2022). Quantitative reduction of soil bacteria and qualitative microbial changes: Biotic components associated to kiwifruit decline. *Plant and Soil, 478*(1–2), 173–188. https://doi.org/10.1007/s11104-022-05470-w

Mazzaglia, A., Turco, S., Taratufolo, M. C., Tatì, M., Rahi, Y. J., Gallipoli, L., & Balestra, G. M. (2021). Improved MLVA typing reveals a highly articulated structure in *Pseudomonas syringae* pv. *actinidiae* populations. *Physiological and Molecular Plant Pathology, 114*, 101636. https://doi.org/10.1016/j.pmpp.2021.101636

McMurdie, P. J., & Holmes, S. (2013). phyloseq: An R package for reproducible interactive analysis and graphics of microbiome census data. *PLoS ONE, 8*(4), e61217. https://doi.org/10.1371/journal.pone.0061217

Mehmood, N., Saeed, M., Zafarullah, S., Hyder, S., Rizvi, Z. F., Gondal, A. S., Jamil, N., Iqbal, R., Ali, B., Ercisli, S., & Kupe, M. (2023). Multifaceted impacts of plant-beneficial *Pseudomonas* spp. in managing various plant diseases and crop yield improvement. *ACS Omega, 8*(25), 22296–22315. https://doi.org/10.1021/acsomega.3c00870

Mian, G., Cipriani, G., Firrao, G., & Martini, M. (2023). Genetic diversity of *Actinidia* spp. shapes the oomycete pattern associated with Kiwifruit Vine Decline Syndrome (KVDS). *Scientific Reports, 13*(1), 16942. https://doi.org/10.1038/s41598-023-43754-y

Mosca, S., Aci, M. M., Procopio, G., Vadalà, V., Vizzari, G., Francomano, E., Mohamed, N. Z., Li Destri Nicosia, M. G., Agosteo, G. E., Spadaro, D., Schena, L., & Malacrinò, A. (2024). Integrated analyses of the plant and soil microbiome identify *Phytopythium vexans* as agent of the Kiwifruit Vine Decline Syndrome. *Plant and Soil, 486*(1–2), 1–17. https://doi.org/10.1007/s11104-024-06891-5

Mukhtar, T., Rehman, S., Smith, D., Sultan, T., Seleiman, M. F., Alsadon, A. A., Amna, Ali, S., Chaudhary, H. J., Solieman, T. H. I., Ibrahim, A. A., & Saad, M. A. O. (2020). Mitigation of heat stress in *Solanum lycopersicum* L. by ACC-deaminase and exopolysaccharide-producing *Bacillus cereus*: Effects on biochemical profiling. *Sustainability*, 12(6), 2159. https://doi.org/10.3390/su12062159

Pantigoso, H. A., Newberger, D., & Vivanco, J. M. (2022). The rhizosphere microbiome: Plant–microbial interactions for resource acquisition. *Journal of Applied Microbiology*, 133(5), 2864–2876. https://doi.org/10.1111/jam.15686

Paudel, S., Dobhal, S., Alvarez, A. M., & Arif, M. (2020). Taxonomy and phylogenetic research on *Ralstonia solanacearum* species complex: A complex pathogen with extraordinary economic consequences. *Pathogens*, 9(11), 886. https://doi.org/10.3390/pathogens9110886

Poveda, J., & González-Andrés, F. (2021). *Bacillus* as a source of phytohormones for use in agriculture. *Applied Microbiology and Biotechnology*. https://doi.org/10.1007/s00253-021-11492-8

Prencipe, S., Savian, F., Nari, L., Ermacora, P., Spadaro, D., & Martini, M. (2020). First report of *Phytopythium vexans* causing decline syndrome of *Actinidia deliciosa* "Hayward" in Italy. *Plant Disease*. https://doi.org/10.1094/PDIS-10-19-2101-PDN

Prencipe, S., Schiavon, G., Rosati, M., Nari, L., Schena, L., Spadaro, D. (2023). Characterization of *Phytopythium* species involved in the establishment and development of Kiwifruit Vine Decline Syndrome. *Microorganisms*, 11(1), 216. https://doi.org/10.3390/microorganisms11010216

Priya, P., Aneesh, B., & Harikrishnan, K. (2021). Genomics as a potential tool to unravel the rhizosphere microbiome interactions on plant health. *Journal of Microbiological Methods*. https://doi.org/10.1016/j.mimet.2021.106215

Quast, C., Pruesse, E., Yilmaz, P., Gerken, J., Schweer, T., Yarza, P., Peplies, J., Glöckner, F. O. (2013). The SILVA ribosomal RNA gene database project: Improved data processing and web-based tools. *Nucleic Acids Research*, 41, D590–D596. https://doi.org/10.1093/nar/gks1219

Reid, J. B., Tate, K. G., Brown, N. S., & Cheah, L. H. (1991). Effects of flooding and alluvium deposition on kiwifruit (*Actinidia deliciosa*): 1. Early vine decline. *New Zealand Journal of Crop and Horticultural Science*, 19(3), 247–257. https://doi.org/10.1080/01140671.1991.10421808

Reinhold-Hurek, B., Bünger, W., Burbano, C. S., Sabale, M., & Hurek, T. (2015). Roots shaping their microbiome: Global hotspots for microbial activity. *Annual Review of Phytopathology*, 53, 403–424. https://doi.org/10.1146/annurev-phyto-082712-102342

Safni, I., Cleenwerck, I., De Vos, P., Fegan, M., Sly, L., Kappler, U. (2014). Polyphasic taxonomic revision of the *Ralstonia solanacearum* species complex: Proposal to emend the descriptions of *Ralstonia solanacearum* and *Ralstonia syzygii* and reclassify current *R. syzygii* strains as *Ralstonia syzygii* subsp. *syzygii* subsp. nov., *R. solanacearum* phylotype IV strains as *Ralstonia syzygii* subsp. i*ndonesiensis* subsp. nov., banana blood disease bacterium strains as *Ralstonia syzygii* subsp. *celebesensis* subsp. nov., and *R. solanacearum* phylotype I and III strains as *Ralstonia pseudosolanacearum* sp. nov. *International Journal of Systematic and Evolutionary Microbiology*, 64(9), 3087–3103. https://doi.org/10.1099/ijs.0.066712-0

Santoyo, G. (2022). How plants recruit their microbiome? New insights into beneficial interactions. *Journal of Advanced Research*, 40, 45–58. https://doi.org/10.1016/j.jare.2021.11.020

Savian, F., Ginaldi, F., Musetti, R., Sandrin, N., Tarquini, G., Pagliari, L., Firrao, G., Martini, M., & Ermacora, P. (2020). Studies on the aetiology of kiwifruit decline: Interaction between soil-borne pathogens and waterlogging. *Plant and Soil*, 456(1–2), 113–128. https://doi.org/10.1007/s11104-020-04671-5

Savian, F., Marroni, F., Ermacora, P., Firrao, G., & Martini, M. (2022). A metabarcoding approach to investigate fungal and oomycete communities associated with Kiwifruit Vine Decline Syndrome in Italy. *Phytobiomes Journal*, 6, 290–304. https://doi.org/10.1094/PBIOMES-03-22-0019-R

Savian, F., Musetti, R., Sandrin, N., Ermacora, P., & Martini, M. (2019). Etiological studies over Kiwifruit Decline reveal the involvement of both flooding and biotic factors. Proceedings of the Abstracts of Presentations at the XXV Congress of the Italian Phytopathological Society (SIPaV). *Journal of Plant Pathology*, 101(3), 811–848.

Savian, F., Prencipe, S., Filippini, N., Nari, L., Martini, M., Ermacora, P., & Spadaro, D. (2021). Pathogenicity of *Phytopythium chamaehyphon*: A new player in Kiwifruit Vine Decline Syndrome of *Actinidia chinensis* var. *deliciosa* 'Hayward' in Italy. *Plant Disease*. https://doi.org/10.1094/PDIS-01-21-0143-SC

Saxena, A. K., Kumar, M., Chakdar, H., Anuroopa, N., & Bagyaraj, D. J. (2020). *Bacillus* species in soil as a natural resource for plant health and nutrition. *Journal of Applied Microbiology*, 129(2), 375–392. https://doi.org/10.1111/jam.14506

Shi, S., Nuccio, E., Herman, D. J., Rijkers, R., Estera, K., Li, J., da Rocha, U. N., He, Z., Pett-Ridge, J., Brodie, E. L., Zhou, J., & Firestone, M. (2015). Successional trajectories of rhizosphere bacterial communities over consecutive seasons. *MBio*, 6(4), e00746-15. https://doi.org/10.1128/mBio.00746-15

Schlatter, D., Kinkel, L., Thomashow, L., Weller, D., & Paulitz, T. (2017). Disease suppressive soils: New insights from the soil microbiome. *Phytopathology*, 107(11), 1284–1297. https://doi.org/10.1094/PHYTO-07-17-0227-R

Sorrenti, G., Toselli, M., & Spinelli, F. (2016). Implicazioni della gestione idrica nella "Moria del kiwi" del veronese. *Italian Journal of Agronomy*.

Spigaglia, P., Barbanti, F., Marocchi, F., Mastroleo, M., Baretta, M., Ferrante, P., Caboni, E., Lucioli, S., & Scortichini, M. (2020). *Clostridium bifermentans* and *C. subterminale* are associated with Kiwifruit Vine Decline, known as moria, in Italy. *Plant Pathology*, 69(4), 765–774. https://doi.org/10.1111/ppa.13161

Tacconi, G., Paltrinieri, S., Mejia, J. F., Fuentealba, S. P., Bertaccini, A., Tosi, L., Giacopini, A., Mazzucchi, U., Favaron, F., Sella, L., & Bertaiola, F. (2015). Vine decline in kiwifruit: Climate change and effect on waterlogging and *Phytophthora* in North Italy. *Acta Horticulturae*, 1096, 93–97. https://doi.org/10.17660/ActaHortic.2015.1096.7

Tacconi, G., Giacopini, A., & Tosi, L. (2014). La moria del kiwi nel veronese. *Kiwi Informa,* 4–6, 5–23.

Tosi, L., Tacconi, G., & Giacopini, A. (2015). La moria del kiwi, situazione e prospettive. *L'Informatore Agrario*, 44, 67–70.

Turco, S., Brugneti, F., Giubilei, I., Silvestri, C., Petrovic, M., Drais, M. I., Cristofori, V., Speranza, S., Mazzaglia, A., Contarini, M., & Rossini, L. (2024a). A bud's life: Metabarcoding analysis to

characterise hazelnut big buds microbiome biodiversity. *Microbiological Research*, 127851. https://doi.org/10.1016/j.micres.2024.127851

Turco, S., Ferrucci, A., Drais, M. I., & Mazzaglia, A. (2024b). A genome-wide comparative analysis to characterise the phylogenetic relationship and the pathogenicity of *Pseudomonas syringae* pv. *actinidiae* strains. *European Journal of Plant Pathology*, 168, 97–107. https://doi.org/10.1007/s10658-023-02731-x

Türkkan, M., Özer, G., Karaca, G., Erper, I., & Derviş, S. (2022). Characterization and pathogenicity of *Pythium*-like species associated with root and collar rot of kiwifruit in Turkey. *Plant Disease*, 106(3), 854–863. https://doi.org/10.1094/PDIS-05-21-0961-RE

Wang, Z., Luo, W., Cheng, S., Zhang, H., Zong, J., & Zhang, Z. (2023). *Ralstonia solanacearum* – A soil-borne hidden enemy of plants: Research development in management strategies, their action mechanism and challenges. *Frontiers in Plant Science*, 14, 1141902. https://doi.org/10.3389/fpls.2023.1141902

Yang, C., Mai, J., Cao, X., Burberry, A., Cominelli, F., & Zhang, L. (2023). ggpicrust2: An R package for PICRUSt2 predicted functional profile analysis and visualization. *Bioinformatics*, 39(4), 1320–1321. https://doi.org/10.1093/bioinformatics/btad470

Yeates, C., Gillings, M. R., Davison, A. D., Altavilla, N., & Veal, D. A. (1998). Methods for microbial DNA extraction from soil for PCR amplification. *Biological Procedures Online*, 1, 40–47. https://doi.org/10.1251/bpo6

Zhou, J., Bruns, M. A., & Tiedje, J. M. (1996). DNA recovery from soils of diverse composition. *Applied and Environmental Microbiology*, 62(2), 316–322. https://doi.org/10.1128/aem.62.2.316-322.1996

2.6 Supplementary material

Figure S2.1 - Sampling site. Area A (red) is characterized by a higher prevalence of KVDS-affected plants and Area B (green) where the majority of the plants exhibit no symptoms on the canopy related to KVDS. Each dot (blue, purple and yellow) represents a group of plants (3 plants/group) asymptomatic (ASM), and symptomatic (KVDS)

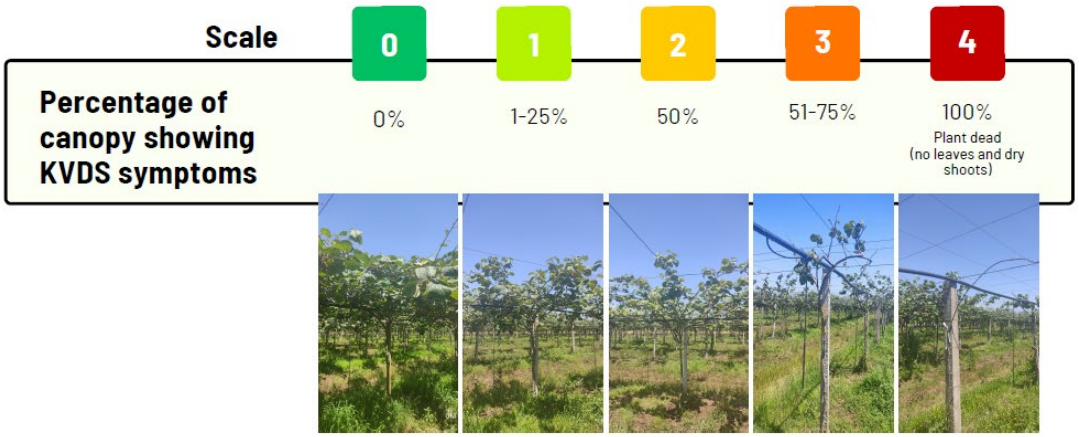

Figure S2.2 - Symptomatology scale based on percentage of canopy showing symptoms related to KVDS. Class 2 and 3 plants were selected for this study.

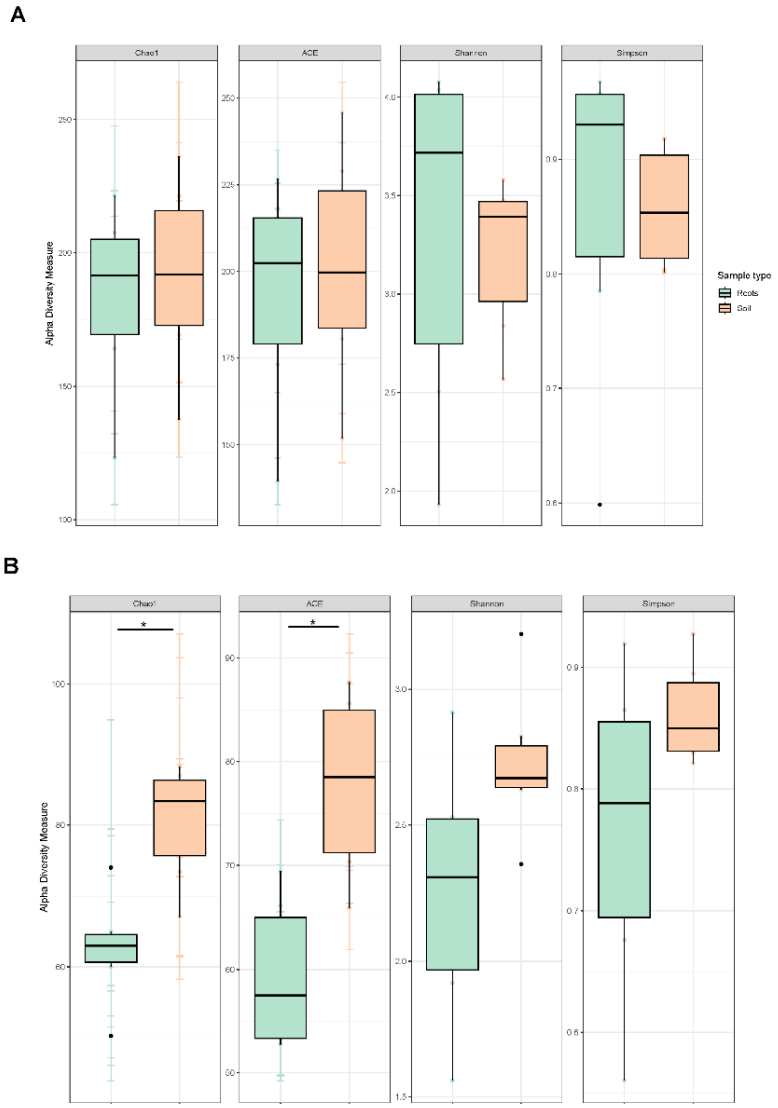

Figure S2.3 - Alpha-diversity of bacterial (A) and fungal (B) communities in roots (green) and soil (pink). Alpha diversity metrics summarize the structure of microbial community with respect to its richness (Chao1 and ACE indexes), and within-sample diversity expressed by Shannon and Simpson indexes. Significant differences (*p≤0.05*) were observed in the fungal community across Chao1 and ACE indexes.

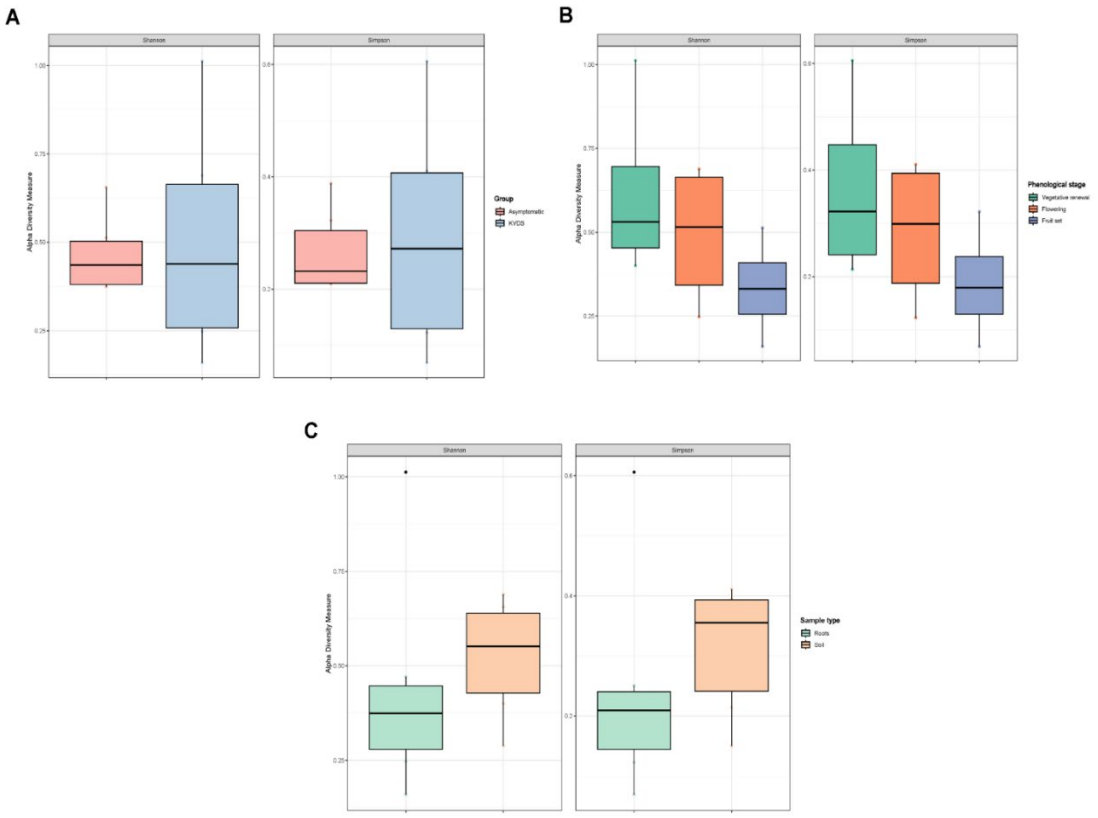

Figure S2.4 - Alpha-diversity of oomycetes communities in asymptomatic (pink) and KVDS (purple) samples (panel A), during the vegetative season: vegetative renewal (green), flowering (orange) (panel B), and fruit set (purple)in roots (green) and soil (pink) (panel C). Alpha diversity metrics summarize the structure of microbial community within-sample diversity expressed by Shannon and Simpson indexes.

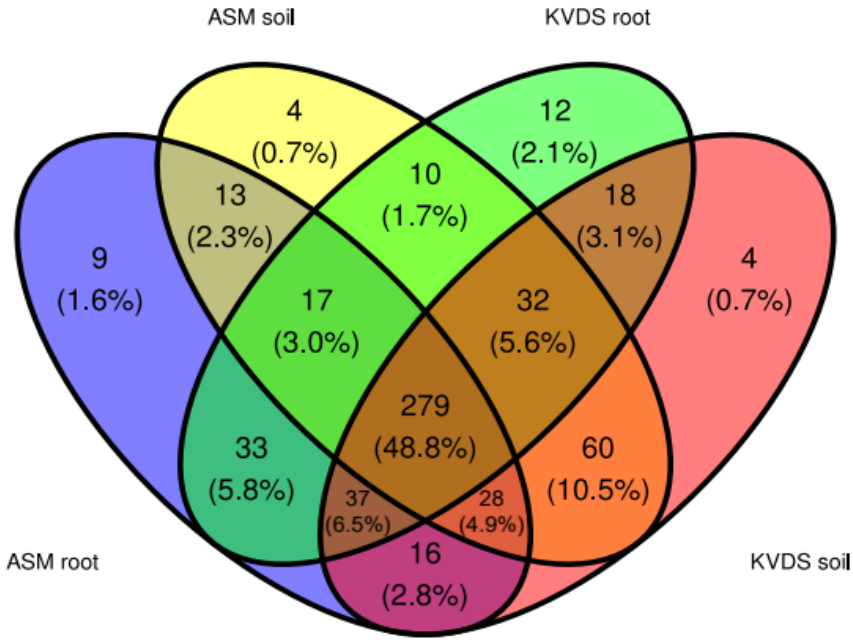

Figure S2.5 - Venn diagram depicting unique and shared bacterial ASVs among asymptomatic and KVDS roots and soil samples

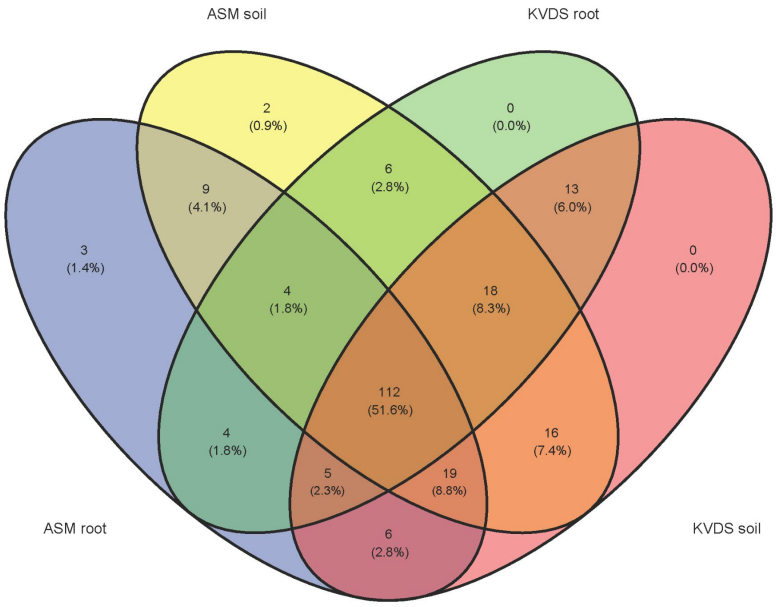

Figure S2.6 - Venn diagram depicting unique and shared fungal ASVs among asymptomatic and KVDS roots and soil samples

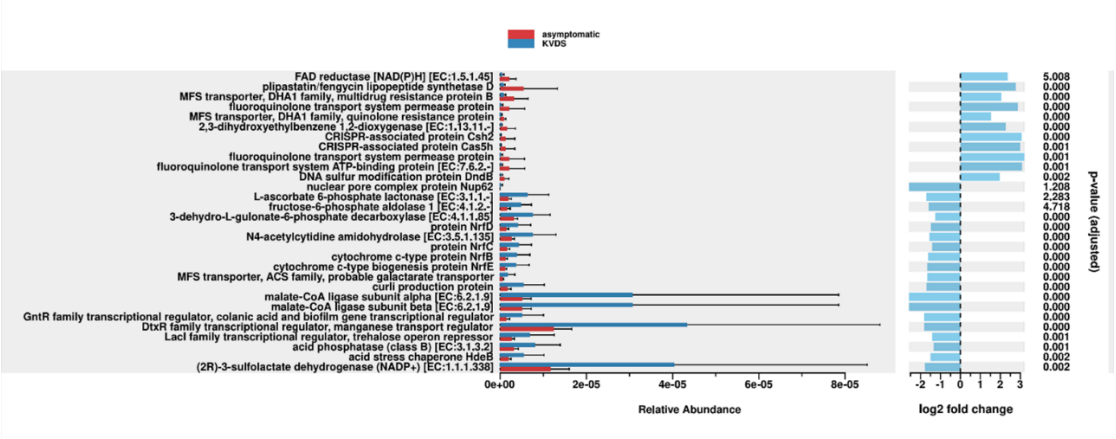

Figure S2.7 - Predicted differential KEGG pathways in asymptomatic and KVDS samples. The extended error barplot shows the predicted differential KEGG pathways using PICRUSt2 analysis. The barplot on the left shows the relative abundance of the KEGG pathway, while the bars on the right show the log2fold change in ASVs relative abundance between the two groups (effect size).

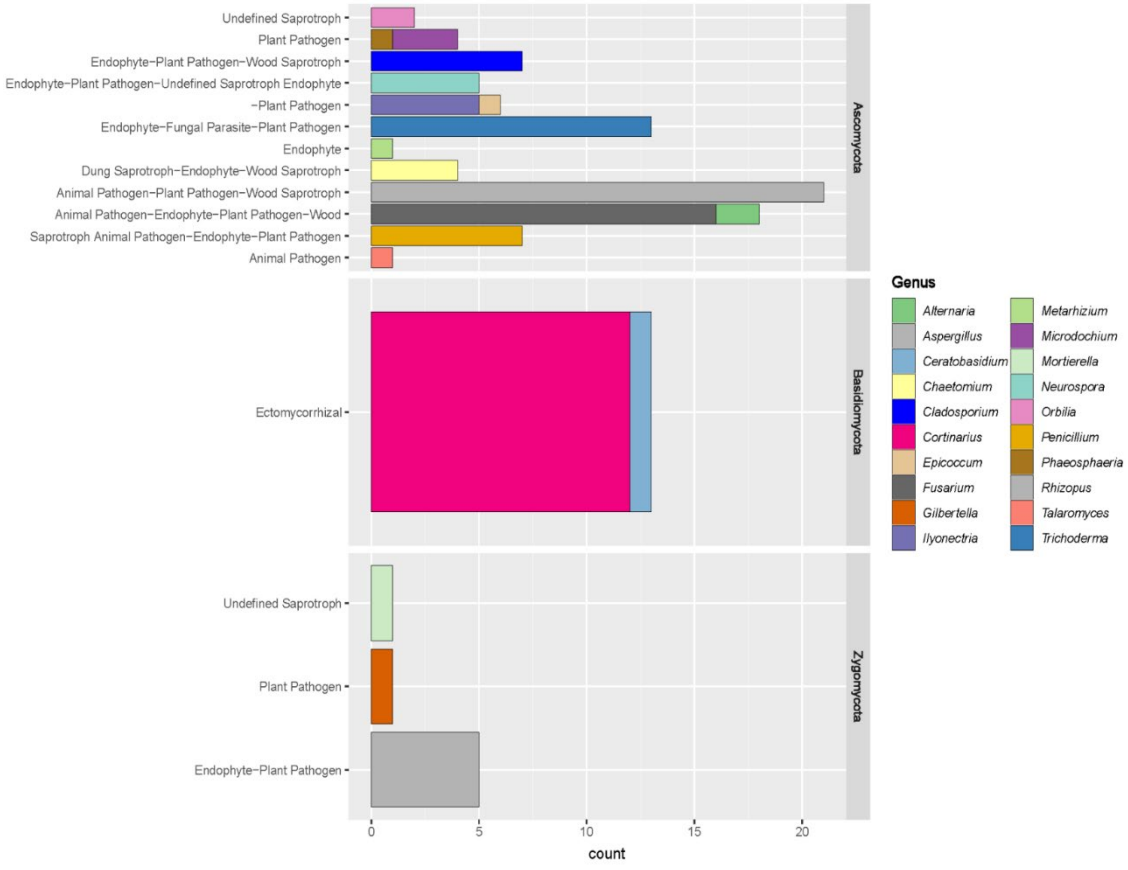

Figure S2.8 - FUNGuild analysis of fungal functional groups and a count of each fungal genera and their functional classification

Table S2.1 - Physical and chemical soil analysis

Parameter	***Value (%)***	***Parameter***	***Value***
Sand	39	*pH*	7.3 (neutral)
Silt	15	*Electrical conductivity*	0.233 mS/cm
Clay	46	*Limestone*	trace elements
Texture	Clay	*Organic matter*	1.66 % (low)

Table S2.2 - Average of quality metrics and percentage of reads

ITS

Group	Sample type	Time point	Input	Filtered	% of input passed filter	Denoised	Non-chimeric	% of input non-chimeric	ASVs
Asymptomatic	Roots	Flowering	246.517	245.114	99,43	243999	231020	93,71	672
Asymptomatic	Roots	Fruit set	357.209	353.390	98,93	351761	343372	96,13	859
Asymptomatic	Roots	Vegetative renewal	298.082	291.862	97,91	290493	288536	96,8	692
Asymptomatic	Soil	Flowering	378.822	374.152	98,77	372398	364807	96,3	1.178
Asymptomatic	Soil	Fruit set	253.450	251.980	99,42	250617	246369	97,21	802
Asymptomatic	Soil	Vegetative renewal	115.445	114.553	99,23	113386	107782	93,36	848
KVDS	Roots	Flowering	185.959	180.682	97,16	179962	178314	95,89	559
KVDS	Roots	Fruit set	377.582	370.576	98,14	369025	362517	96,01	859
KVDS	Roots	Vegetative renewal	352.421	345.728	98,1	344594	341851	97	656
KVDS	Soil	Flowering	361.988	356.290	98,43	354624	347457	95,99	963
KVDS	Soil	Fruit set	298.808	296.374	99,19	294803	287026	96,06	884
KVDS	Soil	Vegetative renewal	371.265	368.528	99,26	366452	355434	95,74	1.171

16S

Group	Sample type	Time point	Input	Filtered	% of input passed filter	Denoised	Non-chimeric	% of input non-chimeric	ASVs
Asymptomatic	Roots	Flowering	101.863	97.346	95,57	89945	87073	85,48	2.568
Asymptomatic	Roots	Fruit set	197.400	189.221	95,86	182153	159604	80,85	2.156
Asymptomatic	Roots	Vegetative renewal	167.496	160.190	95,64	149530	144355	86,18	3.337
Asymptomatic	Soil	Flowering	241.990	229.253	94,74	225663	217999	90,09	2.290
Asymptomatic	Soil	Fruit set	221.492	211.291	95,39	209503	202125	91,26	1.790
Asymptomatic	Soil	Vegetative renewal	163.210	156.412	95,83	152563	145375	89,07	2.858
KVDS	Roots	Flowering	195.326	186.297	95,38	176382	166761	85,38	3.518
KVDS	Roots	Fruit set	161.491	154.783	95,85	145266	130092	80,56	2.909
KVDS	Roots	Vegetative renewal	261.725	251.416	96,06	244781	240173	91,77	2.357
KVDS	Soil	Flowering	149.996	142.334	94,89	131301	125317	83,55	3.196
KVDS	Soil	Fruit set	253.338	240.137	94,79	236294	231274	91,29	1.843
KVDS	Soil	Vegetative renewal	320.055	307.971	96,22	304634	293108	91,58	2.525

Table S2.3 - PERMANOVA results of bacterial communities' composition indicating the partitioning of variation and tests for group (asymptomatic and KVDS), sample type (roots and soil) and phenological stage (vegetative renewal, flowering and fruit set)

	Df	*Sum of Sqs*	*R^2*	*F*	*P(>F)*
GROUP	1	0.09999	0.04483	0.6058	0.798
SAMPLE TYPE	1	0.39835	0.17857	2.4135	0.024 *
PHENOLOGICAL STAGE	2	0.57705	0.25868	1.7481	0.047 *
RESIDUAL	7	1.15534	0.51792		

*Signif. codes: 0 '***' 0.001 '**' 0.01 '*' 0.05 '.' 0.1 ' ' 1*

Table S2.4 - PERMANOVA results of fungal communities' composition indicating the partitioning of variation and tests for group (asymptomatic and KVDS), sample type (roots and soil) and phenological stage (vegetative renewal, flowering and fruit set)

	Df	*Sum of Sqs*	*R^2*	*F*	*P(>F)*
GROUP	1	0.14966	0.07840	1.2808	0.188
SAMPLE TYPE	1	0.21638	0.11334	1.8518	0.065
PHENOLOGICAL STAGE	2	0.72506	0.37980	3.1025	0.003 **
RESIDUAL	7	0.8179	0.42846		

*Signif. codes: 0 '***' 0.001 '**' 0.01 '*' 0.05 '.' 0.1 ' ' 1*

Table S2.5 - PERMANOVA results of oomycetes communities' composition indicating the partitioning of variation and tests for group (asymptomatic and KVDS), sample type (roots and soil) and phenological stage (vegetative renewal, flowering and fruit set)

	Df	*Sum of Sqs*	*R^2*	*F*	*P(>F)*
GROUP	1	0.16086	0.10224	1.3341	0.303
SAMPLE TYPE	1	0.12461	0.07920	1.0335	0.366
PHENOLOGICAL STAGE	2	0.44389	0.28212	1.8407	0.222
RESIDUAL	7	0.84405	0.53644		

*Signif. codes: 0 '***' 0.001 '**' 0.01 '*' 0.05 '.' 0.1 ' ' 1*

Chapter 3

Deciphering Kiwifruit Vine Decline Syndrome: insights into microbial communities, gene expression, and hormonal dynamics

Antonella Cardacino[1], Silvia Turco[1], Leandro Pereira-Dias[2,3], Paulo Ricardo Oliveira-Pinto[3], Conceição Santos[3], Giorgio Mariano Balestra[1]

[1] *Department of Agriculture and Forest Sciences, University of Tuscia, Viterbo, Italy*

[2]*Instituto de Conservación y Mejora de la Agrodiversidad Valenciana, Universitat Politècnica de València, Valencia, Spain*

[3]*Department of Biology, Faculty of Sciences, University of Porto, Porto, Portugal*

Abstract

Since its emergence in 2012, Kiwifruit Vine Decline Syndrome (KVDS) has been spreading rapidly across Italian orchards, leading to significant reductions in production and substantial economic losses. By being multifaced disease, involving both abiotic and biotic stressors as causal agents, this syndrome requires a multifactorial approach. Hence, this study aimed to characterize the microbiome associated with the root endosphere, analyze gene expression modulation, and quantify the hormonal response of the vine to enhance the understanding of the plant's fitness and adaptability to KVDS. For these reasons, root samples were collected from symptomatic plants at two key stages of the growing season: the end of flowering (June 2023) and during fruit set (July 2023), together with roots from asymptomatic plants serving as controls. Metagenomic analysis revealed distinct differences in microbial communities (bacteria and fungi) between diseased and asymptomatic samples, confirming the involvement of specific genera previously identified as putative causal agents of KVDS. The relative expression of 17 genes associated with plant immunity responses (ROS detoxification, PR proteins and R proteins synthesis, PRRs, and hormone biosynthesis and signalling) demonstrated significant differences between asymptomatic and KVDS samples at both time points for all examined pathways. Furthermore, to elucidate the hormonal

regulatory networks activated in response to the disease and assess their impact on plant fitness, concentrations of GA3, 6-BA, IAA, SA, ABA, JA, and MeJA were quantified using high-performance liquid chromatography (HPLC). These findings contribute to a more comprehensive understanding of the epidemiology of KVDS and may provide critical insights for effective disease management strategies.

Keywords: microbiome, gene expression, hormonal response, KVDS

3.1 Introduction

Plants, as sessile organisms, have evolved complex defense mechanisms to protect themselves against a wide range of pathogens, including bacteria, fungi, oomycetes, and viruses. These defense responses are tightly regulated at the molecular and physiological levels to ensure effective immunity while minimizing fitness costs. The ability of plants to resist pathogen attacks largely depends on their innate immune system, which consists of two major layers: pattern-triggered immunity (PTI) and effector-triggered immunity (ETI) (Boutrot and Zipfel, 2017). PTI is activated when pattern recognition receptors (PRRs) detect conserved pathogen-associated molecular patterns (PAMPs), such as bacterial flagellin or fungal chitin, leading to a cascade of signalling events, including calcium ion fluxes, production of reactive oxygen species (ROS), and activation of mitogen-activated protein kinase (MAPK) pathways. This ultimately results in the transcriptional reprogramming of defense-related genes and reinforcement of cell walls to prevent further pathogen invasion (Bigeard et al., 2015). However, some pathogens deploy effector proteins to suppress PTI and facilitate infection. In response, plants have evolved intracellular nucleotide-binding leucine-rich repeat (NLR) receptors that recognize these effectors, either directly or indirectly, leading to a more robust immune response known as ETI. This second layer of immunity often triggers localized cell death, known as the hypersensitive response (HR), which limits pathogen spread (Wang et al., 2019). ETI is also associated with systemic acquired resistance (SAR), a long-lasting immune response that protects the plant against future infections (Shah et al., 2014). Emerging studies highlight that PTI and ETI function as a continuum rather than independent layers, with extensive crosstalk between their signalling components (Ngou et al., 2022). Understanding plant responses and defence mechanisms against complex diseases is crucial for developing mitigation and control strategies. To unravel the complexity of plant-pathogen interactions, researchers are increasingly adopting multi-omics approaches. The integrated analysis of genomics, transcriptomics, proteomics, and metabolomics provides a holistic view of plant-pathogen interactions, revealing molecular responses across multiple levels. This integrative approach is indispensable for elucidating complex diseases driven by the interplay of multiple environmental and biological stressors.

One of the critical plant diseases affecting kiwifruit (*Actinidia* spp.) is Kiwifruit Vine Decline Syndrome (KVDS), an emerging threat that has been particularly devastating in Italy during the last decade. KVDS is characterised by a progressive decline in plant health with symptoms including leaf wilting, canopy collapse and extensive root necrosis, often leading to plant death (Savian et al., 2022). The aetiology of KVDS is complex and involves both abiotic and biotic factors. Studies have identified soil compaction, poor drainage and excessive irrigation as predisposing factors that create a suitable environment for soil-borne pathogens (Tosi et al., 2015; Sorrenti et al., 2016). In addition, shifts in the soil microbiome have been observed in orchards affected by KVDS, with an increase in pathogenic fungal communities and a decrease in beneficial microorganisms that support plant health (Savian et al., 2022; Guaschino et al., 2024; Cardacino et al., 2025).

Nevertheless, the study of plant adaptation and response to the syndrome remains an understudied concept. Given the complex etiology of KVDS, this study employed a metagenomic approach to characterize and compare the root endosphere microbiome of KVDS-infected and asymptomatic plants. This method enables a comprehensive analysis of microbial community composition and structure, providing key insights into the potential roles of various microorganisms in both disease progression and plant health. Furthermore, to investigate the plant's response to the disease at a molecular level, a gene expression analysis of 17 key genes directly involved in the plant's immune response was conducted. This targeted approach focused on genes critical to plant defense pathways, offering deeper insights into the specific immune responses that are activated or suppressed during disease progression. In addition to gene expression analysis, the study included a quantification of key plant hormones, particularly those involved in defense signalling pathways. This hormonal profiling aimed to assess their dynamics during the critical phases when KVDS symptoms are most pronounced, providing insights into the hormonal regulation of the plant’s response to the disease. By integrating microbiome analysis, immune gene expression, and hormone quantification, this study offers a comprehensive approach to unravelling the complex interactions between the kiwifruit plant, its associated microbial community, and KVDS progression.

3.2 Materials and methods

3.2.1 Experimental field

Root samples were collected from *Actinidia chinensis* var. *deliciosa* "BO-ERICA®" plants cultivated in an orchard located in Cisterna di Latina (Lazio Region, Central Italy, 41°33'34.0344''N, 12°47'32.7948''E). Since 2020, the orchard has been subject to monitoring, during which two distinct areas have been identified: area A, characterised by a prevalence of KVDS-affected plants, and area B which is predominantly made up of asymptomatic plants that exhibit no symptoms on the canopy and roots that can be attributed to KVDS (Figure S3.1).

3.2.2 Roots sampling, DNA and RNA isolation, cDNA synthesis

Eighteen plants were selected during the spring of 2023. The sample population consisted of nine asymptomatic plants and nine plants exhibiting symptoms of KVDS. Root samples (~500 g) were collected from each plant at two distinct developmental stages: the end of flowering (June) and the end of the fruit set (July). Immediately following collection, samples were stored on ice. Root samples were prepared for downstream analyses following the protocol described by Simmons et al. (2018). Briefly, roots were initially washed with sterile distilled water, followed by a phosphate buffer solution containing 6.75 g KH_2PO_4, 8.75 g K_2HPO_4, and 1 mL Triton X-100 per liter. To separate the rhizosphere soil from the root tissue, samples were sonicated in an ultrasonic bath for 10 minutes, applying 160 W pulses for 30 seconds, alternating with 30-second intervals. Subsequently, the samples were transferred to a chilled (4°C) sterile 50 mL tubes. To remove residual rhizosphere soil, roots were washed with 20 mL of chilled (4°C) sterile water and vigorously shaken. The wash water was discarded, and the cleaned roots were flash frozen in liquid nitrogen and stored at -80°C. Prior to nucleic acid extraction, root samples were ground to a fine powder using a mortar and pestle and lyophilized for 36 hours.

For total gDNA extraction, 1 mL of CTAB extraction buffer [2% CTAB, 100 mM Tris-HCl (pH 8.0), 20 mM EDTA, 1.4 M NaCl, 1% PVP-40] was added to 200 mg of lyophilized tissue and incubated at room temperature for 20 minutes. Subsequently, 500 µL of chloroform:isoamyl alcohol (24:1) was added, followed by centrifugation

at 12,000 rpm for 10 minutes at 4°C. The aqueous phase was transferred to a new clean tube, and an additional chloroform-based extraction was performed as described above. A solution of 10% CTAB and 0.7 M NaCl, preheated to 65°C, was added to the aqueous phase. Subsequently, 500 µL of chloroform:isoamyl alcohol (24:1) was added, followed by vigorous vortexing and centrifugation. Total DNA was precipitated by adding cold isopropanol and 3M sodium acetate. After gentle inversion and centrifugation at 12,000 rpm for 10 minutes at 4°C, the DNA pellet was washed twice with cold 70% ethanol and dried in a speed vacuum for 10 minutes. The DNA was eluted in 50 µL of TE buffer and incubated at room temperature for 20 minutes. DNA concentration was determined with Qubit™ fluorometer 1.01 (Invitrogen, United States) using the Qubit™ dsDNA BR Assay Kit (Thermo Fisher Scientific, United States).

RNA was extracted from 50 mg of lyophilized tissue using the Plant Tissue RNA Purification Protocol provided by the GeneMATRIX Universal RNA Purification Kit (EURx Ltd, Poland). The extracted RNA was resuspended in RNase-free water, immediately placed on ice, and quantified using µDrop™ plate (Thermo Fisher Scientific, MA, USA). The synthesis of the cDNA was performed using 250 ng of RNA following the instructions provided by NZY First-Strand cDNA Synthesis Kit (NZYTech, Portugal) adding DNase I to remove gDNA contamination in a final volume of 25 µL.

3.2.3 Amplification of 16S and ITS sequencing

Amplification, library preparation and Illumina NovaSeq sequencing were carried out by Novogene (Cambridge, UK). Briefly, all PCR reactions were carried out with 15 µL of Phusion® High - Fidelity PCR Master Mix (New England Biolabs), 0.2 µM of forward and reverse primers, and 10 ng of template DNA. Thermal cycling consisted of initial denaturation at 98 °C for 1 min, followed by 30 cycles of denaturation at 98°C for 10 s, annealing at 50°C for 30 s, and elongation at 72°C for 30 s and 72°C for 5 min. The list of primers used is shown in Table 3.1. Sequencing libraries were generated, and indexes were added. The library was checked with Qubit™ dsDNA BR Assay Kit (Thermo Fisher Scientific, MA, United States) and real-time PCR for quantification and Bioanalyzer (Agilent, USA) for size distribution detection.

Quantified libraries were pooled and sequenced on Illumina NovaSeq 6000 platform, according to effective library concentration and data amount required.

Table 3.1 - List of primers used for Illumina sequencing

Types	Amplified region	Primers	Sequences (5'- 3')
Bacterial 16S	**V3-V4**	341F	CCTAYGGGRBGCASCAG
		806R	GGACTACNNGGGTATCTAAT
Fungal ITS	**ITS1**	ITS5-1737F	GGAAGTAAAAGTCGTAACAAGG
		ITS2-2043R	GCTGCGTTCTTCATCGATGC

3.2.4 Bioinformatic analysis

The microbiome characterization followed the Quantitative Insight into Microbial Ecology 2 (QIIME2, v.2023.2.0; Bolyen et al., 2019) pipeline, with adjustments described in Turco et al. (2024) and in Cardacino et al. (2025). Raw merged reads (R1 and R2) were demultiplexed, chimeras removed, and denoised using DADA2 (Divisive Amplicon Denoising Algorithm) to generate a feature table containing Amplicon Sequence Variants (ASVs) and representative sequences in FASTA format. Fungal ASVs were taxonomically classified using the *classify-consensus-blast* algorithm against an *in-house* database constructed with the rescript QIIME2 plugin. This database included *Actinidia chinensis* sequences (taxID 3625) and the NCBI Fungi RefSeq ITS project (PRJNA177353). Bacterial ASVs were classified using *classify-consensus-blast* against the SILVA 138 database (Quast et al., 2013). A phylogenetic tree was constructed for bacterial representative sequences using MAFFT and FastTree implemented within QIIME2. After filtering out host-related sequences (chloroplast, mitochondria), uncharacterized or uncultured sequences, and low-frequency ASVs (following Bokulich et al., 2013), the four key files (feature table, taxonomy, representative sequences, and phylogenetic tree) were imported into R (v.4.2.3) and processed using *phyloseq* package (v1.42.0; McMurdie & Holmes, 2013). Rarefaction curves were generated using the *vegan* package (v.2.6; Dixon, 2003). Alpha diversity (within-sample diversity) was assessed using Shannon and Simpson indices, while richness was evaluated using Chao1 and ACE indices. Kruskal-Wallis tests were applied to identify significant differences in alpha

diversity among factors. Beta diversity (dissimilarity between samples) was evaluated using Non-metric Multidimensional Scaling (NMDS) and Principal Coordinate Analysis (PCoA) plots based on the Bray-Curtis dissimilarity index. PERMANOVA (permutational multivariate analysis of variance; 1,000 permutations) was employed for statistical testing of beta diversity. The relative abundance of the 20 most abundant genera was visualized, with remaining taxa grouped as "<1%."

3.2.5 Gene expression analysis: selection of candidate genes and RT-qPCR settings

The list of the target genes selected for gene expression analysis are reported in Table S3.1 together with their respective biological functions, and the primer pairs employed for RT-qPCR analysis. For the primer pairs designed in this study, *in silico* sequence similarity searches were performed using BLASTN (National Center for Biotechnology Information, NCBI; [https://blast.nlm.nih.gov/]) against known sequences retrieved from Gramene (accessed November 2023; [https://www.gramene.org/]). Specific primers for qRT-PCR were designed within exonic regions using Primer3 (ELIXIR - European research infrastructure for biological information; [https://primer3.ut.ee/]). The optimal annealing temperature for each primer pair was determined by gradient PCR. The relative expression levels of these genes were determined using the $2^{-\Delta\Delta Cq}$ method (Schmittgen and Livak, 2008). This calculation was based on Cq values obtained from three technical replicates within four independent biological replicates for each experimental group (asymptomatic and KVDS). *AcACT*, *AcGADPH*, and *Ac18S* served as reference genes and asymptomatic group was used to normalize the relative expression levels. qRT-PCR analysis was performed using the CFX 96 Real-TimePCR Detection System device (Bio-Rad Hercules, CA, USA). The reaction was prepared in a final volume of 10 µl containing the following concentrations: 5 µl of NZYSupreme qPCR Green Master Mix (2x), (NZYtech, Portugal), 0.8 µM of each primer and 1 µl of cDNA. The qRT-PCR program had the following conditions: 95°C for 3 min, followed by 39 cycles at 95°C for 10 sec and 56-60°C for 30 sec. A melting curve was generated over the range 75–95°C, with 0.5°C increments at 5 s/step.

3.2.6 Hormones extraction and quantification

Phytohormones, including abscisic acid (ABA), 6-Benzylaminopurine (BAP), gibberellic acid 3 (GA3), indole-acetic-acid (IAA), jasmonic acid (JA), methyl-jasmonate (MeJA), and salicylic acid (SA), were extracted following the method of Van Meulebroek et al. (2012) with modifications described by Oliveira-Pinto et al. (2022) and Oliveira-Fernandes et al. (2023). Briefly, 150 mg of lyophilized root tissue were homogenized with 1 mL of cold (−20°C) extraction buffer (75% methanol, 20% formic acid, 5% Milli-Q water) using a Bead Mill 24 homogenizer (Fisher Scientific, Hampton, NH, USA) with 3 × 2.8 mm ceramic beads for 10 s at 6 m/s, with 2 min pauses on ice between cycles. The homogenate was incubated at −20°C for 12 h, centrifuged at 14,000 × g for 5 min at 4°C, and the supernatant was stored at −80°C. Prior to HPLC injection, the supernatant was concentrated using a 30 kDa Amicon® Ultra centrifugal filter unit at 14,000 × g for 20 min at 4°C, followed by filtration through a 0.22 µm nylon filter (Branchia, Barcelona, Spain). Chromatographic separation was performed using an HPLC Shimadzu LC-20AD system equipped with an SPD-M20A Prominence Diode Array Detector (DAD), a DGU-20A5R Degassing Unit, and a Rheodyne 7725 six-port external sample injector. A Luna Omega Polar C18 column (250 × 4.6 mm, 5 µm) with a guard column was used as the stationary phase. The mobile phase consisted of 0.1% formic acid in Milli-Q water (solvent A) and 0.1% formic acid in methanol (solvent B). A gradient elution was employed, starting with 0% B for 15 min, increasing to 100% B in 0.01 min, and holding at 100% B for 15.01-37.0 min. The initial conditions were restored in 0.01 min and maintained for 13 min, with a total run time of 50 min. A 20 µL sample was injected at a flow rate of 1.0 mL/min. The column temperature was maintained at room temperature. Peak detection, identification, and quantification were performed using i-PeakFinder™ software integrated with LabSolutions software version 5.60 SP2 (Shimadzu Corporation). Phytohormones were detected at their respective maximum absorption wavelengths: GA3 at 206 nm, IAA at 217 nm, SA at 235 nm, JA and MeJA at 198 nm, ABA at 261 nm, and BAP at 271 nm. Concentrations (mg/g fresh mass) were determined for each group (asymptomatic and KVDS), hormone, and time point.

3.2.7 Phenolic compounds extraction and quantification

Total polyphenol content (TPC) was determined using a modified Folin-Ciocalteu method (Rouphael et al., 2017) and the extraction was performed following a protocol by Lupo et al. (2025). Briefly, 1 g of lyophilized root tissue was extracted with 30 mL of 80% ethanol (pH 2.0, adjusted with HCl) for 2 hours at room temperature on a rotary shaker. After centrifugation at 3,000 × g for 15 minutes, the supernatant was stored at -20°C. For TPC analysis, 200 µL of the ethanolic extract was mixed with 1 mL of diluted Folin-Ciocalteu reagent (1:5) and incubated for 5 minutes at room temperature. Subsequently, 800 µL of 7.5% Na_2CO_3 was added, and the mixture was incubated for 1 hour. The absorbance was measured at 765 nm using the Multiskan™ GO Microplate Spectrophotometer (Thermo Fisher Scientific, MA, USA). TPC was quantified using a gallic acid standard curve and expressed as µg gallic acid equivalents per gram of fresh weight.

3.2.8 Statistical analysis and data visualization

One-way ANOVA was used to analyze the data. Significant differences were determined using Tukey's HSD test at the 0.99 confidence level. All statistical analyses were performed using DSAASTAT v1.022. Data visualization was performed using GraphPad Prism v10.2.0.392 and RStudio v.4.2.3.

3.3 Results

3.3.1 Illumina sequencing and data summary

High-throughput sequencing of the 16S rRNA gene and the Internal Transcribed Spacer (ITS) region was performed using the Illumina platform in paired-end mode. Following sequencing, raw reads were processed using the DADA2 pipeline within the QIIME2 environment. Quality filtering involved the removal of low-quality bases, chimeric sequences, and erroneous reads. After trimming and denoising, a total of 2.693.274 high-quality reads were retained for the 16S dataset and 1.648.223 reads for the ITS dataset (Table S3.2). After filtering out reads classified as host-derived, uncultured, and unassigned to any Amplicon Sequence Variant

(ASV), 2556 bacterial and 678 fungal taxa were imported into the R environment as a *phyloseq* object for further analysis.

3.3.2 Microbial communities' of root endosphere

For the bacteriome, the Shannon index revealed significantly higher microbial richness in asymptomatic samples compared to KVDS-affected samples ($p<0.05$) (Figure S3.2, panel A). Conversely, fungal communities exhibited greater richness in KVDS samples compared to asymptomatic ones, suggesting a shift in microbial composition associated with disease presence, though without significant differences (Figure S3.2, panel B). The alpha diversity of bacterial and fungal communities showed a great variance between phenological stages (Figure S3.3). Bacterial communities (Figure S3.3, panel A), exhibit higher diversity in most indexes during the flowering stage compared to the fruit set ones. In contrast, fungal communities (Figure S3.3, panel B) exhibited a different trend, with the fruit set stage generally displaying higher diversity than the flowering stage. Bray–Curtis beta-diversity metrics, visualized using NMDS, were employed to assess the impact of disease status (asymptomatic vs. KVDS) and phenological stage (flowering vs. fruit set) on bacterial (Figure 3.1, panel A) and fungal (Figure 3.1, panel B) communities composition. Data indicated distinct clustering between asymptomatic and KVDS samples in both bacterial (Table S3.3) and fungal (Table S3.4) communities ($p\leq0.001$), highlighting a clear microbiome variation associated with disease. Additionally, phenological stage significantly influenced the mycobiome composition ($p\leq0.05$), suggesting dynamic shifts in fungal communities throughout two time-points.

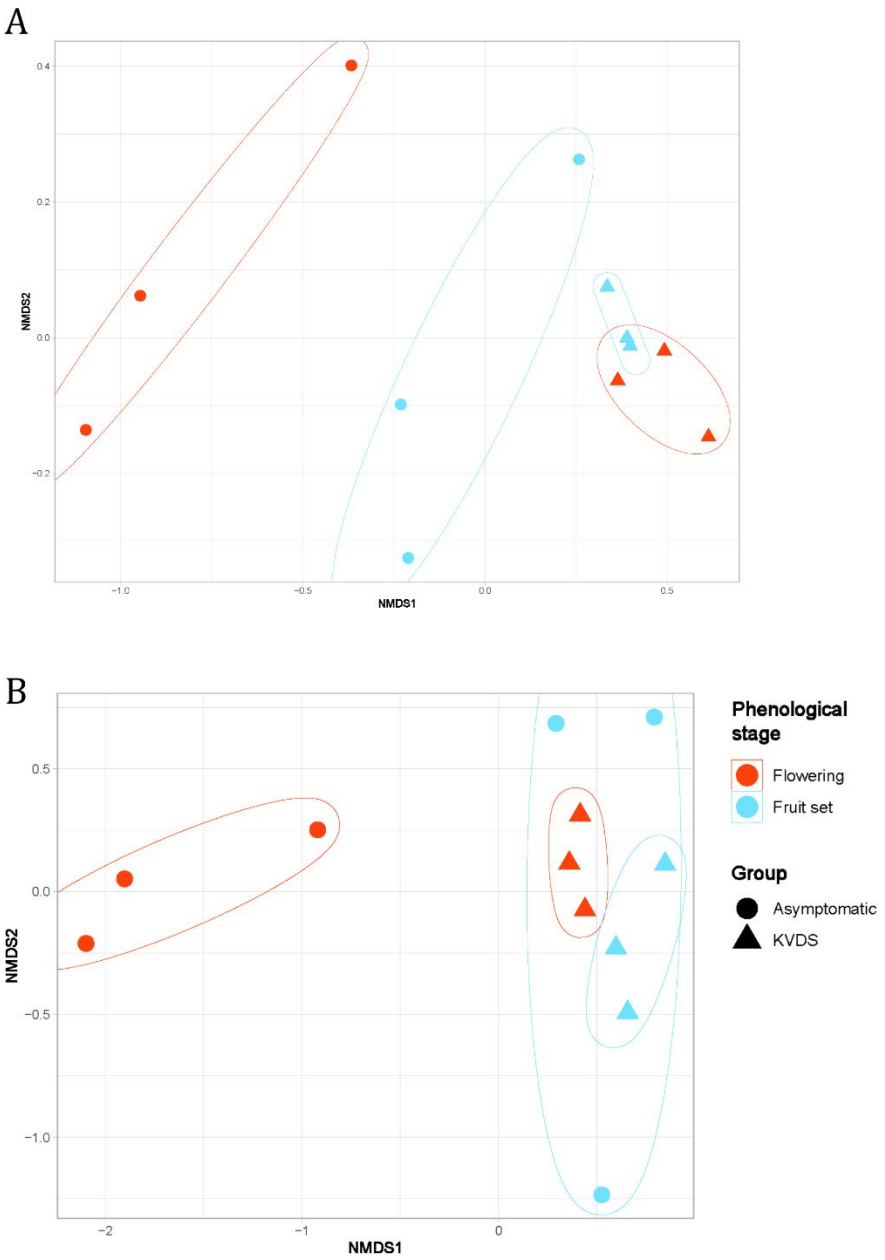

Figure 3.1 - Non-metric Multidimensional Scaling (NMDS) plots based on Bray-Curtis similarity of ASV-based bacterial (A), and fungal (B) communities structure in asymptomatic (circle) and KVDS (triangle) samples during the two time-points (red = flowering, light blue = fruit set).

The bacterial community composition of the root endosphere (Figure 3.2) displayed variation across phenological stages and between KVDS and asymptomatic samples, thereby revealing dynamic shifts in microbial assemblages. During the flowering stage, KVDS samples were dominated by *Bradyrhizobium* (25.8%), followed by *Hyphomicrobium* (12%), *Pelomonas* (9.3%), *Pseudomonas* (7.6%), and *Ralstonia*

(7%). In the fruit set stage, *Bradyrhizobium* remained dominant but exhibited a decline (21.8%), while *Pseudomonas* increased substantially to 19%. *Hyphomicrobium* (10%), *Pelomonas* (8.4%), and *Ralstonia* (5.5%) also persisted, indicating temporal shifts in bacterial prevalence. Conversely, asymptomatic samples displayed a more functionally diverse microbial community. During the flowering stage, *Novosphingobium* and *Allorhizobium/Rhizobium* were the most abundant genera (14% each), followed by *Propionivibrio* (9%) and *Streptomyces* (5.2%). By the fruit set stage, *Pseudomonas* (17.4%) and *Bradyrhizobium* (14.4%) increased in relative abundance, while *Streptomyces* (13.3%) and *Bacillus* (9.7%) became more prominent.

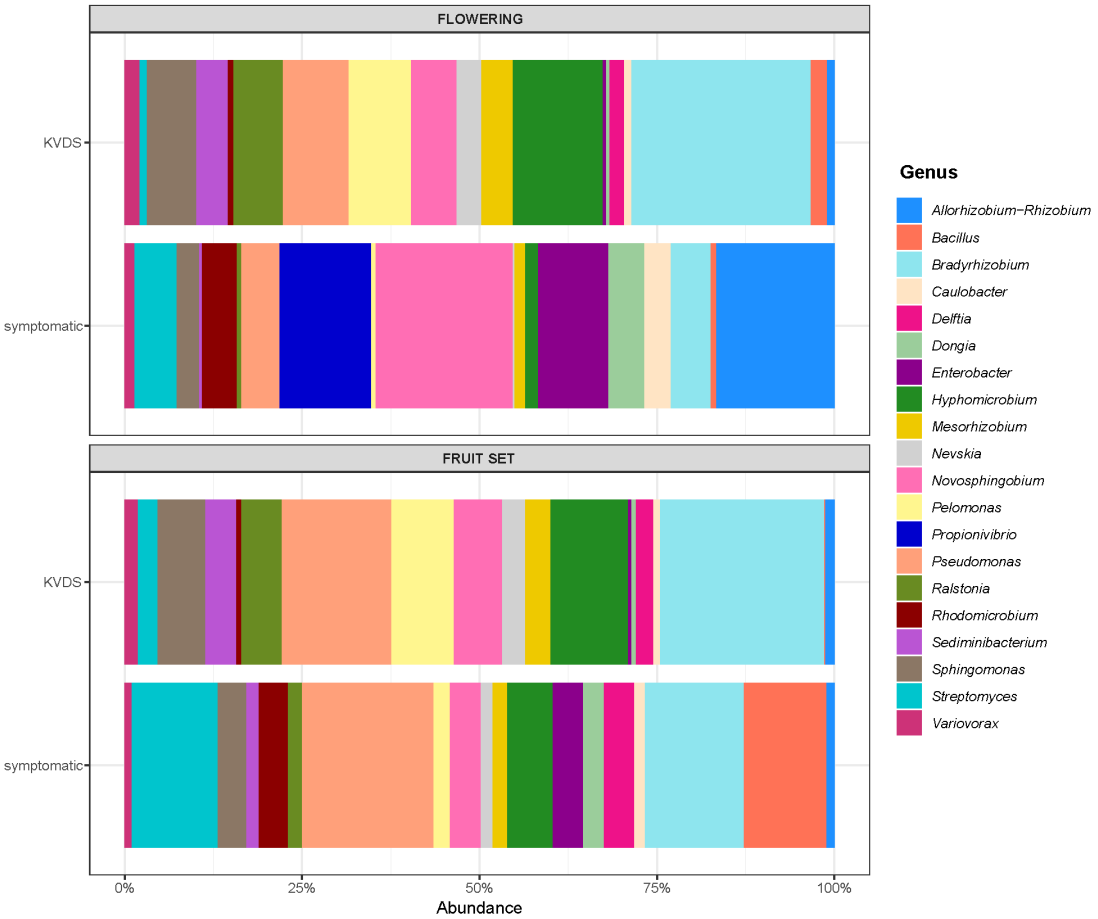

Figure 3.2 - Relative abundance of the top 20 bacterial genera in the roots endosphere in asymptomatic and KVDS samples during the two time-points.

The composition of the fungal community (Figure 3.3) in KVDS samples demonstrated clear dynamic shifts across different phenological stages. During the flowering stage, *Ganoderma* (23%) emerged as the predominant taxon, followed by *Fusarium* (15%), *Epicoccum* (11.2%), *Malassezia* (10.6%), and *Ceratobasidium* (4.6%). During the fruit set stage, *Ganoderma* increased to 29.9%, while *Epicoccum* (13%), *Codinaea* (11.7%), *Fusarium* (5.5%), and *Cladosporium* (5%) were also present. The increased prevalence of *Ganoderma* suggests its potential role as a pathogenic agent, while *Epicoccum* and *Codinaea* may contribute to disease suppression or plant stress responses. Conversely, during the flowering stage, asymptomatic samples exhibited a predominance of *Plectosphaerella* (72%), accompanied by lower abundances of *Exophiala* (6.8%), *Cosmospora* (6.3%), *Fusarium* (6%), and *Ceratobasidium* (3.5%). By the fruit set stage, a shift in the composition of the fungi was observed, with *Ceratobasidium* (17.3%) emerging as the most abundant taxon, followed by *Epicoccum* (9.5%), *Fusarium* (6.8%), *Malassezia* (6.7%), *Cladosporium* (3.2%), and *Alternaria* (3%).

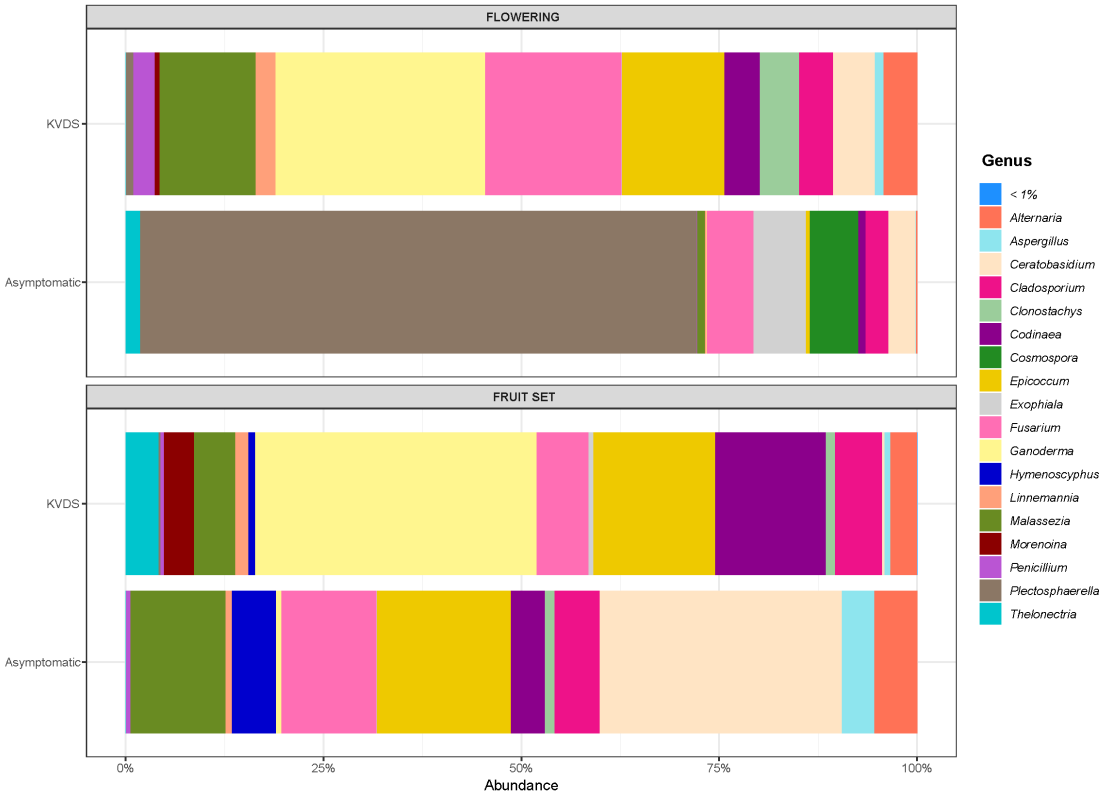

Figure 3.3 - Relative abundance of the top 20 fungal genera in the roots endosphere in asymptomatic and KVDS samples during the two time-points.

3.3.3 Altered gene expression patterns in KVDS-infected vines

Gene expression analysis was conducted on a selection of genes implicated in various pathways involved in the plant immunity response to biotic stressors (Figure 3.4). Data were normalized against asymptomatic controls, and relative gene expression was considered upregulated when exceeding a two-fold change and downregulated when less than 0.5-fold of the control.

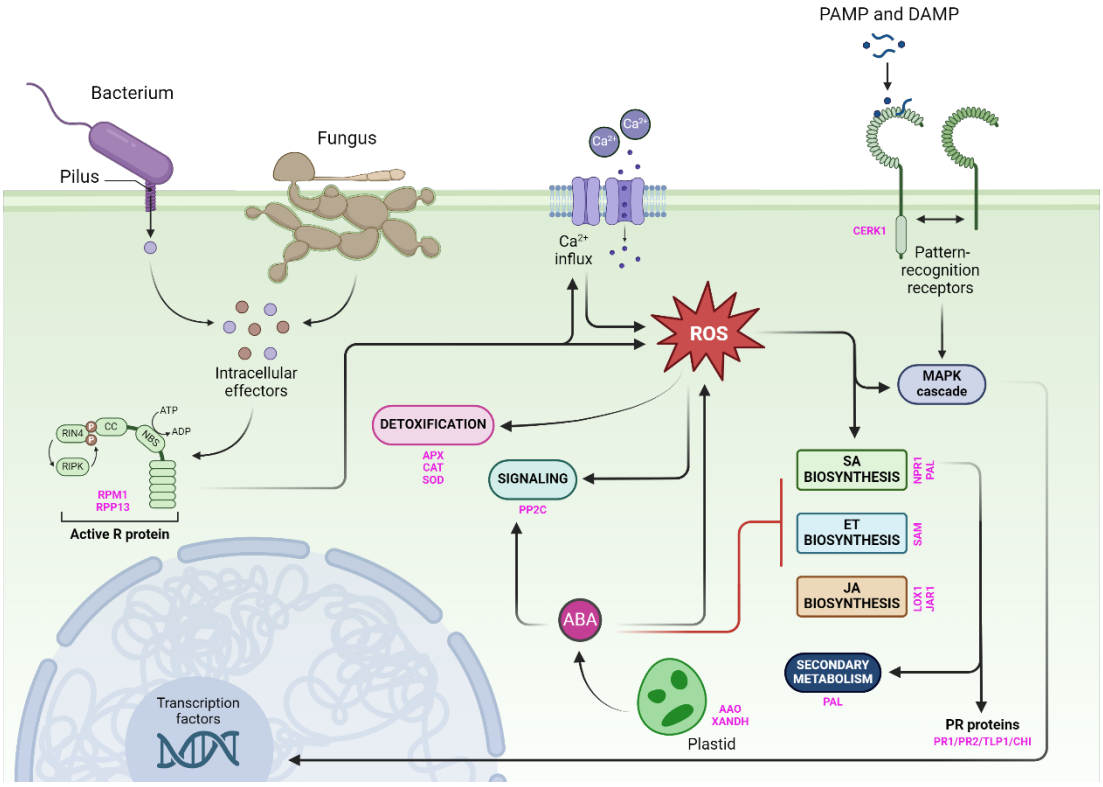

Figure 3.4 - Schematic representation of the plant immunity response to biotic stressors. Based on the existing literature, the primary biosynthetic pathways are illustrated, with key genes involved in these processes highlighted in pink. **Pattern-Triggered Immunity (PTI)** is the first line of defense against pathogens, initiated by the recognition of pathogen-associated molecular patterns (PAMPs) by pattern-recognition receptors (PRRs), such as **CERK1** (chitin elicitor receptor kinase 1). This triggers intracellular signalling pathways, including calcium ion influx and activation of calcium-dependent protein kinases (CDPKs), amplifying the signal. The rapid production of reactive oxygen species (ROS), known as the "oxidative burst," acts as a signalling molecule with antimicrobial properties. Additionally, genes involved in ROS detoxification, such as **SOD** (Superoxide Dismutase), **CAT** (Catalase), and **APX** (Ascorbate Peroxidase), play critical roles in managing oxidative stress. Mitogen-activated protein kinase (MAPK) cascades, involving MAPKKKs, MAPKKs, and MAPKs, activate transcription factors like WRKY proteins, leading to transcriptional reprogramming. Defense-related genes, such as **PR1, TLP1, CHI**, and **PAL**, are upregulated, enhancing antimicrobial compound production, cell wall reinforcement, and signalling. Hormonal signalling molecules—salicylic acid (SA), jasmonic acid (JA), and ethylene (ET)—coordinate local and systemic responses. Key hormone biosynthesis and signalling genes

include **NPR1, PAL, SAM, JAR1, LOX1, AAO, XANDH**, and **PP2C**. **Effector-triggered immunity (ETI)** represents a highly specific immune response triggered by the recognition of pathogen effector molecules by plant resistance (R) proteins, often located in the plant plasma membrane or cytoplasm. R proteins like **RPP13** and **RPM1** are essential for activating immune responses, including ROS production, cell wall reinforcement, and defense gene upregulation.

CERK1 (Chitin Elicitor Receptor Kinase 1) plays a crucial role in the plant's immunity response by recognizing chitin fragments, a key component of fungal cell walls, and is essential for the early stages of Pattern-Triggered Immunity (PTI), facilitating the plant's ability to detect and respond to fungal pathogens (Miya et al., 2007; Cao et al., 2014). *AcCERK1* expression was upregulated at both time points, as illustrated in Figure 3.5, highlighting its consistent role in mediating defense responses during fungal pathogen challenge. Focusing on three major genes—Chitinase, PR1, and TLP1—key players in the synthesis of PR proteins, their expression exhibited distinct patterns across the two time points (Figure 3.5). Chitinase, a critical component of the plant's defence mechanism, plays a pivotal role in the degradation of chitin, a major component of fungal cell walls, conferring resistance to fungal and oomycete pathogens. Along with strengthening plant defense mechanisms, chitinases also improve plant growth and yield (Kumar et al., 2018). PR1 (Pathogenesis-Related 1) is a well-characterised defense-related gene that is rapidly induced during biotic stress. It has been demonstrated that PR1 is involved in the production of antimicrobial compounds and play a crucial role in plant immunity by binding sterols to inhibit pathogen growth, releasing a signaling peptide to activate immune responses, and interacting with other proteins to modulate defense mechanism (Gamir et al., 2017; Han et al., 2023). TLP1 (Thaumatin-like Protein 1) is a defence-related protein that plays a role in the plant's response to both biotic stresses. TLP1 is associated with the reinforcement of the cell wall and acts as a signalling molecule that enhances the plant's defence mechanisms against pathogen invasion (de Jesùs-Pirès et al., 2020). The expression of these genes is often coordinated and regulated by shared signalling pathways, particularly those involving salicylic acid. This coordinated expression, along with their synergistic activities, provides a more robust defense response against pathogens compared to any single protein acting alone. For example, chitinase

weakens the pathogen's cell wall, rendering it more susceptible to the effects of TLP1 and other defense mechanisms. As shown in Figure 3.5, *AcCHI* showed an early up-regulation at the first time point, indicating its active involvement in the early defence response. However, its expression was completely absent at the following time point, suggesting a transient role in the immune process. In contrast, *AcPR1* showed a significant increase in expression at the second time point, while its levels remained comparable to the asymptomatic control at the first time point, indicating its role in later stages of the defence response. Notably, *AcTLP1* showed consistent up-regulation at both time points, indicating its sustained involvement in the plant's immune response throughout the periods observed.

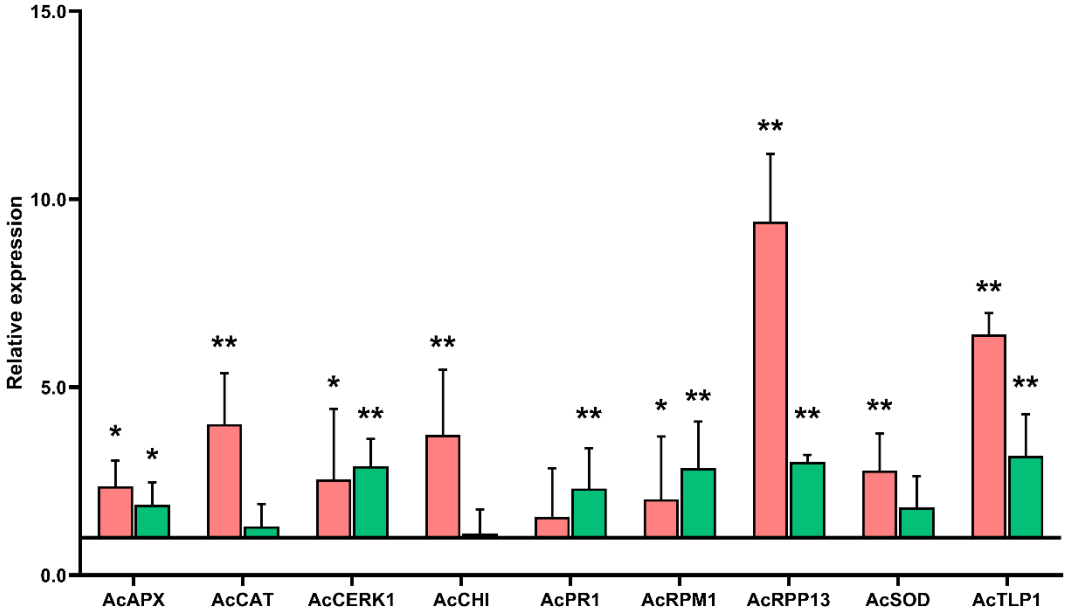

Figure 3.5 - Relative expression of genes involved in PRRs, ROS detoxification, PR and R proteins biosynthesis in KVDS plants during the first time-point (pink) and the second time-point (green). Gene expression levels were determined in relation to the transcription levels of the housekeeping genes *Ac18S, AcACT* and *AcGADPH*. The bar graph represents the mean of three biological replicates, each consisting of four technical replicates, and the line indicates the relative transcription value of the asymptomatic control. The standard deviation is given above each bar. T- test showed relative expression values with significant ("*", $p \leq 0.05$) and highly significant ("**", $p \leq 0.01$) differences compared to the control

Catalase (CAT), superoxide dismutase (SOD), and ascorbate peroxidase (APX) play pivotal roles in the plant's immune response by regulating reactive oxygen species (ROS) levels, which are crucial for both defense signalling and antimicrobial activity. Although ROS act as signalling molecules to trigger downstream immune responses and possess direct pathogen-inhibitory properties, their excessive accumulation can lead to cellular damage. These enzymes work synergistically to maintain ROS homeostasis: SOD catalyzes the conversion of superoxide radicals into hydrogen peroxide, CAT breaks down hydrogen peroxide into water and oxygen, and *APX* further detoxifies hydrogen peroxide using ascorbate as an electron donor (Apel and Hirt, 2004; Mittler et al., 2022). Gene expression analysis revealed that *AcCAT*, *AcAPX*, and *AcSOD* were significantly upregulated exclusively during the first time point, suggesting their critical involvement in the early stages of the plant's immune response by balancing ROS production and detoxification (Figure 3.5).

The biosynthesis of abscisic acid (ABA), salicylic acid (SA), jasmonic acid (JA) and ethylene (ET) is a complex process involving intricate regulatory networks that encompass transcriptional and post-transcriptional regulation. The analysis herein focuses on the genes that are implicated in hormonal biosynthesis and regulation (Figure 3.6). The AAO (aldehyde oxidase) and XanDH (xanthoxin dehydrogenase) genes are critical components of the ABA biosynthesis pathway, each contributing to distinct stages. AAO enzymes, particularly AAO3, are responsible for the final conversion of abscisic aldehyde to abscisic acid (ABA), the active form of the hormone. Meanwhile, XanDH enzymes catalyze the conversion of xanthoxin to abscisic aldehyde, a pivotal intermediate in the pathway (Xiong & Zhu, 2003). In addition to biosynthesis, PP2C (Protein Phosphatase 2C) genes play a fundamental role in ABA signalling. These phosphatases act as negative regulators by dephosphorylating and inactivating key signalling proteins in the absence of ABA. However, when ABA levels rise, PP2C activity is inhibited, allowing downstream signalling components to be activated and ABA-mediated responses to occur (Hirayama & Shinozaki, 2007; Umezawa et al., 2009). Gene expression analysis revealed a significant upregulation of *AcAAO*, *AcXANDH*, and *AcPP2C* specifically at the second time point, indicating their involvement in late-stage ABA biosynthesis and signalling.

NPR1 (Nonexpressor of Pathogenesis-Related genes 1) and PAL (Phenylalanine Ammonia-Lyase) are critical components of the salicylic acid (SA) signalling pathway, playing distinct yet interconnected roles in plant immunity. NPR1 serves as a central regulator of systemic acquired resistance (SAR) and induced systemic resistance (ISR) (Pieterse et al., 1998). It acts as a master regulator in the plant defense network, mediating crosstalk between SA and jasmonic acid/ethylene (JA/ET) signaling pathways (Backer et al., 2019). Upon SA accumulation, NPR1 undergoes redox-mediated structural changes, facilitating its oligomerization and nuclear translocation. In the nucleus, NPR1 interacts with transcription factors such as TGA proteins to activate the expression of pathogenesis-related (PR) genes, which are vital for establishing immunity (Despres et al., 2000; Zhou et al., 2000; Backer et al., 2019). PAL, on the other hand, is a key enzyme in the phenylpropanoid pathway, a metabolic pathway that leads to the production of various secondary metabolites, including SA. Specifically, PAL catalyses the conversion of phenylalanine to trans-cinnamic acid, an essential step in SA biosynthesis (Huang et al., 2010; Zhong et al., 2021). Interestingly, SA itself can induce the expression of PAL genes, creating a positive feedback loop that enhances SA production and strengthens the plant's defence response. *AcNPR1* exhibited notable upregulation during the second time point. In contrast, *AcPAL* showed upregulation at both time points compared to the asymptomatic control, indicating its sustained involvement in salicylic acid biosynthesis and the phenylpropanoid pathway throughout the defense process (Figure 3.5 and 3.6).

The SAM gene, encoding S-adenosylmethionine synthetase (SAMS), plays a crucial role in ethylene (ET) biosynthesis by producing SAM (S-adenosylmethionine), the essential precursor for ET production (Yang and Hoffman, 1984; Wang et al., 2002). The *AcSAM* gene exhibited significant upregulation during the first time point, highlighting its active involvement in the early stages of the plant's immune response. However, its expression was nearly absent at the second time point, suggesting a transient role in the defense process, possibly linked to the initial activation of ethylene biosynthesis or signalling pathways (Figure 3.6).

The genes LOX1 (Lipoxygenase 1) and JAR1 (Jasmonate-Resistant 1) play pivotal roles in the biosynthesis and signalling of jasmonic acid (JA). LOX1 is involved in the

early steps of JA biosynthesis, catalyzing the oxygenation of linolenic acid, a polyunsaturated fatty acid derived from membrane lipids. The activity of LOX1 is essential for initiating the JA biosynthetic pathway and is tightly regulated during stress responses to ensure timely JA production (Creelman and Mullet, 1997; Feussner and Wasternack, 2002). JAR1 functions downstream in the JA signalling pathway, where it encodes an enzyme that conjugates JA to isoleucine, forming jasmonoyl-isoleucine (JA-Ile), the bioactive form of JA (Staswick and Tiryaki, 2004). JA-Ile, the active form of jasmonic acid (JA), plays a crucial role in activating plant defences by binding to the SCF^COI1 complex. This interaction facilitates the ubiquitination and subsequent degradation of JAZ (Jasmonate ZIM-domain) proteins, which act as repressors of JA-responsive transcription factors. The release of these transcription factors, consequent to the degradation of JAZ proteins, facilitates the activation of defense-related genes, including those involved in the production of secondary metabolites, protease inhibitors and antimicrobial compounds (Staswick and Tiryaki, 2004; Fonseca et al., 2009). During the first time point, the expression levels of *AcLOX1* and *AcJAR1* were reduced compared to the asymptomatic control group, suggesting a subdued activation of the jasmonic acid (JA) pathway during this phase. However, at the subsequent time point, both genes exhibited increased expression levels, indicating a later activation of the JA biosynthesis and signalling pathway, likely in response to escalating biotic stress or as part of a secondary defense response.

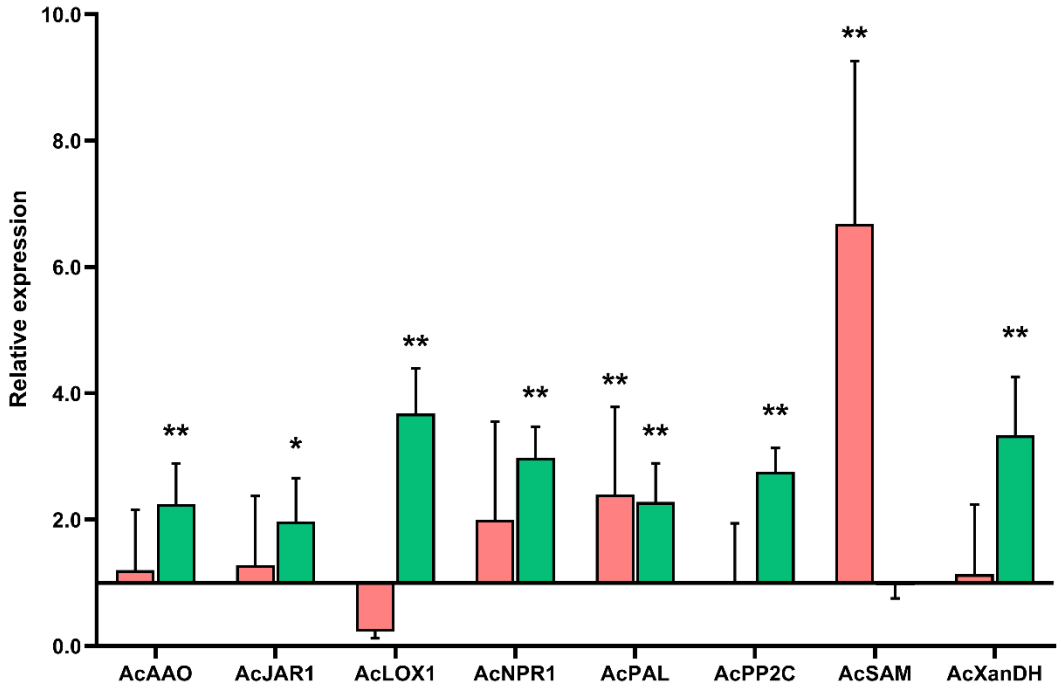

Figure 3.6 - Relative expression of genes involved in hormones biosynthesis and signalling. Gene expression levels were determined in relation to the transcription levels of the housekeeping genes *Ac18S, AcACT* and *AcGADPH*. The bar graph represents the mean of three biological replicates, each consisting of four technical replicates, and the line indicates the relative transcription value of the asymptomatic control. The standard deviation is given above each bar. T- test showed relative expression values with significant ("*", $p \leq 0.05$) and highly significant ("**", $p \leq 0.01$) differences compared to the control

R-genes have been shown to play a crucial role in plant immunity by encoding resistance proteins that recognise pathogen effectors and activate defence responses (Gurunani et al., 2012; Movahedi et al., 2022; Waheed et al., 2022). Among these, RPM1 and RPP13 are well-characterised resistance genes involved in pathogen recognition (Baggs et al., 2017). RPM1 has been shown to detect specific bacterial effectors, triggering a hypersensitive response (HR), a form of programmed cell death at the infection site that limits pathogen spread (Boyes et al., 1998; Wang et al., 2020). Conversely, RPP13 offers resistance against *Peronospora parasitica* in *A. thaliana* through highly polymorphic recognition mechanisms, with different alleles recognising distinct *Peronospora parasitica* effector variants. This suggests a diversifying selection pressure on RPP13, where different alleles confer resistance to different pathogen strains, reflecting its role in adaptive immune responses (Bittner-Eddy et al., 2000). As illustrated in Figure 3.5, KVDS samples

exhibited an upregulation of *AcRPM1* compared to the asymptomatic control at the second time point, suggesting its potential role in a late-stage defense response. In contrast, *AcRPP13* showed a highly significant upregulation at both time points, indicating its consistent involvement in the plant's immune response throughout the infection process (Figure 3.5). The differential expression patterns of these resistance genes highlight their distinct roles in pathogen recognition and defense activation, with *AcRPM1* potentially contributing to race-specific resistance and *AcRPP13* playing a broader role in basal immunity.

3.3.4 Phytohormones profiles in asymptomatic and KVDS-affected plants

Plant immunity is intricately regulated by a complex network of phytohormones, including gibberellic acid (GA3), 6-benzylaminopurine (6-BA), indole-3-acetic acid (IAA), abscisic acid (ABA), salicylic acid (SA), and jasmonic acid (JA) (Yang et al., 2012). GA3 exerts a primary influence on the trade-off between growth and defence, frequently exhibiting antagonistic effects on SA-mediated defences while concurrently enhancing JA-mediated resistance against necrotrophic pathogens (Yang et al., 2012). Cytokinins, such as 6-BA, have been shown to enhance plant resistance by stimulating the expression of defence-related genes and contributing to systemic signalling pathways (Akhtar et al., 2020; Li et al., 2021). IAA, an auxin, plays dual roles in plant immunity. While it can contribute to cell wall fortification, it can also be exploited by certain pathogens to suppress host defences (Kazan and Manners, 2009; Naseem et al., 2015). Furthermore, it has been demonstrated that ABA plays a crucial role in modulating immune responses through intricate crosstalk with SA and JA/ethylene (ET) signalling pathways (Li et al., 2019). It frequently acts antagonistically to SA-mediated defenses against biotrophic pathogens while promoting JA-mediated resistance against necrotrophic pathogens (Ton et al., 2009; Denancé et al., 2013). SA occupies a central position in plant defence against biotrophic pathogens, orchestrating systemic acquired resistance (SAR) and inducing the expression of pathogenesis-related (PR) genes (Vlot et al., 2009). JA is critical for effective defence against necrotrophic pathogens and herbivory, activating the expression of genes involved in the biosynthesis of

secondary metabolites and antimicrobial proteins (Wasternack and Hause, 2013). During the first time point, neither 6-BA, IAA, nor ABA were detected in either asymptomatic or KVDS samples (Figure 3.7).

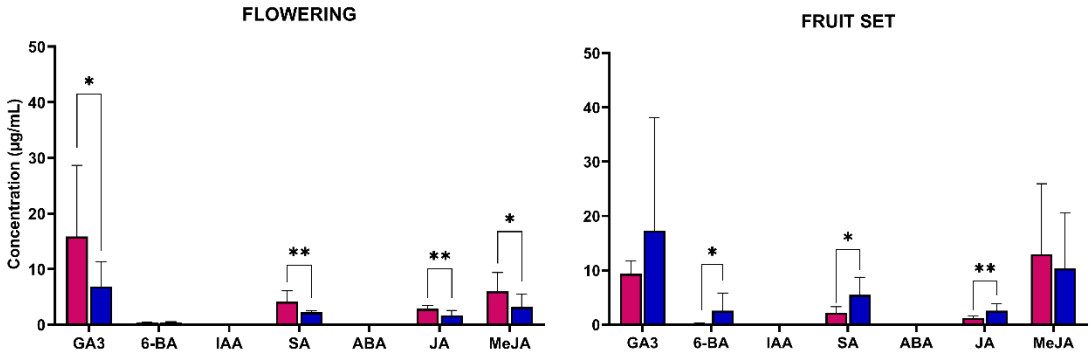

Figure 3.7 - Phytohormones concentration (µg/mL) in asymptomatic (magenta) and symptomatic (blue) root samples during the two sampling times. The bar graph represents the mean of three biological replicates, each consisting of three technical replicates. The standard deviation is given above each bar. Significant differences are indicated by '**' (*p≤0.01*) and '*' (*p≤0.05*)

However, asymptomatic samples exhibited significantly higher concentrations of GA3, SA, JA, and MeJA compared to KVDS-affected samples, suggesting a more robust hormonal balance in healthy plants during the early stage. By the fruit set stage, this trend shifted notably: KVDS samples displayed increased concentrations of GA3, 6-BA, SA, and JA compared to asymptomatic controls, indicating a dynamic hormonal adjustment in response to disease stress (Figure 3.7). These observations are consistent with the gene expression analysis, which revealed significant upregulation of genes involved in the biosynthesis of these hormones in KVDS samples at the second time point. Notably, while genes linked to ABA biosynthesis and signalling were also upregulated at this stage, the hormone itself remained undetectable, raising intriguing questions about post-transcriptional or post-translational regulation mechanisms influencing ABA accumulation under these conditions.

3.3.5 The role of *AcPAL* gene in modulating phenolic content and SA biosynthesis in response to KVDS

To investigate the role of the PAL gene in plant defense, particularly in the biosynthesis of salicylic acid (SA) and phenolic compounds, these metabolites were quantified using a spectrophotometric method. The results demonstrated distinct patterns of accumulation between KVDS-affected and asymptomatic samples across two time points (Figure 3.8).

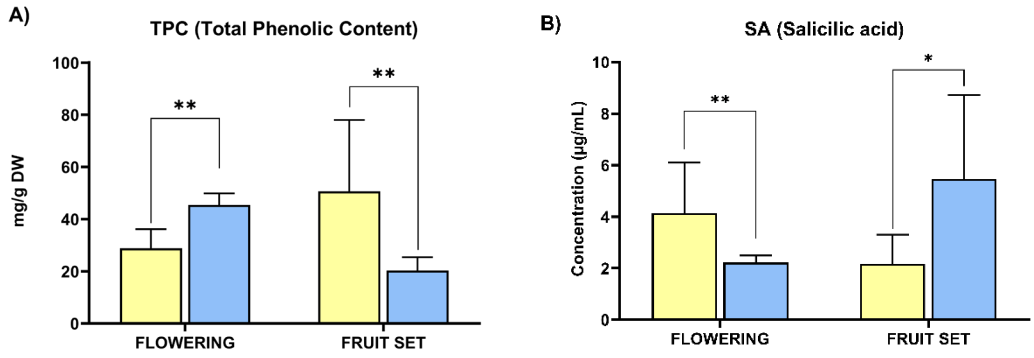

Figure 3.8 - (A) Total phenolic content (TPC) and (B) Salicylic acid (SA) concentration in asymptomatic (yellow) and symptomatic (blue) root samples during the two sampling time points. The bar graph represents the mean of three biological replicates, each consisting of three technical replicates. The standard deviation is given above each bar. Significant differences are indicated by '**' ($p \leq 0.01$) and '*' ($p \leq 0.05$)

During the first time point, KVDS samples exhibited a higher concentration of phenolic compounds (40 mg/g DW) compared to asymptomatic samples (30 mg/g DW), indicating an enhanced production of phenolic compounds in response to stress. In contrast, at the second time point, asymptomatic samples showed a significantly higher accumulation of phenolic compounds (50 mg/g DW) compared to KVDS samples (20 mg/g DW), suggesting a diminished capacity for phenolic production in KVDS-affected plants over time. SA quantification revealed contrasting trends. At the first time point, asymptomatic samples had a higher SA concentration (4 µg/ml) than KVDS samples (approximately 2 µg/ml). However, at the second time point, KVDS samples exhibited a marked increase in SA levels (approximately 5 µg/ml), surpassing the concentration in asymptomatic samples (2 µg/ml). These findings highlight the dynamic role of the PAL gene in modulating

phenolic and SA biosynthesis during stress conditions. Interestingly, Ac*PAL* gene expression was consistently higher in KVDS samples at both time points, confirming its dual role in the defense response. During the first time point, its primary involvement appeared to be in the synthesis of phenolic compounds, while during the second time point, its activity shifted toward increased SA production, reflecting the plant's adaptive strategies to counter biotic stress.

3.4 Discussion

Plants continuously face a trade-off between allocating resources to growth or activating defense mechanisms against pathogens. This evolutionary dilemma is dictated by the costs associated with defense activation, which often leads to reduced photosynthetic capacity, metabolic diversion, and impaired development (Huot et al., 2014). The regulation of this balance is mediated through complex hormonal signalling networks, primarily involving salicylic acid (SA), jasmonic acid (JA), and ethylene (ET) (Yang et al., 2019). The SA pathway is generally associated with resistance to biotrophic pathogens, while JA and ET pathways are more involved in defense against necrotrophic pathogens and herbivores (Pieterse et al., 2012). ABA, traditionally known for its role in abiotic stress responses, also plays a crucial function in modulating plant immunity, often acting as a negative regulator by suppressing SA- and JA-mediated defense pathways (Ton et al., 2009). However, ABA can also contribute to resistance in specific contexts, such as through the regulation of stomatal closure to prevent pathogen entry (Melotto et al., 2006). These interactions highlight the complexity of hormonal crosstalk, further complicating the plant's ability to simultaneously optimize growth and defense (Vos et al., 2015).

At the molecular level, plant immunity is based on a two-tiered defense mechanism: pattern-triggered immunity (PTI) and effector-triggered immunity (ETI) (Jones and Dangl, 2006). PTI is initiated upon the recognition of pathogen-associated molecular patterns (PAMPs) by pattern recognition receptors (PRRs), activating basal defense responses such as reactive oxygen species (ROS) production, callose deposition, and antimicrobial compound synthesis (Boller and Felix, 2009). However, adapted pathogens can suppress PTI through the deployment of effector proteins, leading to

ETI a more robust defense mediated by intracellular nucleotide-binding leucine-rich repeat (NLR) receptors (Cui et al., 2015). The crosstalk between PTI and ETI determines the outcome of plant-pathogen interactions and influences disease resistance. In order to study plant diseases and their complex interactions in an effective manner, a multi-omics approach has proven to be very useful. Multifactorial plant diseases emerge from intricate interactions between genetic predisposition, environmental factors, and pathogen aggressiveness. Integrating genomics, transcriptomics, and metabolomics facilitates a comprehensive understanding of disease mechanisms (Jamil et al., 2020).

The present study has provided a practical application of this approach in addressing the issue of Kiwifruit Vine Decline Syndrome (KVDS), which represents a significant challenge for the Italian kiwifruit industry.

The observed variation in the composition of bacterial and fungal communities across phenological stages and between KVDS and asymptomatic samples suggests that microbiota associated with plants undergo dynamic shifts influenced by host physiological changes and disease states. The present findings are consistent with earlier research suggesting that microbial communities in plant endosphere exhibit fluctuations in response to developmental transitions and environmental cues (Edwards et al., 2015; Compant et al., 2019). The prevalence of *Bradyrhizobium* in KVDS samples during both the flowering (25.8%) and fruit set (21.8%) stages highlights its potential role in nitrogen fixation and plant-microbe interactions under disease stress (Zgadzaj et al., 2016). However, the substantial increase in *Pseudomonas* abundance during the fruit set stage (19%) suggests a possible shift in microbial function, as *Pseudomonas* spp. are known for their plant growth-promoting and pathogen-antagonistic properties (Liu et al., 2020). The persistence of *Hyphomicrobium, Pelomonas*, and *Ralstonia* across stages further suggests their stable association with the plant rhizosphere, though their specific roles in KVDS-affected plants require further investigation. Conversely, asymptomatic samples exhibited greater microbial diversity, with genera such as *Novosphingobium* and *Allorhizobium/Rhizobium* dominating the flowering stage. These taxa have been linked to beneficial plant-microbe interactions, including organic compound degradation and nitrogen fixation (Santoyo et al., 2016). The increased prevalence

of *Streptomyces* (13.3%) and *Bacillus* (9.7%) during the fruit set stage suggests a potential shift towards microbial taxa with biocontrol and antibiotic-producing capabilities, which may contribute to plant health and disease resistance (Mendes et al., 2011; Berendsen et al., 2012). The composition of the fungal community in KVDS samples also exhibited distinct shifts in relation to the phenological stage. During the flowering stage, *Ganoderma* emerged as the predominant taxon, accompanied by *Fusarium, Epicoccum, Malassezia*, and *Ceratobasidium*. During the fruit set stage, *Ganoderma* abundance further increased, while *Epicoccum* and *Codinaea* became more prominent, with *Fusarium* and *Cladosporium* also present. The increase in *Ganoderma* suggests its potential role as a pathogenic agent, whereas *Epicoccum* and *Codinaea* may be involved in disease suppression or plant stress responses. On the other hand, asymptomatic samples exhibited a distinct fungal composition. During the flowering stage, *Plectosphaerella* was identified as the most prevalent taxon, followed by *Exophiala, Cosmospora, Fusarium*, and *Ceratobasidium*. The high abundance of *Plectosphaerella* in asymptomatic samples during flowering may indicate a potential role in plant defence or niche competition, limiting the establishment of pathogenic fungi. By the fruit set stage, a shift in the fungal community was observed, with *Ceratobasidium* emerging as the most abundant taxon, followed by *Epicoccum, Fusarium, Malassezia, Cladosporium*, and *Alternaria*. These changes indicate that asymptomatic plants may harbour fungal taxa associated with beneficial interactions or defence mechanisms against pathogens.

To understand the roles of immune-related genes and hormones in plant defence, the expression of these genes and the levels of hormones were analysed at different phenological stages (flowering and fruit set) in both the asymptomatic and KVDS groups. Overall, KVDS samples exhibited a higher upregulation of genes in comparison to asymptomatic plants. *AcCERK1*, a receptor involved in recognizing fungal chitin fragments, showed upregulation at both time points, indicating its continuous role in early immunity. Genes encoding PR proteins, including Chitinase, PR1, and TLP1, displayed distinct expression patterns. Chitinase was upregulated early but absent at later stages, suggesting a transient role in the initial defense. PR1 showed a significant increase at the later time point, while TLP1 was consistently upregulated, reflecting its sustained role in defense. ROS-related enzymes like

AcCAT, AcAPX, and *AcSOD* were activated early to regulate ROS levels, helping balance defense signaling. Hormonal pathways, including ABA and SA, also exhibited time-specific regulation. *AcAAO, AcXANDH*, and *AcPP2C* involved in ABA biosynthesis and signalling were upregulated at the second time point, indicating their involvement in late-stage immune responses. Similarly, *AcNPR1* and *AcPAL* were upregulated in the later stages, with PAL showing sustained activity and a dynamic role in modulating phenolic and SA biosynthesis during stress conditions. The jasmonic acid pathway, involving *AcLOX1* and *AcJAR1*, was activated at the second time point, suggesting a delayed role in defense. The differential expression of resistance genes like *AcRPM1* and *AcRPP13* indicated their stage-specific contributions to immune responses, with *AcRPM1* linked to later-stage pathogen recognition and *AcRPP13* showing consistent activation throughout the infection. These results emphasize the dynamic and coordinated regulation of immune pathways across different stages of infection.

The hormonal quantification data further complement the gene expression analysis by providing insights into the temporal regulation of plant hormones in response to fungal infection. At the first time point, the absence of detectable levels of 6-BA, IAA, and ABA in both asymptomatic and KVDS samples suggests that these hormones may not play a significant role in the early stages of the immune response. However, the significantly higher concentrations of GA3, SA, JA, and MeJA in asymptomatic plants, compared to KVDS-affected plants, suggest that healthy plants are maintaining a more balanced hormonal profile during the early stages of infection. These hormones are typically associated with growth regulation and defense, and their higher levels in asymptomatic plants may reflect a more robust capacity for growth and development during the initial pathogen encounter. As the plants progressed to the fruit set stage (the second time point), a notable shift in hormonal activity was observed. The increased concentrations of GA3, 6-BA, SA, and JA in KVDS-affected samples relative to asymptomatic controls suggest that plants under disease stress undergo significant hormonal adjustments to cope with stress and activate defense mechanisms. This aligns with the gene expression analysis, which revealed upregulation of genes involved in the biosynthesis of these hormones in KVDS plants at this stage. The increase in GA3 and 6-BA indicates that these hormones may play a role in modulating plant growth during periods of stress, while

the rise in SA and JA is consistent with their role in activating defence pathways. Interestingly, despite the upregulation of genes associated with ABA biosynthesis and signalling in the KVDS samples at the second time point, ABA itself was not detected in either asymptomatic or KVDS plants. This finding indicates the possibility of post-transcriptional or post-translational regulatory mechanisms influencing ABA accumulation, thereby hindering detection of the hormone, despite the activity of the genes responsible for its biosynthesis. Consequently, the absence of ABA could be considered a strategic response, whereby the plant diverts from ABA-mediated responses associated with abiotic stress, instead focusing on the activation of the immune system through alternative hormones that are more effective in addressing biotic stress.

The use of multi-omics methods provides a comprehensive understanding of plant responses to pathogens and sheds light on the aetiology of complex diseases such as KVDS. This could facilitate the identification of key biomarkers and potential targets for more precise disease management. In addition, the assessment of soil management and plant-pathogen interactions could facilitate the development of more sustainable agricultural practices and effective disease management strategies.

3.5 References

Akhtar, S., Mekureyaw, M., Pandey, C., & Roitsch, T. (2020). Role of cytokinins for interactions of plants with microbial pathogens and pest insects. *Frontiers in Plant Science*, 10. https://doi.org/10.3389/fpls.2019.01777

Apel, K., & Hirt, H. (2004). Reactive oxygen species: Metabolism, oxidative stress, and signal transduction. *Annual Review of Plant Biology*, 55, 373–399. https://doi.org/10.1146/annurev.arplant.55.031903.141701

Backer, R., Naidoo, S., & van den Berg, N. (2019). The NONEXPRESSOR OF PATHOGENESIS-RELATED GENES 1 (NPR1) and related family: Mechanistic insights in plant disease resistance. *Frontiers in Plant Science*, 10. https://doi.org/10.3389/fpls.2019.00102

Baggs, E., Dagdas, G., & Krasileva, K. V. (2017). NLR diversity, helpers and integrated domains: Making sense of the NLR identity. *Current Opinion in Plant Biology*, 38, 59–67. https://doi.org/10.1016/j.pbi.2017.04.012

Berendsen, R. L., Pieterse, C. M., & Bakker, P. A. (2012). The rhizosphere microbiome and plant health. *Trends in Plant Science*, 17(8), 478–486. https://doi.org/10.1016/j.tplants.2012.04.001

Bigeard, J., Colcombet, J., & Hirt, H. (2015). Signaling mechanisms in pattern-triggered immunity (PTI). *Molecular Plant*, 8(4), 521–539. https://doi.org/10.1016/j.molp.2014.12.022

Bittner-Eddy, P. D., Crute, I. R., Holub, E. B., & Beynon, J. L. (2000). RPP13 is a simple locus in *Arabidopsis thaliana* for alleles that specify downy mildew resistance to different avirulence determinants in *Peronospora parasitica*. *The Plant Journal: For Cell and Molecular Biology*, 21(2), 177–188. https://doi.org/10.1046/j.1365-313x.2000.00664.x

Boller, T., & Felix, G. (2009). A renaissance of elicitors: Perception of microbe-associated molecular patterns and danger signals by pattern-recognition receptors. *Annual Review of Plant Biology*, 60, 379–406. https://doi.org/10.1146/annurev.arplant.57.032905.105346

Bolyen, E., Rideout, J. R., Dillon, M. R., et al. (2019). Reproducible, interactive, scalable and extensible microbiome data science using QIIME 2. *Nature Biotechnology*, 37, 852–857. https://doi.org/10.1038/s41587-019-0209-9

Boutrot, F., & Zipfel, C. (2017). Function, discovery, and exploitation of plant pattern recognition receptors for broad-spectrum disease resistance. *Annual Review of Phytopathology*, 55, 257–286. https://doi.org/10.1146/annurev-phyto-080614-120106

Boyes, D. C., Nam, J., & Dangl, J. L. (1998). The *Arabidopsis thaliana* RPM1 disease resistance gene product is a peripheral plasma membrane protein that is degraded coincident with the hypersensitive response. *Proceedings of the National Academy of Sciences of the United States of America*, 95(26), 15849–15854. https://doi.org/10.1073/pnas.95.26.15849

Cao, Y., Liang, Y., Tanaka, K., Nguyen, C. T., Jedrzejczak, R. P., Joachimiak, A., & Stacey, G. (2014). The kinase LYK5 is a major chitin receptor in *Arabidopsis* and forms a chitin-induced complex with related kinase CERK1. *eLife*, 3. https://doi.org/10.7554/eLife.03766

Cardacino, A., Turco, S., & Balestra, G. M. (2025). Seasonal dynamics of kiwifruit microbiome: A case study in a KVDS-affected orchard. *Microbiological Research*, 292. https://doi.org/10.1016/j.micres.2024.128044

Cellini, A., Fiorentini, L., Buriani, G., Yu, J., Donati, I., Cornish, D. A., Novak, B., Costa, G., Vanneste, J. L., & Spinelli, F. (2014). Elicitors of the salicylic acid pathway reduce incidence of bacterial canker of kiwifruit caused by *Pseudomonas syringae* pv. *actinidae*. *Annals of Applied Biology*, 165, 441–453. https://doi.org/10.1111/aab.12150

Compant, S., Samad, A., Faist, H., & Sessitsch, A. (2019). A review on the plant microbiome: Ecology, functions, and emerging trends in microbial application. *Journal of Advanced Research*, 19, 29–37. https://doi.org/10.1016/j.jare.2019.03.004

Creelman, R. A., & Mullet, J. E. (1997). Biosynthesis and action of jasmonates in plants. *Annual Review of Plant Physiology and Plant Molecular Biology*, 48. www.annualreviews.org

Cui, H., Tsuda, K., & Parker, J. E. (2015). Effector-triggered immunity: From pathogen perception to robust defense. *Annual Review of Plant Biology*, 66, 487–511. https://doi.org/10.1146/annurev-arplant-050213-040012

de Jesús-Pires, C., Ferreira-Neto, J. R. C., Pacifico Bezerra-Neto, J., Kido, E. A., de Oliveira Silva, R. L., Pandolfi, V., Wanderley-Nogueira, A. C., Binneck, E., da Costa, A. F., Pio-Ribeiro, G., Pereira-Andrade, G., Sittolin, I. M., Freire-Filho, F., & Benko-Iseppon, A. M. (2020). Plant thaumatin-like proteins: Function, evolution and biotechnological applications. *Current Protein & Peptide Science*, 21(1), 36–51. https://doi.org/10.2174/1389203720666190318164905

Denancé, N., Sánchez-Vallet, A., Goffner, D., & Molina, A. (2013). Disease resistance or growth: The role of plant hormones in balancing immune responses and fitness costs. *Frontiers in Plant Science*, 4. https://doi.org/10.3389/fpls.2013.00155

Despres, C., DeLong, C., Glaze, S., Liu, E., & Fobert, P. R. (2000). The *Arabidopsis* NPR1/NIM1 protein enhances the DNA binding activity of a subgroup of the TGA family of bZIP transcription factors. *Plant Cell*, 12, 279–290. https://doi.org/10.1105/tpc.12.2.279

Edwards, J., Johnson, C., Santos-Medellín, C., Lurie, E., Podishetty, N. K., Bhatnagar, S., Eisen, J. A., & Sundaresan, V. (2015). Structure, variation, and assembly of the root-associated microbiomes of rice. *Proceedings of the National Academy of Sciences of the United States of America*, 112(8), E911–E920. https://doi.org/10.1073/pnas.1414592112

Ferradás, Y., Rey, L., Martínez, Ó., Rey, M., & González, M. V. (2016). Identification and validation of reference genes for accurate normalization of real-time quantitative PCR data in kiwifruit. *Plant Physiology and Biochemistry*, 102, 27–36. https://doi.org/10.1016/j.plaphy.2016.02.011

Feussner, I., & Wasternack, C. (2002). The lipoxygenase pathway. *Annual review of plant biology, 53*, 275–297. https://doi.org/10.1146/annurev.arplant.53.100301.135248

Fonseca, S., Chico, J. M., & Solano, R. (2009). The jasmonate pathway: the ligand, the receptor and the core signalling module. *Current opinion in plant biology, 12*(5), 539–547. https://doi.org/10.1016/j.pbi.2009.07.013

Francesconi, S., Tagliavento, V., Ciarroni, S., Sestili, F., & Balestra, G. M. (2024). Chitosan- and gallic acid-based (NPF) displayed antibacterial activity against three *Pseudomonas* spp. plant pathogens and boosted systemic acquired resistance in kiwifruit and olive plants. *Pest Management Science, 80*(3), 1300–1313. https://doi.org/10.1002/ps.7861

Gamir, J., Darwiche, R., van't Hof, P., Choudhary, V., Stumpe, M., Schneiter, R., & Mauch, F. (2017). The sterol-binding activity of PATHOGENESIS-RELATED PROTEIN 1 reveals the mode of action of an antimicrobial protein. *Plant Journal, 89*(3), 502–509. https://doi.org/10.1111/tpj.13398

Guaschino, M., Garello, M., Nari, L., Zhimo, Y. V., Droby, S., & Spadaro, D. (2024). Soil, rhizosphere, and root microbiome in kiwifruit vine decline, an emerging multifactorial disease. *Frontiers in Microbiology, 15*. https://doi.org/10.3389/fmicb.2024.1330865

Gururani, M. A., Venkatesh, J., Upadhyaya, C. P., Nookaraju, A., Pandey, S. K., & Park, S. W. (2012). Plant disease resistance genes: Current status and future directions. *Physiological and Molecular Plant Pathology, 78*, 51–65. https://doi.org/10.1016/j.pmpp.2012.01.002

Han, Z., Xiong, D., Schneiter, R., & Tian, C. (2023). The function of plant PR1 and other members of the CAP protein superfamily in plant–pathogen interactions. *Molecular Plant Pathology, 24*(6), 651–668. https://doi.org/10.1111/mpp.1332

Hirayama, T., & Shinozaki, K. (2007). Perception and transduction of abscisic acid signals: keys to the function of the versatile plant hormone ABA. *Trends in Plant Science, 12*(8), 343–351. https://doi.org/10.1016/j.tplants.2007.06.013

Huang, J., Gu, M., Lai, Z., Fan, B., Shi, K., Zhou, Y. H., Yu, J. Q., & Chen, Z. (2010). Functional analysis of the Arabidopsis PAL gene family in plant growth, development, and response to environmental stress. *Plant Physiology, 153*(4), 1526–1538. https://doi.org/10.1104/pp.110.157370

Huot, B., Yao, J., Montgomery, B. L., & He, S. Y. (2014). Growth-defense tradeoffs in plants: a balancing act to optimize fitness. *Molecular plant, 7*(8), 1267–1287. https://doi.org/10.1093/mp/ssu049

Jamil, I. N., Remali, J., Azizan, K. A., Nor Muhammad, N. A., Arita, M., Goh, H. H., & Aizat, W. M. (2020). Systematic Multi-Omics Integration (MOI) Approach in Plant Systems Biology. *Frontiers in plant science, 11*, 944. https://doi.org/10.3389/fpls.2020.00944

Jones, J. D., & Dangl, J. L. (2006). The plant immune system. *Nature, 444*(7117), 323–329. https://doi.org/10.1038/nature05286

Kazan, K., & Manners, J. M. (2009). Linking development to defense: auxin in plant-pathogen interactions. *Trends in plant science, 14*(7), 373–382. https://doi.org/10.1016/j.tplants.2009.04.005

Kumar, M., Brar, A., Yadav, M., Chawade, A., Vivekanand, V., & Pareek, N. (2018). Chitinases—Potential candidates for enhanced plant resistance towards fungal pathogens. *Agriculture (Switzerland), 8*(7). https://doi.org/10.3390/agriculture8070088

Ledger, S. E., Janssen, B. J., Karunairetnam, S., Wang, T., & Snowden, K. C. (2010). Modified CAROTENOID CLEAVAGE DIOXYGENASE8 expression correlates with altered branching in kiwifruit (*Actinidia chinensis*). *The New phytologist, 188*(3), 803–813. https://doi.org/10.1111/j.1469-8137.2010.03394.x

Li, N., Han, X., Feng, D., Yuan, D., & Huang, L. (2019). Signaling Crosstalk between Salicylic Acid and Ethylene/Jasmonate in Plant Defense: Do We Understand What They Are Whispering?. *International Journal of Molecular Sciences, 20*. https://doi.org/10.3390/ijms20030671

Li, S. M., Zheng, H. X., Zhang, X. S., et al. (2021). Cytokinins as central regulators during plant growth and stress response. *Plant Cell Reports, 40*, 271–282. https://doi.org/10.1007/s00299-020-02612-1

Liu, H., Brettell, L. E., Qiu, Z., & Singh, B. K. (2020). Microbiome-Mediated Stress Resistance in Plants. *Trends in plant science, 25*(8), 733–743. https://doi.org/10.1016/j.tplants.2020.03.014

Lupo, M., Cristofori, V., & Silvestri, C. (2025). Lighting the way: exploring LED-driven enhancements in service tree (*Sorbus domestica* L.) micropropagation and phytochemical contents. *Plant Cell, Tiss Organ Cult, 160*, 3. https://doi.org/10.1007/s11240-025-01929-0

Melotto, M., Underwood, W., & He, S. Y. (2008). Role of stomata in plant innate immunity and foliar bacterial diseases. *Annual review of phytopathology, 46*, 101–122. https://doi.org/10.1146/annurev.phyto.121107.104959

Mendes, R., Kruijt, M., de Bruijn, I., Dekkers, E., van der Voort, M., Schneider, J. H., Piceno, Y. M., DeSantis, T. Z., Andersen, G. L., Bakker, P. A., & Raaijmakers, J. M. (2011). Deciphering the rhizosphere microbiome for disease-suppressive bacteria. *Science, 332*(6033), 1097–1100. https://doi.org/10.1126/science.1203980

Michelotti, V., Lamontanara, A., Buriani, G., Orrù, L., Cellini, A., Donati, I., Vanneste, J. L., Cattivelli, L., Tacconi, G., & Spinelli, F. (2018). Comparative transcriptome analysis of the interaction between *Actinidia chinensis* var. chinensis and *Pseudomonas syringae* pv. *actinidiae* in absence and presence of acibenzolar-S-methyl. *BMC genomics, 19*(1), 585. https://doi.org/10.1186/s12864-018-4967-4

Mittler, R., Zandalinas, S. I., Fichman, Y., & Van Breusegem, F. (2022). Reactive oxygen species signalling in plant stress responses. *Nature Reviews Molecular Cell Biology*, *23*(10), 663–679. https://doi.org/10.1038/s41580-022-00499-2

Miya, A., Albert, P., Shinya, T., Desaki, Y., Ichimura, K., Shirasu, K., Narusaka, Y., Kawakami, N., Kaku, H., & Shibuya, N. (2007). CERK1, a LysM receptor kinase, is essential for chitin elicitor signaling in *Arabidopsis*. *Proceedings of the National Academy of Sciences of the United States of America*, *104*(49), 19613–19618. https://doi.org/10.1073/pnas.0705147104

Movahedi, A., Aghaei-Dargiri, S., Barati, B., Kadkhodaei, S., Wei, H., Sangari, S., Yang, L., & Xu, C. (2022). Plant immunity is regulated by biological, genetic, and epigenetic factors. *Agronomy*, *12*(11), 2790. https://doi.org/10.3390/agronomy12112790

Naseem, M., Kaltdorf, M., & Dandekar, T. (2015). The nexus between growth and defence signalling: auxin and cytokinin modulate plant immune response pathways. *Journal of Experimental Botany*, *66*(16), 4885–4896. https://doi.org/10.1093/jxb/erv29

Ngou, B. P. M., Ding, P., & Jones, J. D. G. (2022). Thirty years of resistance: Zig-zag through the plant immune system. *The Plant Cell*, *34*(5), 1447–1478. https://doi.org/10.1093/plcell/koac041

Nunes da Silva, M., Machado, J., Balestra, G. M., Mazzaglia, A., Vasconcelos, M. W., & Carvalho, S. M. P. (2019). Exploring the expression of defence-related genes in *Actinidia* spp. after infection with *Pseudomonas syringae* pv. *actinidiae* and pv. *actinidifoliorum*: First steps. *European Journal of Horticultural Science*, *84*(4), 206–212. https://doi.org/10.17660/eJHS.2019/84.4.2

Oliveira-Fernandes, J., Oliveira-Pinto, P. R., Mariz-Ponte, N., Sousa, R. M. O. F., & Santos, C. (2023). *Satureja montana* and *Mentha pulegium* essential oils' antimicrobial properties against *Pseudomonas syringae* pv. *actinidiae* and elicitor potential through the modulation of kiwifruit hormonal defenses. *Microbiological Research*, *277*, 127490. https://doi.org/10.1016/j.micres.2023.127490

Oliveira-Pinto, P. R., Mariz-Ponte, N., Gil, R. L., Cunha, E., Amorim, C. G., Montenegro, M. C., Fernandes-Ferreira, M., Sousa, R. M. O. F., Santos, C. (2022). Montmorillonite nanoclay and formulation with *Satureja montana* essential oil as a tool to alleviate *Xanthomonas euvesicatoria* load on *Solanum lycopersicum*. *Applied Nano*, *3*, 126–142. https://doi.org/10.3390/applnano3030009

Petriccione, M., Mastrobuoni, F., Zampella, L., & Scortichini, M. (2015). Reference gene selection for normalization of RT-qPCR gene expression data from *Actinidia deliciosa* leaves infected with *Pseudomonas syringae* pv. *actinidiae*. *Scientific Reports*, *5*, 16961. https://doi.org/10.1038/srep16961

Pieterse, C. M., Van der Does, D., Zamioudis, C., Leon-Reyes, A., & Van Wees, S. C. (2012). Hormonal modulation of plant immunity. *Annual Review of Cell and Developmental Biology*, *28*, 489–521. https://doi.org/10.1146/annurev-cellbio-092910-154055

Pieterse, C. M., van Wees, S. C., van Pelt, J. A., Knoester, M., Laan, R., Gerrits, H., et al. (1998). A novel signaling pathway controlling induced systemic resistance in *Arabidopsis*. *Plant Cell*, *10*, 1571–1580. https://doi.org/10.1105/tpc.10.9.1571

Rouphael, Y., Colla, G., Graziani, G., et al. (2017). Phenolic composition, antioxidant activity, and mineral profile in two seed-propagated artichoke cultivars as affected by microbial inoculants and planting time. *Food Chemistry*, *234*, 10–19. https://doi.org/10.1016/j.foodchem.2017.04.175

Santoyo, G., Moreno-Hagelsieb, G., Orozco-Mosqueda, M. del C., & Glick, B. R. (2016). Plant growth-promoting bacterial endophytes. *Microbiological Research*, *183*, 92–99. https://doi.org/10.1016/j.micres.2015.11.008

Savian, F., Marroni, F., Ermacora, P., Firrao, G., Martini, M. (2022). A metabarcoding approach to investigate fungal and oomycete communities associated with Kiwifruit Vine Decline Syndrome in Italy. *Phytobiomes Journal*, *6*, 290–304. https://doi.org/10.1094/PBIOMES-03-22-0019-R

Schmittgen, T. D., & Livak, K. J. (2008). Analyzing real-time PCR data by the comparative C(T) method. *Nature Protocols*, *3*(6), 1101–1108. https://doi.org/10.1038/nprot.2008.73

Shah, J., Chaturvedi, R., Chowdhury, Z., Venables, B., & Petros, R. A. (2014). Signaling by small metabolites in systemic acquired resistance. *Plant Journal*, *79*(4), 645–658. https://doi.org/10.1111/tpj.12464

Simmons, T., Caddell, D. F., Deng, S., & Coleman-Derr, D. (2018). Exploring the root microbiome: Extracting bacterial community data from the soil, rhizosphere, and root endosphere. *Journal of Visualized Experiments: JoVE*, *135*, 57561. https://doi.org/10.3791/57561

Sorrenti, G., Toselli, M., & Spinelli, F. (2016). Implicazioni della gestione idrica nella "Moria del kiwi" del veronese.

Staswick, P. E., & Tiryaki, I. (2004). The oxylipin signal jasmonic acid is activated by an enzyme that conjugates it to isoleucine in *Arabidopsis*. *The Plant Cell*, *16*(8), 2117–2127. https://doi.org/10.1105/tpc.104.023549

Ton, J., Flors, V., & Mauch-Mani, B. (2009). The multifaceted role of ABA in disease resistance. *Trends in Plant Science*, *14*(6), 310–317. https://doi.org/10.1016/j.tplants.2009.03.006

Tosi, L., Tacconi, G., Giacopini, A. (2015). La moria del kiwi, situazione e prospettive. *L'Informatore Agrario*, *44*, 67–70.

Turco, S., Brugneti, F., Giubilei, I., Silvestri, C., Petrovic, M., Drais, M. I., Cristofori, V., Speranza, S., Mazzaglia, A., Contarini, M., Rossini, L. (2024). A bud's life: Metabarcoding analysis to characterize hazelnut big buds microbiome biodiversity. *Microbiological Research*, *127851*. https://doi.org/10.1016/j.micres.2024.127851

Umezawa, T., Sugiyama, N., Mizoguchi, M., Hayashi, S., Myouga, F., Yamaguchi-Shinozaki, K., Ishihama, Y., Hirayama, T., & Shinozaki, K. (2009). Type 2C protein phosphatases directly regulate abscisic acid-activated protein kinases in *Arabidopsis*. *Proceedings of the National Academy of Sciences of the United States of America*, *106*(41), 17588–17593. https://doi.org/10.1073/pnas.0907095106

van Meulebroek, L., vanden Bussche, J., Steppe, K., Vanhaecke, L. (2012). Ultra-high performance liquid chromatography coupled to high resolution Orbitrap mass spectrometry for metabolomic profiling of the endogenous phytohormonal status of the tomato plant. *Journal of Chromatography A*, *1260*, 67–80. https://doi.org/10.1016/j.chroma.2012.08.047

Vlot, A. C., Dempsey, D. A., & Klessig, D. F. (2009). Salicylic acid, a multifaceted hormone to combat disease. *Annual Review of Phytopathology*, *47*, 177–206. https://doi.org/10.1146/annurev.phyto.050908.135202

Vos, I. A., Moritz, L., Pieterse, C. M., & Van Wees, S. C. (2015). Impact of hormonal crosstalk on plant resistance and fitness under multi-attacker conditions. *Frontiers in Plant Science*, *6*, 639. https://doi.org/10.3389/fpls.2015.00639

Waheed, A., Haxim, Y., Islam, W., Kahar, G., Liu, X., & Zhang, D. (2022). Role of pathogen's effectors in understanding host-pathogen interaction. *Biochimica et Biophysica Acta - Molecular Cell Research*, *1869*(12), 119347. https://doi.org/10.1016/j.bbamcr.2022.119347

Wang, J., Hu, M., Wang, J., Qi, J., Han, Z., Wang, G., Qi, Y., Wang, H. W., Zhou, J. M., & Chai, J. (2019). Reconstitution and structure of a plant NLR resistosome conferring immunity. *Science (New York, N.Y.)*, *364*(6435), eaav5870. https://doi.org/10.1126/science.aav5870

Wang, K. L., Li, H., & Ecker, J. R. (2002). Ethylene biosynthesis and signaling networks. *The Plant Cell*, *14*(Suppl), S131–S151. https://doi.org/10.1105/tpc.001768

Wang, T., Jia, Z. H., Zhang, J. Y., Liu, M., Guo, Z. R., & Wang, G. (2020). Identification and analysis of NBS-LRR genes in *Actinidia chinensis* genome. *Plants*, *9*(10), 1350. https://doi.org/10.3390/plants9101350

Wasternack, C., & Hause, B. (2013). Jasmonates: biosynthesis, perception, signal transduction, and action in plant stress response, growth, and development. *Annals of Botany*, *111*(6), 1021–1058. https://doi.org/10.1093/aob/mct067

Wurms, K., Ah Chee, A., Stannard, K., Anderson, R., Jensen, D., Cooney, J., & Hedderley, D. (2022). Defence responses associated with elicitor-induced, cultivar-associated resistance to Latania scale in *Kiwifruit*. *Plants*, *11*(1), 10. https://doi.org/10.3390/plants11010010

Xiong, L., & Zhu, J. K. (2003). Regulation of abscisic acid biosynthesis. *Plant Physiology*, *133*(1), 29–36. https://doi.org/10.1104/pp.103.025395

Yang, D. L., Yao, J., Mei, C. S., Tong, X. H., Zeng, L. J., Li, Q., Xiao, L. T., Sun, T. P., Li, J., Deng, X. W., Lee, C. M., Thomashow, M. F., Yang, Y., He, Z., & He, S. Y. (2012). Plant hormone jasmonate prioritizes defense over growth by interfering with gibberellin signaling cascade. *Proceedings of the National Academy of Sciences of the United States of America*, *109*(19), E1192–E1200. https://doi.org/10.1073/pnas.1201616109

Yang, S. F., & Hoffman, N. E. (1984). Ethylene biosynthesis and its regulation in higher plants. *Annual Review of Plant Physiology*, *35*(1), 159–189. https://doi.org/10.1146/annurev.pp.35.060184.001103

Zgadzaj, R., Garrido-Oter, R., Jensen, D. B., Koprivova, A., Schulze-Lefert, P., & Radutoiu, S. (2016). Root nodule symbiosis in *Lotus japonicus* drives the establishment of distinctive rhizosphere, root, and nodule bacterial communities. *Proceedings of the National Academy of Sciences of the United States of America*, *113*(49), E7996–E8005. https://doi.org/10.1073/pnas.1616564113

Zhong, Q., Hu, H., Fan, B., Zhu, C., Chen, Z., & Pěnčík, A. (2021). Biosynthesis and roles of salicylic acid in balancing stress response and growth in plants. *International Journal of Molecular Sciences*, *22*, 11672. https://doi.org/10.3390/ijms221111672

Zhou, J. M., Trifa, Y., Silva, H., Pontier, D., Lam, E., Shah, J., et al. (2000). NPR1 differentially interacts with members of the TGA/OBF family of transcription factors that bind an element of the PR-1 gene required for induction by salicylic acid. *Molecular Plant-Microbe Interactions*, *13*(2), 191–202. https://doi.org/10.1094/MPMI.2000.13.2.191

3.6 Supplementary material

Figure S3.1 - Sampling sites showing Area A (red), characterized by a higher prevalence of KVDS-affected plants, and Area B (blue), where most plants exhibit no canopy symptoms related to KVDS. Each dot represents a group of three plants (asymptomatic [ASM] and symptomatic [KVDS]).

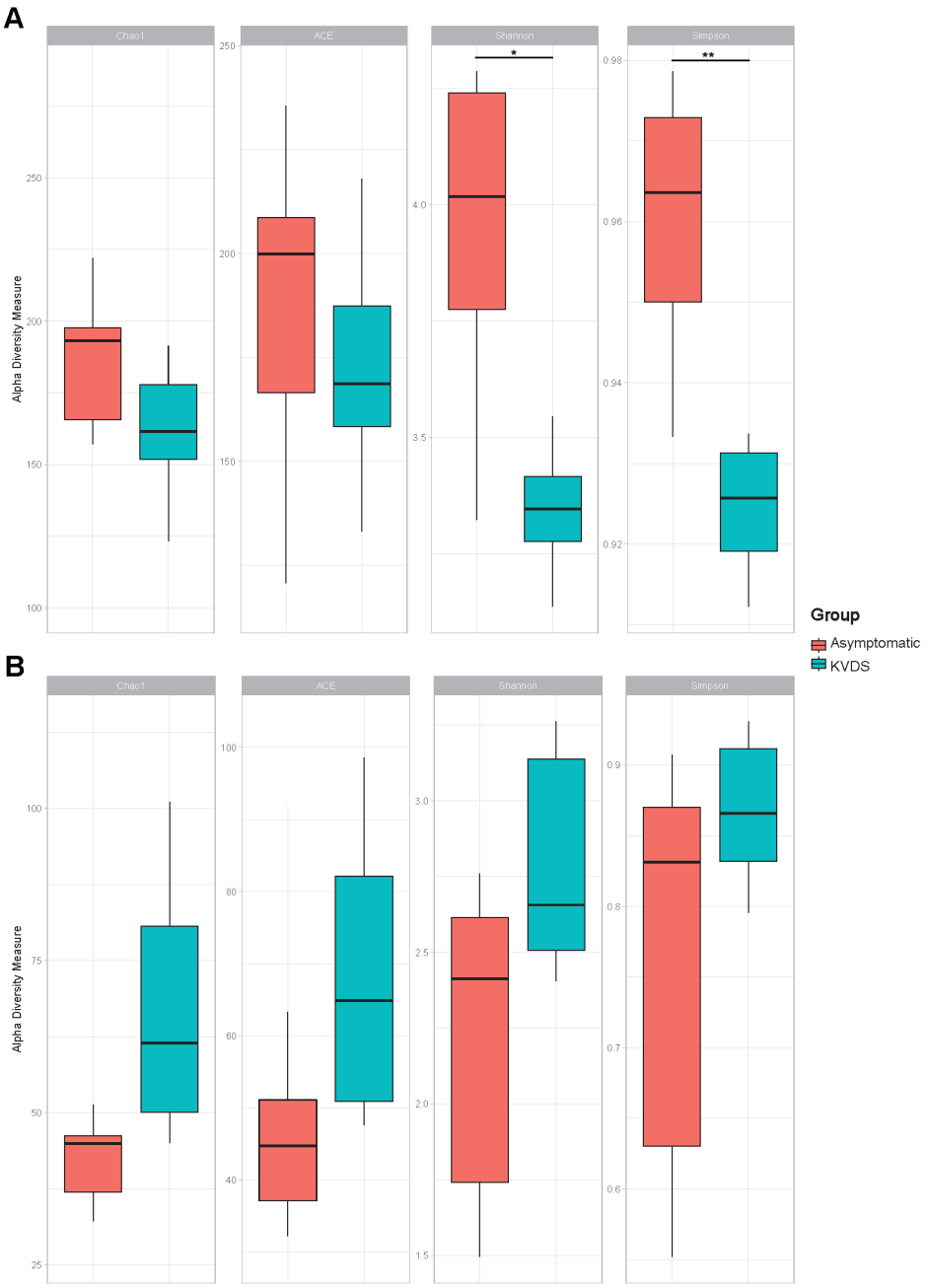

Figure S3.2 - Alpha diversity of the bacterial (A) and fungal (B) communities in asymptomatic (pink) and KVDS (blue) samples. Diversity metrics include richness indicators (Chao1 and ACE indexes) and within-sample diversity measures (Shannon and Simpson indexes). Significant differences ($p < 0.05$) were observed in the Shannon index, while highly significant differences ($p < 0.01$) were observed in the Simpson index in bacterial communities. No significant differences were observed in fungal communities.

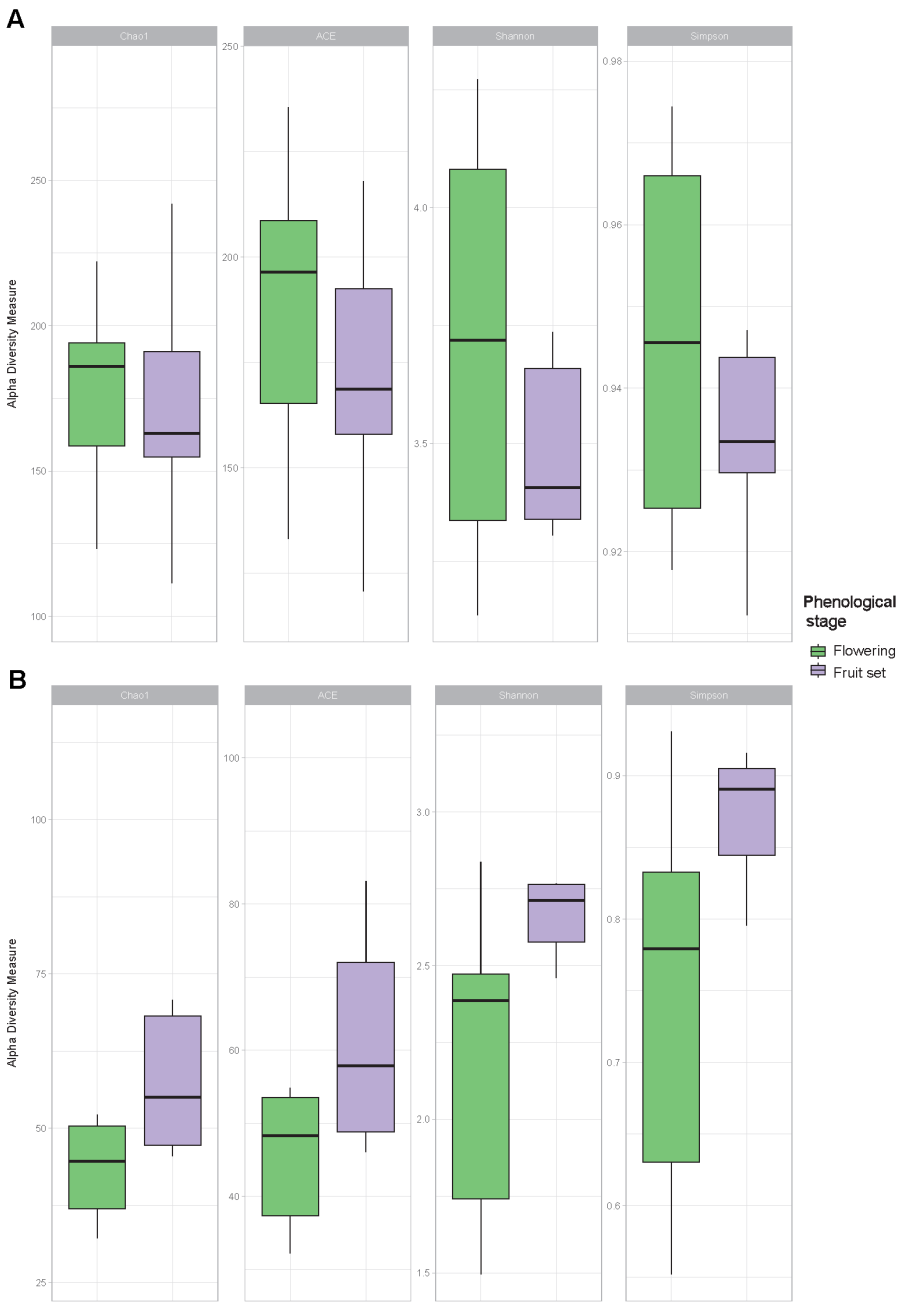

Figure S3.3 - Alpha diversity of the bacterial (A) and fungal (B) communities during the flowering (green) stage and the fruit set (purple) stage. Diversity metrics include richness indicators (Chao1 and ACE indexes) and within-sample diversity measures (Shannon and Simpson indexes). No significant differences were observed in both communities in all indexes.

Table S3.1 - List of target genes, accession numbers, gene functions, and primer pairs

Gene	Function	Primers	Sequences (5'-3')	ID or reference
Ac18S	18S rRNA	Ac18S_F Ac18S_R	CTGTGAAACTGCGAATGGCTC TTCCAGAAGTCGGGGTTTGT	Ferradás et al., 2016
AcAAO	Indole-3-acetaldehyde oxidase	AcAAO_F AcAAO_R	AAGTATGACCCTGTGCGTGA CGTGGAAACCCGAAAACCTT	*De novo* CEY00_Acc16452
AcACT	Actin	AcACT_F AcACT_R	CCAAGGCCAACAGAGAGAAG GACGGAGGATAGCATGAGGA	Ledger et al., 2010
AcAPX	Ascorbate peroxidase	AcAPX_F AcAPX_R	GGAGCCGATCAAGGAACAGT AACGGAATATCAGGGCCTCC	Petriccione et al., 2015
AcCAT	Catalase	AcCAT_F AcCAT_R	GCTTGGACCCAACTATCTGC TTGACCTCCTCATCCCTGTG	Petriccione et al., 2015
AcCERK1	LysM domain receptor-like kinase 3	AcCERK1_F AcCERK1_R	TGGCGACTCAAAACTATGCG CCAAAGTATCACCCGGCCTA	*De novo* CEY00_Acc19243
AcCHI	Chitinase	AcCHI_F AcCHI_R	GAACCATCCGGAATACATCG GCCAAAGTGTCGTTCTTGGT	Francesconi et al., 2024
AcGADPH	Glyceraldehyde 3-phosphate dehydrogenase	AcGADPH_F AcGADPH_R	GTTCCCACTGTCGATGTCTCA CCCTTCATCTTGCCCTCAGA	Petriccione et al., 2015
AcJAR1	Jasmonate resistant 1	AcJAR1_F AcJAR1_R	TTCATTTGCCCACAGCA TTTGGCTTGAGCAGTTTTGA	Wurms et al., 2022
AcLOX1	Lipoxygenase	AcLOX1_F AcLOX1_R	GTTAGAGGGGTGGTGACTCT CTTTAGCACTGCTTGGTTGC	Nunes da Silva et al., 2019
AcNPR1	Non-expresser of PR genes 1	AcNPR1_F AcNPR1_R	TCTAACCAAGGGTGCCCGAC CCAGGCAACGGATCTCTCCT	Francesconi et al., 2024
AcPAL	Phenylalanine ammonia lyase	AcPAL_F AcPAL_R	CGGAGCAACACAACCAAGA CTGACATAGTGCGACTACATAG	Cellini et al., 2014
AcPP2C	Protein phosphatase-2C	AcPP2C_F AcPP2C_R	TTTTGCGGGAGGAGATGTCT ATTATCACGAGGCACCGACA	*De novo* CEY00_Acc11393
AcPR1	Pathogenesis-related protein 1	AcPR1_F AcPR1_R	GAGAAGCCCGACTATAAC CGAACCAAGACCCCACTAT	Michelotti et al., 2018
AcRPM1	RPM1-interacting protein 4-like	AcRPM1_F AcRPM1_R	AGTTCTAGCCCTTCCTCTGA GTCTTGACACTTCCTTTGGC	*De novo* CEY00_Acc00158
AcRPP13	Disease resistance RPP13-like protein	AcRPP13_F AcRPP13_R	TCCAACACCAGTGACAATGA CCTGATAGGCCTGGTTGATT	*De novo* CEY00_Acc17404
AcSAM	S-Adenosyl-L-methionine synthetase	AcSAM_F AcSAM_R	GAATAGTACTTGCCCCTGGC TACAAATCGACCAGAGGGGT	Nunes da Silva et al., 2019
AcSOD	Superoxide dismutase	AcSOD_F AcSOD_R	CACAAGAAGCACCACCAGAC TCTGCAATTTGACGACGGTG	Petriccione et al., 2015
AcTLP1	Thaumatin-like protein	AcTLP1_F AcTLP1_R	CAACCCCCTAACACACTAGC ATTTCCGGAGTTGCAACAGT	Nunes da Silva et al., 2019
AcXanDH	Xanthoxin dehydrogenase	AcXanDH_F AcXanDH_R	ACATGCATACACTGGGTCCA GAGTTAGCCACATCAGCAGC	*De novo* CEY00_Acc09261

Table S3.2 - Average of quality metrics and percentage of reads

16S								
Group	Time point	Input	Filtered	% of input passed filter	Denoised	Non-chimeric	% of input non-chimeric	ASVs
Asymptomatic	Flowering	737.883	683.897	92,69	677.086,00	669.718,00	91	5.866
Asymptomatic	Fruit set	731.551	681.863	93,21	677.735,00	674.772,00	92,23	3.221
KVDS	Flowering	763.306	711.520	93,2	706.758,00	701.708,00	91,9	4.335
KVDS	Fruit set	723.791	658.784	91,02	653.496,00	647.076,00	89,4	5.202

ITS								
Group	Time point	Input	Filtered	% of input passed filter	Denoised	Non-chimeric	% of input non-chimeric	ASVs
Asymptomatic	Flowering	705.225	468.741	66,4	467.663,00	454.413,00	64	1.046
Asymptomatic	Fruit set	679.452	382.012	56,25	381.249,00	376.333,00	55,41	830
KVDS	Flowering	639.573	369.437	57,69	368.583,00	364.595,00	56,93	1.110
KVDS	Fruit set	769.376	479.035	62,27	477.184,00	452.882,00	58,86	1.287

Table S3.3 – PERMANOVA results of bacterial communities' composition, indicating the partitioning of variation based on group (asymptomatic and KVDS), sampling time-point (flowering and fruit set).

	Df	*Sum of Sqs*	*R^2*	*F*	*P(>F)*
GROUP	1	0.66105	0.40688	7.7380	0.001 **
PHENOLOGICAL STAGE	1	0.19476	0.11987	2.2797	0.075
RESIDUAL	9	0.76886	0.47324		

*Signif. codes: 0 '***' 0.001 '**' 0.01 '*' 0.05 '.' 0.1 ' ' 1*

Table S3.4 – PERMANOVA results of fungal communities' composition, indicating the partitioning of variation based on group (asymptomatic and KVDS), sampling time-point (flowering and fruit set).

	Df	*Sum of Sqs*	*R^2*	*F*	*P(>F)*
GROUP	1	0.67516	0.22759	3.2612	0.001 **
PHENOLOGICAL STAGE	1	0.42816	0.14433	2.0682	0.050 *
RESIDUAL	9	1.86323	0.62808		

*Signif. codes: 0 '***' 0.001 '**' 0.01 '*' 0.05 '.' 0.1 ' ' 1*

Chapter 4

Assessing the fungal rhizosphere microbiome of *Ficus* as a potential replacement crop for KVDS-affected *Actinidia* orchards

Antonella Cardacino[1], Mattia Animobono[1], Silvia Turco[1], Giorgio Mariano Balestra[1]

[1] *Department of Agriculture and Forest Sciences, University of Tuscia, Viterbo, Italy*

Abstract

Since 2012, Kiwifruit Vine Decline Syndrome (KVDS) has significantly impacted kiwifruit production and cultivation across all Italian orchards. Various agronomic interventions, including bed-forming, improved irrigation, shading nets, and enhanced soil aeration, have been implemented to mitigate and contain the disease. However, the containment of KVDS remains challenging. Alternatively, the replacement of kiwifruit with different tree species was considered, since replanting is not allowed and is strongly discouraged. Plants belonging to the *Ficus* genus, known for their adaptability to different environments and disease resistance, were considered a promising replacement crop. In this study, to assess the potential impact of this strategy, fig trees were cultivated in a portion of an aged kiwifruit orchard located in Cisterna di Latina (Lazio Region, Italy) where the KVDS-affected plants had been removed. The rhizosphere fungal microbiome of both *Actinidia* plants affected by KVDS and *Ficus* plants was then investigated to characterize the fungal communities in the rhizosphere, identify significant differences in their fungal microbiome composition, and evaluate the ability of fig plants to influence and potentially reshape the rhizosphere microbiome.

Keywords: metagenomics, microbiome, microbial communities, KVDS, rhizosphere

4.1 Introduction

Kiwifruit Vine Decline Syndrome (KVDS) is a significant threat to Italian agriculture, threatening both the productivity and long-term sustainability of kiwifruit orchards. Over the past decade, this emerging disease has resulted in substantial economic losses, with damages estimated to reach 300,000 euros in 2020 alone (Mian et al., 2023). Italy is the world's third largest producer of kiwifruit, after China and New Zealand, with a total production volume of 391,100 tons in 2023 (FAOSTAT, 2024). The first documented outbreaks of Kiwifruit Vine Decline Syndrome (KVDS) in Italy occurred in 2012, affecting multiple orchards in the Veneto region. Since then, the disease has spread rapidly, impacting major kiwifruit-producing regions across northern (Veneto, Piedmont, and Friuli Venezia Giulia), central (Lazio and Emilia-Romagna), and southern Italy (Calabria) (Sorrenti et al., 2019). Savian et al. (2020) estimate that KVDS has affected approximately 25% of Italian orchards, highlighting the severity of its impact on national kiwifruit production. Although KVDS is primarily concentrated in Italy, similar disorders have recently been reported in other countries, including Turkey (Kurbetli et al., 2013) and China (Wang et al., 2015). These cases were associated with environmental factors such as waterlogging, which are similar to the conditions associated with the onset of KVDS. This suggests a potential risk of the syndrome spreading to other kiwifruit-producing regions in the absence of effective mitigation strategies.

The syndrome is characterized by foliar symptoms such as leaf curling, and twig wilting, along with root system damage, including browning cortex detachment, and loss of feeding roots (Donati et al., 2020). While its exact etiology remains under investigation, KVDS is now recognized as a multifactorial disease influenced by both biotic and abiotic factors. Imbalances in the root microbiome and adverse soil and climatic conditions such as waterlogging, rising temperatures, and hypoxia are key contributors. Pathogens, including oomycetes (*Phytophthora spp.*, *Pythium spp.*, *Phytopythium spp.*), fungi (*Cylindrocarpon spp.*, *Fusarium spp.*), and bacteria (*Clostridium spp.* and *Ralstonia sp.*), have been identified in plants affected by KVDS (Bardi et al., 2020; Spigaglia et al., 2020; Savian et al., 2022; Cardacino et al., 2025). However, the presence of these microorganisms alone does not fully explain KVDS

onset, as environmental stressors and host susceptibility play crucial roles, underscoring the complexity of the syndrome.

Abiotic stressors, particularly waterlogging, are major contributors to KVDS. Kiwifruit plants are highly susceptible to hypoxic conditions caused by waterlogged soils because their roots have a limited capacity for oxygen diffusion (Reid et al., 1992; Smith et al., 1989). Even short-term episodes of waterlogging can severely impair root functionality (Jackson and Drew, 1984). The intensification of waterlogging due to climate change, specifically through altered rainfall patterns and an increased frequency of intense precipitation events, is further compounded by the characteristics of heavy soils common in affected regions. High temperatures play a significant role in the onset and progression of Kiwifruit Vine Decline Syndrome (KVDS). Elevated temperatures can exacerbate abiotic stress on kiwifruit plants, particularly by increasing evapotranspiration rates and further compromising root system functionality (Spadaro et al., 2020). As the plants' roots become damaged, their ability to uptake water and nutrients is reduced, leading to enhanced susceptibility to the syndrome. In addition, high temperatures can amplify soil moisture deficits, contributing to conditions such as waterlogging, which are known to trigger KVDS symptoms. The combined effects of heat stress and compromised root systems create a favourable environment for the syndrome to manifest, underlining the importance of temperature regulation and environmental management in mitigating the disease. On the other hand, repeated cropping on the same soils may also contribute to KVDS through replant diseases that deplete soil fertility and select harmful microbiomes. Pathogens such as *Dactylonectria spp.* and *Fusarium spp.*, commonly associated with replant disease, have been linked to KVDS (Manici et al., 2021, 2024). The rhizosphere, the soil zone immediately adjacent to plant roots, is critical to plant health because it harbours a wide variety of organisms that interact with the plant in beneficial, commensal, or pathogenic ways (Hinsinger et al., 2009; Bonkowski et al., 2009). Beneficial bacteria and fungi promote plant growth by producing phytohormones and enhancing nutrient uptake (Compant et al., 2019; Rascovan et al., 2016). In addition, these microorganisms enhance plant defence against pathogens through commensal-pathogen interactions, antibiotic production, emission of pathogen-suppressing volatiles, or induction of systemic resistance (Babalola et al., 2020). Conversely, the depletion of beneficial microbes

and the proliferation of pathogens in the rhizosphere exacerbate the decline in plant health and increase disease susceptibility (Bergamaschi et al., 2024). This was demonstrated by Guaschino et al. (2024), who found that oomycetes associated with KVDS were negatively correlated with saprobes and plant growth-promoting fungal genera in the rhizosphere of kiwifruit plants affected by the syndrome, in contrast to the rhizosphere of healthy plants. Thus, the composition of the plant-associated microbiome is influenced by complex interactions between host plants, environmental factors, and microbial communities. Root exudates, acting as substrates, chemotactic agents, or signalling molecules, play a key role in shaping this microbiome (Chaparro et al., 2014). Environmental factors, including plant developmental stage, soil and climatic conditions, and plant health, also significantly influence microbiome composition. Climate change has emerged as a critical factor that may reduce plants' control over their microbiomes, thereby increasing the likelihood of dysbiosis and increased susceptibility to disease (Trivedi et al., 2022). For example, waterlogging can promote the production of stress-related hormones (e.g., ethylene) and metabolites (e.g., ethanol) by altering oxygen availability, shifting microbial communities, and modifying root exudate profiles. These changes can attract root pathogens such as *Fusarium spp*. and *Phytophthora spp*. (Smucker and Erickson, 1987; Blokhina et al., 2003; Voesenek et al., 2013; Martínez-Arias et al., 2022). To address the effects of KVDS, farmers have explored various agronomic strategies, including improving soil structure, using tolerant rootstocks, and optimizing irrigation practices (D'Ippolito et al., 2022; Mian et al., 2022). However, these approaches have not consistently provided definitive solutions. A promising alternative is the introduction of other crops, such as those belonging to the *Ficus* genera, like fig (*Ficus carica*), known to be highly resistant to biotic stressors, thanks to physical defenses such as tough leaves and trichomes, as well as biochemical strategies such as alkaloids, terpenoids, phenolics, and defense proteins (Villard et al., 2019). Furthermore, fig trees thrive in warm climates with hot summers and mild winters but can also adapt to less favourable conditions and grow in a variety of soils, from sandy to heavy clay, without significant nutrient deficiencies (Khadivi et al., 2018). Hence, incorporating fig into crop rotations could reduce economic losses from KVDS and promote sustainable agriculture by enhancing beneficial microbial communities (Rahmani et al., 2017). The fig tree (*Ficus carica* L.) is one of

the oldest cultivated plants, native to the Middle East and domesticated in the Mediterranean region (Ayuso et al., 2022), which currently accounts for approximately 70% of the world's fig production (FAO, 2023). Understanding the mechanisms that govern microbiome selection in the rhizosphere, along with the implementation of sustainable strategies such as crop diversification, are crucial steps in mitigating this syndrome. While transitioning to alternative crops might appear as a drastic measure, climate change is an inevitable force that will increasingly influence agronomic practices. In particular, the Mediterranean region is projected to experience temperature increases 25% faster than the global average (Alrteimei et al., 2022). Therefore, selecting crops that are well-suited to the local environment and exhibit enhanced resilience to the mounting pressures of climate change represents a pragmatic approach to ensuring both sustainable agricultural production and food security.

This study aimed to characterize the rhizosphere microbiomes of *Actinidia chinensis* var. *deliciosa* and *Ficus carica* cv. 'Paradiso,' the latter grown in soil previously affected by *Actinidia* plants suffering from KVDS. Additionally, the microbiome evolution was analyzed during two critical phases of the growing season, which are pivotal for the development and onset of KVDS.

4.2 Materials and methods

4.2.1 Site description

The experimental field chosen for this study is located in Cisterna di Latina (LT), Italy, at 41 m above sea level. It consists of two plantations: a kiwifruit orchard covering 10,791.83 m^2 and a fig orchard covering 7,368.8 m^2 (Figure S4.1). The kiwifruit orchard (*Actinidia chinensis* var. *deliciosa* cv. 'Hayward'), established in 1998, was managed conventionally, including weed control, pest monitoring, and pruning. A micro-sprinkler system provided irrigation for both orchards with estimated seasonal volumes of 10,000 m^3/ha. Fertilization employed a combined approach, utilizing organic inputs such as manure and other organic fertilizers, supplemented by a fertigation system delivering nitrogen, phosphorus, potassium, and micronutrients. Phytosanitary interventions were limited to applying tribasic

copper sulfate to control *Pseudomonas viridiflava*. To mitigate waterlogging, bed forming was implemented in the root zone to improve aeration and root development. In 2018, a section of the old kiwifruit orchard was replaced with a fig orchard (*Ficus carica* cv. 'Paradiso'). The soil exhibits a predominantly sandy texture with a pH of 6.8 and normal electrical conductivity (Table S4.1) with high levels of nitrogen, phosphorus, calcium, and magnesium, along with a substantial organic matter content (Table S4.2).

4.2.2 Samples collection and DNA extraction

Roots from *Actinidia* plants displaying leaf symptoms consistent with Kiwifruit Vine Decline Syndrome (KVDS) (Figure 4.1) were sampled for further analysis. No discernible disease symptoms were observed on *Ficus carica* plants.

Figure 4.1 - Actinidia plants observed in October 2022 (on the left), and leaf symptoms appearing in early July 2023 (on the right)

Plants were grouped according to a randomized complete block design. For both kiwifruit and fig, three blocks were established, each consisting of four plants, resulting in a total of 24 plants. Sampling was carried out at two time points: during kiwifruit flowering (in May 2022) and its fruit set (in July 2022).

Soil cores (40-50 cm depth) were extracted within a 50 cm radius of each plant using a hand-held core drill. Three cores per plant were collected and combined to form a

single composite sample. Samples were collected in sterile bags, stored at 4°C, air-dried, and sieved (2- and 4-mm mesh) to separate roots from soil. Cleaned roots were stored at -20°C. Actinidia roots exhibited characteristic symptoms of KVDS, including reddish-brown discoloration and rotting, as previously described by Savian et al. (2020) and D'Ippolito et al. (2022) (Figure 4.2).

Figure 4.2 - Actinidia roots showing symptoms of KVDS, taken from one of the observed plants

Rhizosphere soil was removed from roots by sonication in an ultrasonic bath (20°C, 40 kHz, 60-second pulses with 15-second pauses). Roots were subsequently washed three times with sterile phosphate-buffered saline (PBS; 1x, pH 7.4) to remove residual soil particles, and stored at -80°C until DNA extraction. Before DNA extraction, root samples were freeze-dried, ground to a fine powder using a mortar and pestle and then processed. Genomic DNA (gDNA) was extracted from both soil and root samples using the NucleoSpin® Soil kit (Macherey-Nagel) according to the manufacturer's instructions. Approximately 150 mg of soil and 100 mg of root tissue were used for each extraction. A total of 96 samples were processed. Extracted DNA was eluted in 50 µl of TE buffer and stored at -20°C until further analysis. DNA concentration was measured with Qubit™ dsDNA BR Assay Kit.

4.2.3 ITS amplification and sequencing

DNA amplification, library preparation, and Illumina NovaSeq sequencing were performed by Novogene (Cambridge, UK). PCR reactions were conducted using 15 µL of Phusion® High-Fidelity PCR Master Mix (New England Biolabs), 0.2 µM of each primer, and 10 ng of template DNA. PCR cycling conditions included an initial denaturation at 98°C for 1 min, followed by 30 cycles of denaturation at 98°C for 10 s, annealing at 50°C for 30 s, and extension at 72°C for 30 s, with a final extension at 72°C for 5 min. Fungal ITS2 region was amplified using primers ITS3-2024F (5'-GCATCGATGAAGAACGCAGC-3') and ITS4-2409R (5'- TCCTCCGCTTATTGATATGC-3'). Sequencing libraries were prepared, indexed, and quantified using Qubit™ and a real-time qPCR. Library size distribution was assessed using a Bioanalyzer (Agilent, USA). Quantified libraries were pooled and sequenced on the Illumina NovaSeq platform according to library concentration and sequencing depth requirements.

4.2.4 Bioinformatic analysis

Microbiome characterization was performed using the QIIME2 pipeline (QIIME2 v.2023.2.0, Bolyen et al., 2019) adapted by Cardacino et al., (2025) and Turco et al., (2024). Briefly, raw sequence reads were demultiplexed, chimera-filtered, and denoised with DADA2 to generate a feature table containing amplicon sequence variants (ASVs) and representative sequences in FASTA format (Table S4.3). Fungal taxonomic classification employed the classify-consensus-blast algorithm against a custom database built with *Actinidia chinensis* (taxID 3625) and *Ficus carica* sequences (taxID 3494) and the NCBI Fungi RefSeq ITS project (PRJNA177353). Following removal of host-related, uncharacterized, and low-frequency ASVs (Bokulich et al., 2013), the processed data (feature table, taxonomy, representative sequences, and phylogenetic tree) were imported into R RStudio v.2024.09.0 and analyzed with *phyloseq* v.1.50.0 (McMurdie and Holmes, 2013). Rarefaction curves were generated using *vegan* R v.2.6.8 (Dixon, 2003). Alpha diversity (within-sample) was assessed using Shannon, Simpson, Chao1, and ACE indices. Kruskal-Wallis tests were used to compare alpha diversity between factors. Beta diversity

(between-sample dissimilarity) was evaluated using NMDS and PCoA plots based on the Bray-Curtis index. Permutational multivariate analysis of variance (PERMANOVA, 1,000 permutations) was used for statistical testing of beta diversity. Relative abundance of the 30 most abundant genera was visualized, with the least abundant taxa grouped as "<1%." Functional guilds of the identified fungal ASVs were assigned using the *fungaltraits* v.0.0.3 package which leverages information from both the FunGuild and FunFun databases for functional guild assignment (Põlme et al., 2020; Turco et al., 2024).

4.3 Results

4.3.1 Sequencing data summary

Illumina sequencing generated a total of 4.8M reads, with an average of 600K reads per sample (Table S4.2). Following the removal of reads classified as host, uncultured, or unassigned to any Amplicon Sequence Variant (ASV), a total of 775 fungal taxa were imported into the R environment as a *phyloseq* object for subsequent analyses.

4.3.2 Communities richness and diversity

Estimates of microbial richness, based on ACE and Chao1 indices, did not differ significantly between *Actinidia* and *Ficus* rhizosphere communities (Figure 4.3) at either sampling time point (Figure S4.2). In contrast, soil samples exhibited significantly higher richness compared to root samples, as shown in Figure S4.3. Analysis of microbial diversity, using the Simpson and Shannon indices, revealed higher values in *Actinidia* rhizosphere samples compared to *Ficus* rhizosphere samples. Samples collected at the second time point (July) generally exhibited higher diversity compared to the first time point (May). Furthermore, soil samples tended to exhibit higher diversity compared to root samples. However, statistical analyses did not reveal significant differences among these groups.

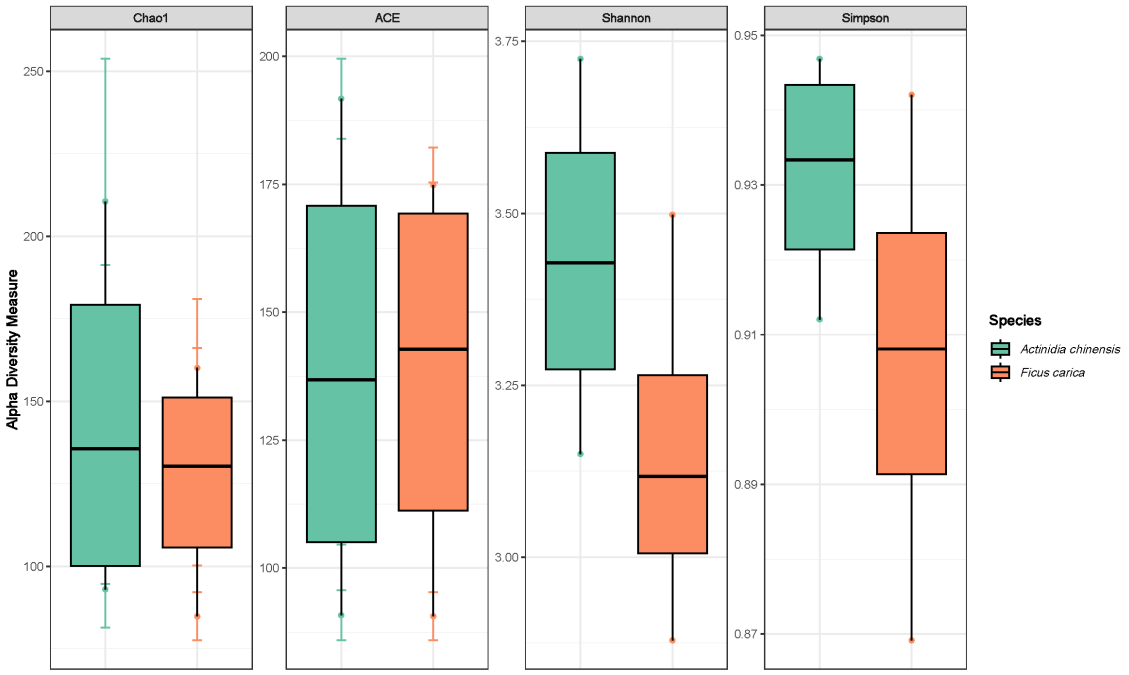

Figure 4.3 - Alpha-diversity of fungal communities in kiwifruit and fig rhizosphere. Box plots represent the distribution of alpha-diversity indices: Chao1 (richness), ACE (richness estimate), Shannon (diversity), and Simpson (dominance). No significant differences (*p≤0.05*) were observed between the two plant rhizospheres for any of the evaluated indices.

4.3.3 Beta-diversity and microbial dissimilarities

Non-metric multidimensional scaling (NMDS) and principal coordinate analysis (PCoA) were employed to assess community dissimilarity. Results revealed distinct clustering of microbial communities associated with *Actinidia* and *Ficus* rhizospheres, highlighting the influence of plant host on rhizosphere microbiome composition (Figure 4.4). Furthermore, significant differences in community structure were observed between sampling time points. These observations were further supported by permutational multivariate analysis of variance (PERMANOVA), which demonstrated significant effects of both plant species (R^2 = 0.423; P < 0.01) and sampling time (R^2 = 0.164; P < 0.05) on fungal community composition (Table S4.4).

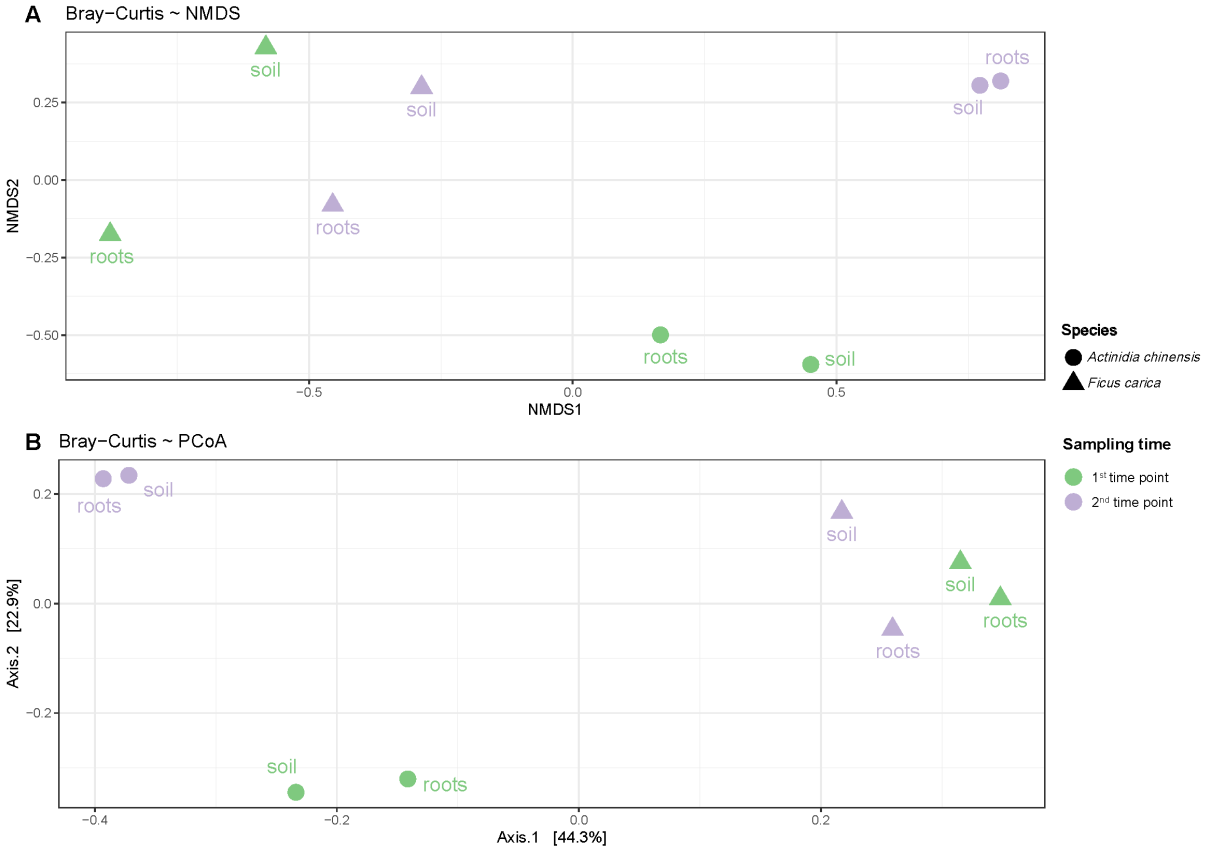

Figure 4.4 - NMDS and PCoA ordinations based on Bray-Curtis dissimilarity of fungal communities (ASV level) in kiwifruit (circles) and fig (triangles) rhizospheres. Samples are color-coded by sampling time: green = May, purple = July.

4.3.4 Exploring the fungal rhizosphere communities

The fungal communities associated with the *Actinidia* rhizosphere were predominantly composed of Ascomycota (67.6%), Basidiomycota (22%), and Mucoromycota (10.4%). Similarly, *Ficus* rhizosphere samples exhibited a high prevalence of Ascomycota (61.6%), Basidiomycota (17.8%), and Mucoromycota (11.6%).

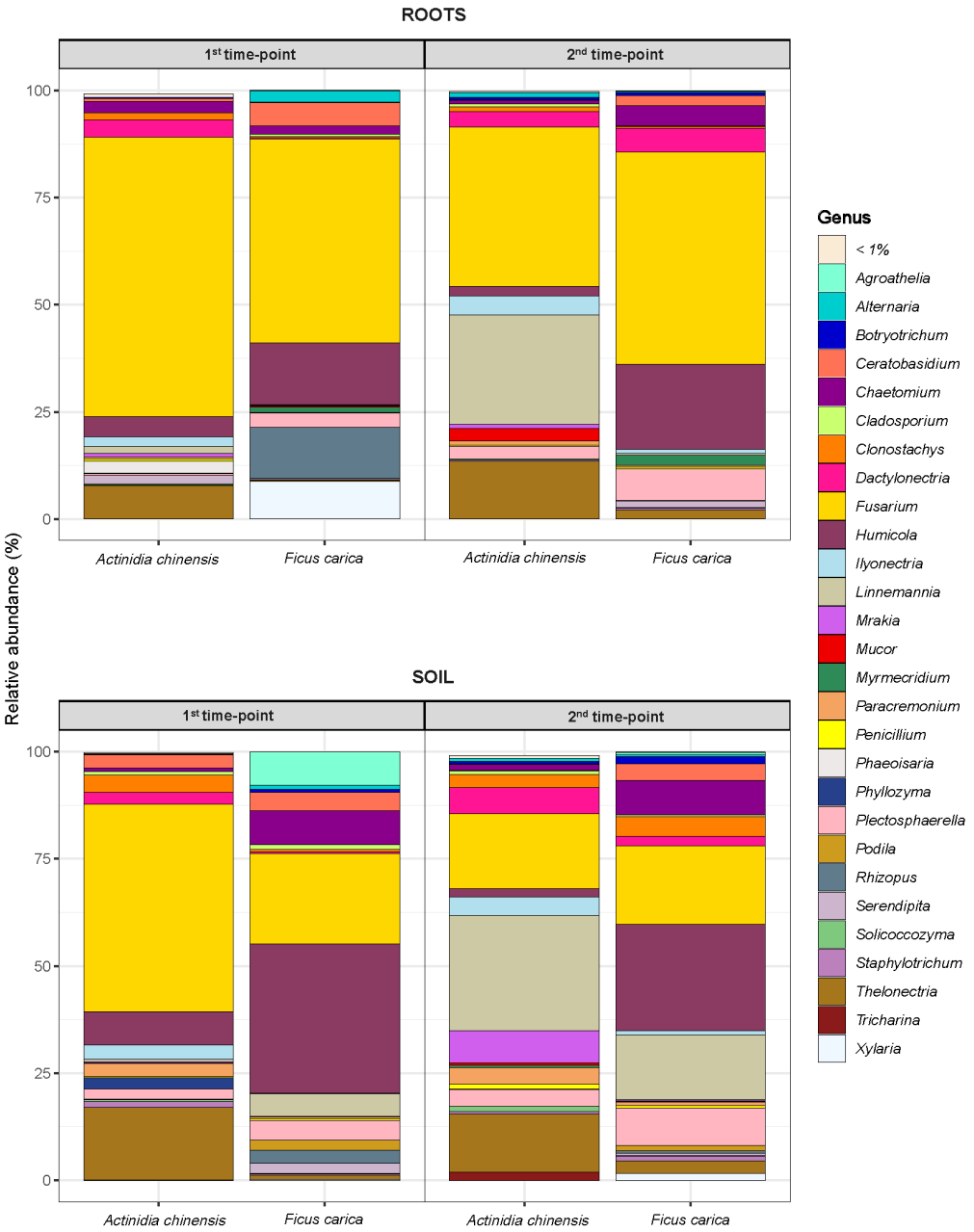

Figure 4.5 - Relative abundance of the top 30 fungal genera in kiwifruit and fig samples – both roots and soil - collected in May and July. Genera are ranked by mean relative abundance across all samples.

At the first collection point in May, *Actinidia* root samples exhibited a high prevalence of *Fusarium* spp. (65.1%), followed by *Thelonectria* (7.8%), *Humicola* (5%), and *Dactylonectria* (4%) (Figure 4.5). Other genera, including *Phaeoisaria, Chaetomium,* and *Ilyonectria*, were present in smaller proportions. Soil samples exhibited a similar fungal community composition, with *Fusarium* spp. identified as the most abundant genus at 48.5%, followed by *Humicola* (7.7%), *Clonostachys* (4%), *Ilyonectria* (3.2%), *Ceratobasidium* (3%), and *Paracremonium* (3%). At the second sampling time point, kiwifruit roots exhibited a distinct fungal community profile, with *Fusarium* spp. dominating at 37%, followed by *Linnemannia* spp. (25.6%) and *Thelonectria* spp. (13.4%). Soil samples exhibited a fungal community composition similar to that of roots, with *Linnemannia* spp. dominating at 27%, followed by *Fusarium* spp. (17.4%) and *Thelonectria* spp. (13.5%). *Mrakia*, *Dactylonectria*, *Ilyonectria*, and *Plectosphaerella* were present at lower relative abundances.

At the first sampling time point, fig root samples exhibited a high prevalence of *Fusarium* sp. (47.5%) genus. Notably, *Humicola* sp. (14.4%), *Rhizopus* sp. (12%), and *Xylaria* sp. (8%) were also prominent members of the fungal community. Fig soil samples demonstrated a distinct fungal community profile compared to kiwifruit samples. *Humicola* sp. was the most prevalent genus in fig soil, accounting for 34.8% of the community. *Fusarium* sp. followed at 21.2%, with *Chaetomium* sp. (7.9%) and *Agroathelia* sp. (7.8%) also present in notable proportions. At the second sampling time point, *Fusarium* spp. was prevalent in both fig root and soil samples, constituting 49.5% of the root community and 18% of the soil community. *Humicola* spp. and *Plectosphaerella* spp. were also abundant, comprising 19.8% and 7.4% of the root community, respectively, and 25% and 8.6% of the soil community. Notably, *Linnemannia* spp. was found at a prevalence of 15% in the soil samples.

The distribution of fungal taxa within the different species and sample types (roots and soil) was investigated and visualized using a Venn diagram (Figure 4.6). A core of 70 ASVs (9% of the total) was shared between soil and root samples across both *Actinidia* and *Ficus* species. The *Actinidia* core microbiota encompassed 75 ASVs (9.7%), predominantly represented by *Thelonectria*, *Fusarium*, *Phyllozyma*, *Penicillium*, *Mortierella*, *Clonostachys*, *Apiotrichum*, *Dactylonectria*, *Chaetomium*, and

Linnemannia. *Ficus* samples exhibited a core of 57 ASVs (7.4%) with *Xylaria*, *Ceratobasidium*, *Chaetomium*, *Fusarium*, *Agroathelia*, and *Serendipita* as the most representative genera. Soil samples from both species demonstrated a high degree of unique ASVs, with 196 and 152 unique ASVs observed in *Actinidia* and *Ficus* soil, respectively. Only two ASVs, *Penicillium* and *Phaeosphaeria*, were shared between *Actinidia* and *Ficus* root samples. In contrast, *Actinidia* and *Ficus* soil samples shared a core of 37 ASVs (4.8%).

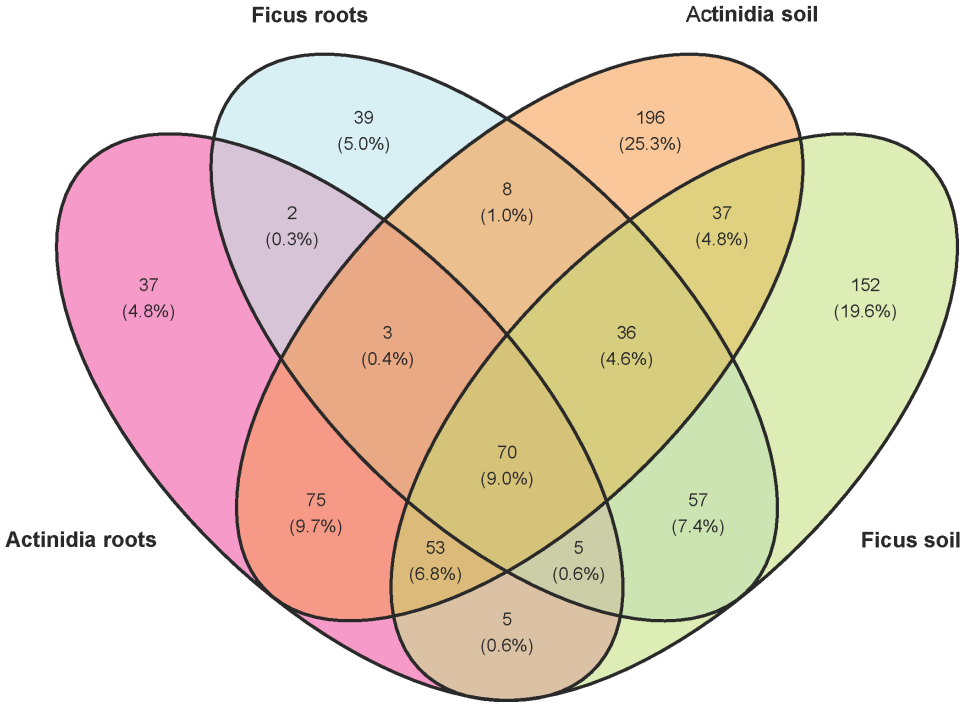

Figure 4.6 - Venn diagram illustrating the number of unique and shared fungal amplicon sequence variants (ASVs) between kiwifruit and fig rhizosphere samples

4.3.5 Assigning ecological functions to microbial communities

The ecological function of the identified fungal taxa, assessed using FungalTraits, revealed a predominance of plant pathogens within the Ascomycota phylum (Figure 4.7), notably represented by *Fusarium*, *Cladosporium*, *Penicillium*, and *Alternaria*. Other fungal taxa were classified as endophytes (*Ilyonectria* and *Chaetomium*) or wood saprophytes (*Xylaria*, *Fusarium*, and *Alternaria*). *Serendipita* and

Ceratobasidium, belonging to the Basidiomycota phylum, were classified as endophytic and ectomycorrhizal fungi, respectively. Within the Zygomycota phylum, *Rhizopus* and *Mucor* were classified as endophytes/plant pathogens.

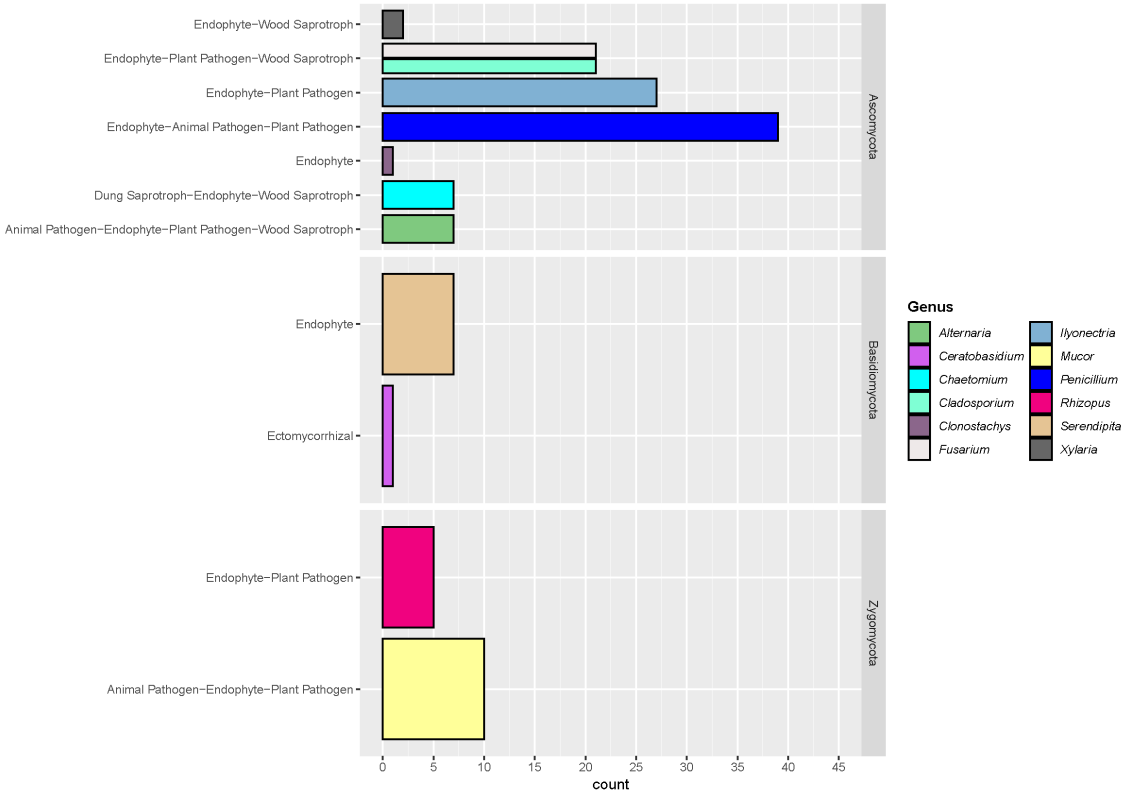

Figure 4.7 - FungalTraits-based assessment of fungal species and their ecological roles within the rhizospheres of kiwifruit and fig plants

4.4 Discussion

The rhizosphere microbiome, a complex community of microorganisms associated with plant roots, plays a crucial role in plant health, growth, and resilience. This microbiome is shaped by various factors, including plant species, soil type, and agricultural practices, all of which influence its structure and function. Different plant species, even when cultivated in homogenous soil, exhibit distinct rhizosphere microbiome compositions, indicating active plant participation in shaping these communities (Berendsen et al., 2012; Qu et al., 2020). This selective recruitment of beneficial microorganisms can contribute to enhanced plant growth and disease

resistance (Pérez-Jaramillo et al., 2015; Qu et al., 2020). Plants exert an influence on the rhizosphere microbiome through the secretion of root exudates and alterations in abiotic conditions. These factors, in turn, affect the composition and function of the microbial community (Berg and Smalla, 2009; Fu et al., 2023). These interactions are crucial for nutrient cycling and pathogen resistance (Hu et al., 2020). The assembly of the rhizosphere microbiome is a multifaceted process influenced by intricate interactions between plant roots and soil microorganisms. Root architecture and exudation patterns have been identified as pivotal factors in this process (Pérez-Jaramillo et al., 2015; Park et al., 2023). However, the influence of plant species on rhizosphere microbiome composition is often less pronounced than that of edaphic factors or agricultural practices. For example, research on wheat has demonstrated that plant genotype explains only a small proportion of the observed variance in rhizosphere microbiome composition (Simonin et al., 2020). Similar observations have been reported in studies conducted across tropical and subtropical regions of China, where site- and soil-related factors exerted a greater influence on the rhizosphere microbiome than plant species (Xu et al., 2019). Soil type is a recognized primary driver of rhizosphere microbiome composition, frequently exhibiting a more substantial impact than plant species. Different studies have established a strong correlation between soil properties and microbial community structure and diversity (Berg and Smalla, 2009; Simonin et al., 2020). These properties, including but not limited to pH, nutrient content, and texture, create distinct environmental niches that favour specific microbial taxa. Furthermore, agricultural practices, particularly fertilization regimes, significantly influence the rhizosphere microbiome. Long-term fertilization, for instance, can induce more substantial alterations in microbial abundance and diversity within the rhizosphere than plant species, potentially through shifts in soil nutrient availability and subsequent effects on microbial community assembly (Semenov et al., 2020). This suggests that anthropogenic influences can override the selective pressures exerted by plants on their rhizosphere microbiome. Despite the strides made in our understanding of these interactions, the precise mechanisms by which plants shape their rhizosphere microbiome remain largely unknown. Further research is needed to explore these interactions and develop strategies to manipulate the microbiome for improved plant health and productivity.

In this study, we characterized the rhizosphere fungal microbiome in kiwifruit plants exhibiting symptoms associated with KVDS and in fig plants grown in a former kiwifruit orchard that had been decommissioned due to the syndrome. The results showed different patterns of microbial genera between the two species during the different time points. This finding was further validated by beta diversity and PERMANOVA analysis.

The most prevalent genus detected in soil and root samples from both species was *Fusarium*, with higher abundance found in actinidia samples. Several *Fusarium* species are linked to kiwifruit diseases, particularly those affecting roots, vascular systems, and postharvest fruit quality. *Fusarium oxysporum* and *Fusarium solani* are the primary species implicated, causing root rot, wilting, vascular discoloration, and plant death. *F. oxysporum* induces vascular wilt, while *F. solani* leads to root and crown rot, reducing kiwifruit yield and vitality (Song et al., 2022). Environmental factors, such as soil moisture, temperature, and irrigation practices, influence the severity and spread of Fusarium infections, with poorly drained soils facilitating disease progression (Yan and Nelson, 2022). Both species have been isolated from kiwifruit roots, manifesting symptoms of KVDS (Savian et al., 2020; D'Ippolito et al., 2022).

The genus *Humicola* was notably present in fig samples from both roots and soil. This genus, from the *Chaetomiaceae* family, is particularly significant in the rhizosphere, where it plays a crucial role in regulating microbial interactions and maintaining plant health. *Humicola* species, including *Humicola phialophoroides*, have been demonstrated a biocontrol potential, such as disease suppression, suggesting their application in plant disease management (Ko et al., 2011). For example, within the rhizosphere of eggplants, the genus *Humicola* was predominant, underscoring its significance in disease suppression and the dynamic equilibrium of the microbiota (Ogundeji et al., 2021). *Linnemannia,* which showed high abundance in kiwifruit samples during the second time point (July), is particularly interesting due to its role in plant health and rhizosphere dynamics. As part of the *Mortierellaceae* family, some species of this genus, like *L. elongata,* promotes plant growth through chitin-based stimulation, attracting beneficial microbes. It enhances shoot and root fresh weight and chlorophyll content in *Arabidopsis thaliana*

(Vandepol et al., 2021; De Tender et al., 2023), likely through auxin production and calcium translocation (De Tender et al., 2023). Its chitinase activity enhances seed germination and plant growth when combined with chitin (De Tender et al., 2023).

The genus *Plectosphaerella*, identified in fig root and soil samples, co-occurs with *Fusarium*, raising interest due to its role as a plant pathogen. *Plectosphaerella* is commonly found in the rhizosphere, where it influences microbial composition. Studies have shown that it often coexists with other pathogens like *Fusarium*, contributing to disease progression (Wang et al., 2021; Jia et al., 2023). Environmental factors, such as irrigation and soil phenolic acid content, affect the abundance and pathogenic behavior of *Plectosphaerella* species (Del Castillo Múnera et al., 2022). The genera *Thelonectria* and *Dactylonectria* were frequently associated with KVDS (references). *Thelonectria* was abundant in actinidia samples, while *Dactylonectria* was detected in both species at both time points. *Dactylonectria* species, responsible for diseases like black foot in grapevines and root rot in kiwifruit, contribute to plant decline through cell wall-degrading enzymes and toxins (Cabral et al., 2012; Álvarez-Pérez et al., 2017; Gramaje et al., 2020). On the other hand, *Thelonectria*, from the *Nectriaceae* family, acts as both a pathogen and saprobe, with species influencing rhizosphere dynamics through complex interactions with other microorganisms (Xiong et al., 2020). Finally, *Chaetomium* was most abundant in fig root and soil samples. Though predominantly a decomposer, some *Chaetomium* species act as opportunistic pathogens, causing root rot, leaf spots, and stem lesions in stressed plants (Guarro et al., 1995). However, *Chaetomium* species, such as *Chaetomium globosum*, also exhibit biocontrol potential, suppressing pathogens like *Fusarium* and *Rhizoctonia* through mechanisms such as mycoparasitism and antifungal compound production (Kato et al., 2004; Harman et al., 2004; Zhang et al., 2021).

The analysis of samples collected at two distinct time points highlighted the influence of phenological stages and pedoclimatic conditions on the composition of fungal communities, with *Fusarium* emerging as the most prevalent genus in the microbiomes of both plant species. The increased abundance of fungal genera, including phytopathogenic species, in the kiwifruit microbiome may be associated with anoxic soil conditions resulting from high irrigation volumes and substantial

rainfall in Cisterna di Latina during May and June 2023 (140 mm and 103 mm, respectively). These conditions can induce stress in root tissues, altering root exudate composition and promoting peroxidase synthesis to mitigate oxidative stress (Blokhina et al., 2003). Turrà et al. (2015) demonstrated that peroxidases attract *Fusarium oxysporum* to host plant roots, while ethanol released from rhizodepositions serves as a chemical attractant for root pathogens, including *Phytophthora* spp. and *Fusarium* spp.

Notably, fig trees (*Ficus carica*) exhibited an absence of KVDS symptoms, alongside a higher prevalence of plant growth-promoting microbial genera. This suggests a potential role in remodeling the rhizosphere microbiome toward a more balanced and disease-suppressive state. Fig trees are well-adapted to Mediterranean climates, demonstrating resilience to soil anoxia, drought conditions, and various biotic stressors. Their ability to establish beneficial microbial associations could contribute to improved soil health, reducing the proliferation of pathogenic fungi linked to KVDS. Furthermore, the lower water demand of fig trees compared to kiwifruit reduces the risk of excessive soil moisture, which is a key factor favoring pathogen proliferation.

Given these characteristics, fig trees emerge as a promising alternative crop for KVDS-affected orchards, potentially mitigating soilborne pathogen pressure while ensuring sustainable agricultural productivity. However, long-term monitoring remains essential to confirm the continued absence of KVDS-related symptoms and to evaluate potential shifts in microbial communities that may influence soil and plant health over time.

4.5 References

Alrteimei, H. A., Ash'aari, Z. H., & Muharram, F. M. (2022). Last decade assessment of the impacts of regional climate change on crop yield variations in the Mediterranean region. *Agriculture*, *12*, 1787. https://doi.org/10.3390/agriculture12111787

Álvarez-Pérez, J., González-García, S., Cobos, R., Olego, M., Ibáñez, A., Diez-Galán, A., Garzón-Jimeno, E., & Coque, J. (2017). Use of endophytic and rhizosphere actinobacteria from *Vitis vinifera* plants to reduce nursery fungal graft infections that lead to young grapevine decline. *Applied and Environmental Microbiology*, *83*. https://doi.org/10.1128/AEM.01564-17

Ayuso, M., Carpena, M., Taofiq, O., Albuquerque, T. G., Simal-Gandara, J., Oliveira, M. B. P., Prieto, M. A., Ferreira, I. C., & Barros, L. (2022). Fig *Ficus carica* L. and its byproducts: A decade of evidence of their health-promoting benefits towards the development of novel food formulations. *Trends in Food Science & Technology*, *127*, 1–13.

Babalola, O., Fadiji, A. E., Enagbonma, B. J., Alori, E. T., Ayilara, M. S., & Ayangbenro, A. S. (2020). The nexus between plant and plant microbiome: Revelation of the networking strategies. *Frontiers in Microbiology*, *11*, 548037. https://doi.org/10.3389/fmicb.2020.548037

Bardi, L. (2020). Early kiwifruit decline: A soil-borne disease syndrome or a climate change effect on plant–soil relations? *Frontiers in Agronomy*, *2*, 3. https://doi.org/10.3389/fagro.2020.00003

Berendsen, R., Pieterse, C., & Bakker, P. (2012). The rhizosphere microbiome and plant health. *Trends in Plant Science*, *17*(8), 478–486. https://doi.org/10.1016/j.tplants.2012.04.001

Berg, G., & Smalla, K. (2009). Plant species and soil type cooperatively shape the structure and function of microbial communities in the rhizosphere. *FEMS Microbiology Ecology*, *68*(1), 1–13. https://doi.org/10.1111/j.1574-6941.2009.00654.x

Bergamaschi, V., Vera, A., Pirone, L., Siles, J. A., López-Mondéjar, R., Luongo, L., Vitale, S., Reverberi, M., Infantino, A., & Bastida, F. (2024). Kiwifruit vine decline syndrome (KVDS) alters soil enzyme activity and microbial community. *Microorganisms*, *12*, 2347. https://doi.org/10.3390/microorganisms12112347

Blokhina, O., Virolainen, E., & Fagerstedt, K. V. (2003). Antioxidants, oxidative damage and oxygen deprivation stress: A review. *Annals of Botany*, *91*(Spec No. 2), 179–194. https://doi.org/10.1093/aob/mcf118

Bokulich, N. A., Subramanian, S., Faith, J. J., Gevers, D., Gordon, J. I., Knight, R., Mills, D. A., & Caporaso, J. G. (2013). Quality-filtering vastly improves diversity estimates from Illumina amplicon sequencing. *Nature Methods*, *10*(1), 57–59. https://doi.org/10.1038/nmeth.2276

Bolyen, E., Rideout, J. R., Dillon, M. R., et al. (2019). Reproducible, interactive, scalable and extensible microbiome data science using QIIME 2. *Nature Biotechnology*, *37*, 852–857. https://doi.org/10.1038/s41587-019-0209-9

Bonkowski, M., Villenave, C., & Griffiths, B. (2009). Rhizosphere fauna: The functional and structural diversity of intimate interactions of soil fauna with plant roots. *Plant and Soil*, *321*, 213–233.

Cabral, A., Groenewald, J. Z., Rego, C., Oliveira, H., & Crous, P. W. (2012). Cylindrocarpon root rot: Multi-gene analysis reveals novel species within the *Ilyonectria radicicola* species complex. *Mycological Progress*, *11*, 655–688. https://doi.org/10.1007/s11557-011-0777-7

Cardacino, A., Turco, S., & Balestra, G. M. (2025). Seasonal dynamics of kiwifruit microbiome: A case study in a KVDS-affected orchard. *Microbiological Research*, *292*. https://doi.org/10.1016/j.micres.2024.128044

Chaparro, J., Badri, D., & Vivanco, J. (2014). Rhizosphere microbiome assemblage is affected by plant development. *ISME Journal*, *8*, 790–803. https://doi.org/10.1038/ismej.2013.196

Compant, S., Samad, A., Faist, H., & Sessitsch, A. (2019). A review on the plant microbiome: Ecology, functions, and emerging trends in microbial application. *Journal of Advanced Research*, *19*, 29–37. https://doi.org/10.1016/j.jare.2019.03.004

D'Ippolito, I., Mang, S., Elshafie, H., Camele, I., Scillitani, G., Mastrodonato, M., Sofo, A., Mininni, A., & Xylogiannis, E. (2022). Morpho-anatomical and microbiological analysis of kiwifruit roots with KVDS symptoms. *Acta Horticulturae*, *1332*, 131–136. https://doi.org/10.17660/ActaHortic.2022.1332.18

De Tender, C., Vandecasteele, M., Ommeslag, S., De Zutter, N., Vandenbussche, E., Haegeman, A., Audenaert, K., Li, L., Vandecasteele, B., Voorthuijzen, F., Maenhout, K., Beirinckx, S., Barneveldt, R., Goormachtig, S., & Debode, J. (2023). *Linnemannia elongata*: A key species in chitin-based plant growth promotion. *Phytobiomes Journal*. https://doi.org/10.1094/pbiomes-05-23-0031-r

Del Castillo Múnera, J., Poret-Peterson, A., & Swett, C. (2022). Changes in fungal and oomycete community composition following irrigation reductions aimed at increasing water use efficiency in a containerized nursery crop. *Phytobiomes Journal*. https://doi.org/10.1094/pbiomes-09-21-0058-r

Dixon, P. (2003). VEGAN, a package of R functions for community ecology. *Journal of Vegetation Science*, *14*, 927–930. https://doi.org/10.1111/j.1654-1103.2003.tb02228.x

Donati, I., Cellini, A., Sangiorgio, D., Caldera, E., Sorrenti, G., & Spinelli, F. (2020). Pathogens associated with kiwifruit vine decline in Italy. *Agriculture*, *10*, 119. https://doi.org/10.3390/agriculture10040119

Fu, X., Huang, Y., Fu, Q., Qiu, Y., Zhao, J., Li, J., Wu, X., Yang, Y., Liu, H., Yang, X., & Chen, H. (2023). Critical transition of soil microbial diversity and composition triggered by plant

rhizosphere effects. *Frontiers in Plant Science, 14*, Article 1252821. https://doi.org/10.3389/fpls.2023.1252821

Gramaje, D., Berlanas, C., Martínez-Diz, M. d. P., Diaz-Losada, E., Antonielli, L., Beier, S., Gorfer, M., Schmoll, M., & Compant, S. (2020). Comparative genomic analysis of *Dactylonectria torresensis* strains from grapevine, soil, and weed highlights potential mechanisms in pathogenicity and endophytic lifestyle. *Journal of Fungi, 6*(4), Article 255. https://doi.org/10.3390/jof6040255

Guarro, J., Soler, L., & Rinaldi, M. G. (1995). Pathogenicity and antifungal susceptibility of *Chaetomium* species. *European Journal of Clinical Microbiology & Infectious Diseases, 14*(7), 613–618. https://doi.org/10.1007/BF01690737

Guaschino, M., Garello, M., Nari, L., Zhimo, Y. V., Droby, S., & Spadaro, D. (2024). Soil, rhizosphere, and root microbiome in kiwifruit vine decline, an emerging multifactorial disease. *Frontiers in Microbiology, 15*, Article 1330865. https://doi.org/10.3389/fmicb.2024.1330865

Harman, G. E., Howell, C. R., Viterbo, A., Chet, I., & Lorito, M. (2004). *Trichoderma* species—opportunistic, avirulent plant symbionts. *Nature Reviews Microbiology, 2*(1), 43–56. https://doi.org/10.1038/nrmicro797

Hinsinger, P., Bengough, A. G., Vetterlein, D., & Young, I. M. (2009). Rhizosphere: Biophysics, biogeochemistry and ecological relevance. *Plant and Soil, 321*, 117–152. https://doi.org/10.1007/s11104-009-9923-7

Hu, J., Wei, Z., Kowalchuk, G., Xu, Y., Shen, Q., & Jousset, A. (2020). Rhizosphere microbiome functional diversity and pathogen invasion resistance build up during plant development. *Environmental Microbiology, 22*(6), 2497–2510. https://doi.org/10.1111/1462-2920.15097

Jackson, M. B., & Drew, M. C. (1984). Effects of flooding on growth and metabolism of herbaceous plants. In T. T. Kozlowski (Ed.), *Flooding and plant growth* (pp. 47–128). Academic Press.

Jia, C., An, Y., Du, Z., Gao, H., Su, J., & Xu, C. (2023). Differences in soil microbial communities between healthy and diseased *Lycium barbarum* cv. Ningqi-5 plants with root rot. *Microorganisms, 11*, Article 694. https://doi.org/10.3390/microorganisms11030694

Khadivi, A., Anjam, R., & Anjam, K. (2018). Morphological and pomological characterization of edible fig (*Ficus carica* L.) to select the superior trees. *Scientia Horticulturae, 238*, 66–74. https://doi.org/10.1016/j.scienta.2018.04.031

Ko, W., Yang, C., Lin, M., Chen, C., & Tsou, Y. (2011). *Humicola phialophoroides* sp. nov. from soil with potential for biological control of plant diseases. *Botanical Studies, 52*, 197–202. https://doi.org/10.1186/1999-3110-52-197

Kurbetli, I., & Ozan, S. (2013). Occurrence of *Phytophthora* root and stem rot of kiwifruit in Turkey. *Journal of Phytopathology, 161*, 887–889. https://doi.org/10.1111/jph.12055

Kurt, Ş., Uysal, A., Soylu, E. M., et al. (2020). Characterization and pathogenicity of *Fusarium solani* associated with dry root rot of citrus in the eastern Mediterranean region of Turkey. *Journal of General Plant Pathology, 86*, 326–332. https://doi.org/10.1007/s10327-020-00922-6

Manici, L. M., Caboni, E., Caputo, F., Frattarelli, A., & Lucioli, S. (2021). Phytotoxins from *Dactylonectria torresensis* involved in replant disease of fruit trees. *Rhizosphere, 17*, Article 100300. https://doi.org/10.1016/j.rhisph.2020.100300

Manici, L. M., Caputo, F., Luccioli, S., Frattarelli, A., & Caboni, E. (2024). Phytotoxicity of *Dactylonectria* spp. exudates on kiwifruit vine and profile of secondary metabolites for understanding their relationship with the host plant. *Rhizosphere, 30*, Article 100906. https://doi.org/10.1016/j.rhisph.2024.100906

Martínez-Arias, C., Witzell, J., Solla, A., Martin, J. A., & Rodríguez-Calcerrada, J. (2022). Beneficial and pathogenic plant-microbe interactions during flooding stress. *Plant, Cell & Environment, 45*(10), 2875–2897. https://doi.org/10.1111/pce.14403

McMurdie, P. J., & Holmes, S. (2013). Phyloseq: An R package for reproducible interactive analysis and graphics of microbiome census data. *PLOS ONE, 8*(4), Article e61217. https://doi.org/10.1371/journal.pone.0061217

Mian, G., Cipriani, G., Firrao, G., et al. (2023). Genetic diversity of *Actinidia* spp. shapes the oomycete pattern associated with Kiwifruit Vine Decline Syndrome (KVDS). *Scientific Reports, 13*, Article 16449. https://doi.org/10.1038/s41598-023-43754-y

Mian, G., Cipriani, G., Saro, S., Martini, M., & Ermacora, P. (2022). Potential of different *Actinidia* genotypes as resistant rootstocks for preventing Kiwifruit Vine Decline Syndrome. *Horticulturae, 8*, Article 627. https://doi.org/10.3390/horticulturae8070627

Ogundeji, A., Li, Y., Liu, X., Meng, L., Sang, P., Mu, Y., Wu, H., Hou, Z., & Li, S. (2021). Eggplant by grafting enhanced with biochar recruits specific microbes for disease suppression of Verticillium wilt. *Applied Soil Ecology, 167*, Article 103912. https://doi.org/10.1016/j.apsoil.2021.103912

Park, I., Seo, Y., & Mannaa, M. (2023). Recruitment of the rhizo-microbiome army: Assembly determinants and engineering of the rhizosphere microbiome as a key to unlocking plant potential. *Frontiers in Microbiology, 14*, Article 1163832. https://doi.org/10.3389/fmicb.2023.1163832

Pérez-Jaramillo, J., Mendes, R., & Raaijmakers, J. (2015). Impact of plant domestication on rhizosphere microbiome assembly and functions. *Plant Molecular Biology, 90*, 635–644. https://doi.org/10.1007/s11103-015-0337-7

Põlme, S., Abarenkov, K., Nilsson, R. H., et al. (2020). FungalTraits: A user-friendly traits database of fungi and fungus-like stramenopiles. *Fungal Diversity, 105*, 1–16. https://doi.org/10.1007/s13225-020-00466-2

Qu, Q., Zhang, Z., Peijnenburg, W., Liu, W., Lu, T., Hu, B., Chen, J., Chen, J., Lin, Z., Qian, H., & Qian, H. (2020). Rhizosphere microbiome assembly and its impact on plant growth. *Journal of Agricultural and Food Chemistry, 68*(7), 2146–2155. https://doi.org/10.1021/acs.jafc.0c00073

Rahmani, A., & Aldebasi, Y. (2017). *Ficus carica* and its constituents role in management of diseases. *Asian Journal of Pharmaceutical and Clinical Research*, 10(6), 49. https://doi.org/10.22159/ajpcr.2017.v10i6.17832

Rascovan, N., Carbonetto, B., Perrig, D., Díaz, M., Canciani, W., Abalo, M., et al. (2016). Integrated analysis of root microbiomes of soybean and wheat from agricultural fields. *Scientific Reports*, 6, 28084. https://doi.org/10.1038/srep28084

Reid, J. B., Tate, K. G., & Brown, N. S. (1992). Effects of flooding and alluvium deposition on kiwifruit (*Actinidia deliciosa*). *New Zealand Journal of Crop and Horticultural Science*, 20(3), 283–288. https://doi.org/10.1080/01140671.1992.10422745

Savian, F., Ginaldi, F., Musetti, R., Sandrin, N., Tarquini, G., Pagliari, L., et al. (2020). Studies on the aetiology of kiwifruit decline: Interaction between soil-borne pathogens and waterlogging. *Plant and Soil*, 456, 113–128. https://doi.org/10.1007/s11104-020-04671-5

Savian, F., Marroni, F., Ermacora, P., Firrao, G., & Martini, M. (2022). A metabarcoding approach to investigate fungal and oomycete communities associated with Kiwifruit Vine Decline Syndrome (KVDS) in Italy. *Phytobiomes Journal*, 6. https://doi.org/10.1094/PBIOMES-03-22-0019-R

Semenov, M., Krasnov, G., Semenov, V., & Van Bruggen, A. (2020). Long-term fertilization rather than plant species shapes rhizosphere and bulk soil prokaryotic communities in agroecosystems. *Applied Soil Ecology*, 154, 103641. https://doi.org/10.1016/j.apsoil.2020.103641

Simonin, M., Da Silva, C., Terzi, V., Ngonkeu, E., Diouf, D., Kane, A., Béna, G., & Moulin, L. (2020). Influence of plant genotype and soil on the wheat rhizosphere microbiome: Evidence for a core microbiome across eight African and European soils. *FEMS Microbiology Ecology*, 96(10), fiaa067. https://doi.org/10.1093/femsec/fiaa067

Smith, G. S., Buwalda, J. G., Green, T. G. A., & Clark, C. J. (1989). Effect of oxygen supply and temperature at the root on the physiology of kiwifruit vines. *New Phytologist*, 113(4), 431–437. https://doi.org/10.1111/j.1469-8137.1989.tb00318.x

Smucker, A., & Erickson, A. (1987). Anaerobic stimulation of root exudates and disease of peas. *Plant and Soil*, 99, 423–433. https://doi.org/10.1007/BF02370887

Song, W., Song, S., Lan, J., Zheng, D., Xu, X., Huang, L., Yan, C., Liu, Y., & Tang, W. (2022). First report of root rot caused by *Fusarium solani* and *F. breve* on kiwifruit in China. *Plant Disease*. Advance online publication. https://doi.org/10.1094/PDIS-09-22-2103-PDN

Sorrenti, G., Tacconi, G., Tosi, L., Vittone, G., Nari, L., Savian, F., et al. (2019). Avanza la "moria del kiwi": Evoluzione e primi riscontri della ricerca. *Rivista Frutticoltura*, 81, 34–42.

Spigaglia, P., Barbanti, F., Marocchi, F., Mastroleo, M., Baretta, M., Ferrante, P., Caboni, E., Lucioli, S., & Scortichini, M. (2020). *Clostridium bifermentans* and *C. subterminale* are associated with kiwifruit vine decline, known as moria, in Italy. *Plant Pathology*, 69, 765–774. https://doi.org/10.1111/ppa.13157

Trivedi, P., Batista, B. D., Bazany, K. E., & Singh, B. K. (2022). Plant–microbiome interactions under a changing world: Responses, consequences, and perspectives. *New Phytologist*, 234(6), 1951–1959. https://doi.org/10.1111/nph.18016

Turco, S., Brugneti, F., Giubilei, I., Silvestri, C., Petrovic, M., Drais, M. I., Cristofori, V., Speranza, S., Mazzaglia, A., Contarini, M., Rossini, L. (2024). A bud's life: Metabarcoding analysis to characterise hazelnut big buds microbiome biodiversity. *Microbiological Research*, 127851. https://doi.org/10.1016/j.micres.2024.127851

Turrà, D., El Ghalid, M., Rossi, F., & Di Pietro, A. (2015). Fungal pathogen uses sex pheromone receptor for chemotropic sensing of host plant signals. *Nature*, 527(7579), 521–524. https://doi.org/10.1038/nature15516

Vandepol, N., Liber, J., Yocca, A., Matlock, J., Edger, P., & Bonito, G. (2021). *Linnemannia elongata* (Mortierellaceae) stimulates *Arabidopsis thaliana* aerial growth and responses to auxin, ethylene, and reactive oxygen species. *PLoS ONE*, 17(2), e0261908. https://doi.org/10.1371/journal.pone.0261908

Villard, C., Larbat, R., Munakata, R., & Hehn, A. (2019). Defence mechanisms of *Ficus*: Pyramiding strategies to cope with pests and pathogens. *Planta*, 249(3), 617–633. https://doi.org/10.1007/s00425-019-03152-w

Voesenek, L. A. C. J., & Sasidharan, R. (2013). Ethylene—and oxygen signalling—drive plant survival during flooding. *Plant Biology*, 15(3), 426–435. https://doi.org/10.1111/plb.12014

Wang, B., Xia, Q., Li, Y., Zhao, J., Yang, S., Wei, F., Huang, X., Zhang, J., & Cai, Z. (2021). Root rot-infected Sanqi ginseng rhizosphere harbors dynamically pathogenic microbiotas driven by the shift of phenolic acids. *Plant and Soil*, 465, 385–402. https://doi.org/10.1007/s11104-021-05034-4

Wang, K. X., Xie, Y. L., Yuan, G. Q., Li, Q. Q., & Lin, W. (2015). First report of root and collar rot caused by *Phytopythium helicoides* on kiwifruit (*Actinidia chinensis*). *Plant Disease*, 99, 725. https://doi.org/10.1094/PDIS-12-14-1409-PDN

Xiong, W., Song, Y., Yang, K., Gu, Y., Wei, Z., Kowalchuk, G., Xu, Y., Jousset, A., Shen, Q., & Geisen, S. (2020). Rhizosphere protists are key determinants of plant health. *Microbiome*, 8, 90. https://doi.org/10.1186/s40168-020-00799-9

Xu, S., Tian, L., Chang, C., Li, X., & Tian, C. (2019). Plants exhibit significant effects on the rhizospheric microbiome across contrasting soils in tropical and subtropical China. *FEMS Microbiology Ecology*, 95(9), fiz100. https://doi.org/10.1093/femsec/fiz100

Yan, H., & Nelson, B. (2022). Effects of soil type, temperature, and moisture on development of *Fusarium* root rot of soybean by *Fusarium solani* (FSSC 11) and *Fusarium tricinctum*. *Plant Disease*, 106(11), 2974–2983. https://doi.org/10.1094/PDIS-12-21-2738-RE

Zhang, Y., Zhu, H., Ye, Y., & Tang, C. (2021). Antifungal activity of chaetoviridin A from *Chaetomium globosum* CEF-082 metabolites against *Verticillium dahliae* in cotton. *Molecular Plant-Microbe Interactions*, 34(7), 758–769. https://doi.org/10.1094/MPMI-02-21-0032-R

4.6 Supplementary material

Figure S4.1- Sampling site. The green area has been designated for kiwifruit cultivation, while the blue area has been designated for fig cultivation

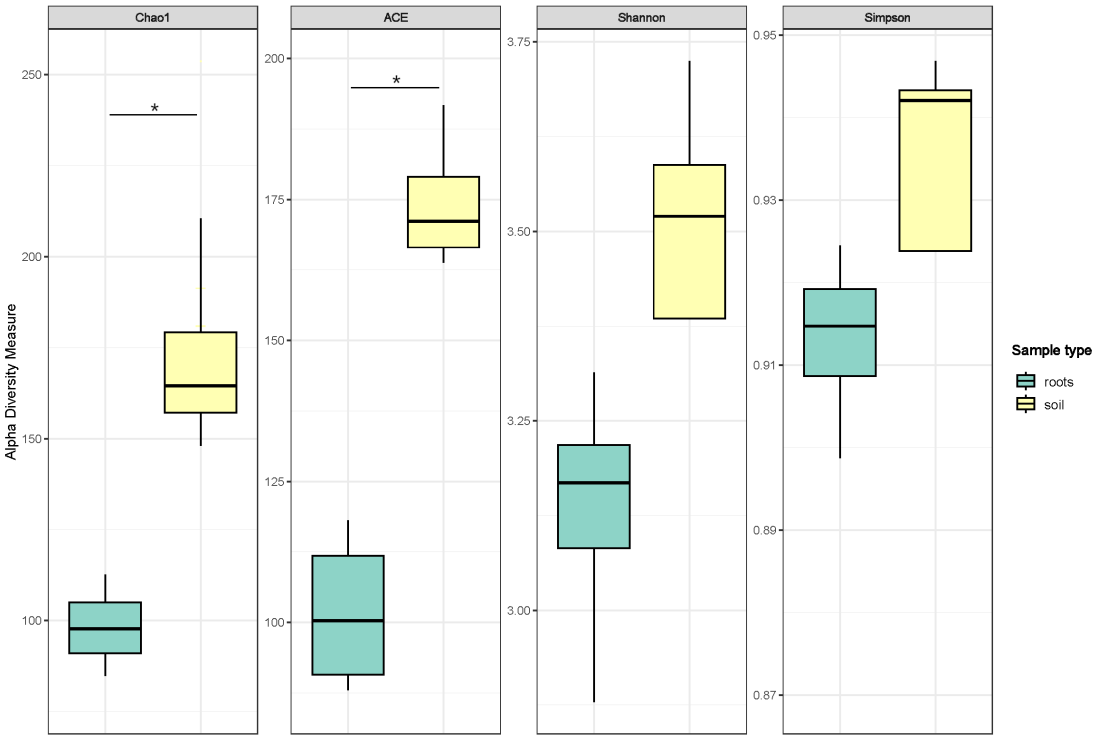

Figure S4.2 - Alpha-diversity of fungal communities in roots (green) and soil (yellow). Alpha diversity metrics summarize the structure of microbial community with respect to its richness (Chao1 and ACE indexes), and within-sample diversity expressed by Shannon and Simpson indexes. Significant differences (*p≤0.05*) were observed in the fungal community across Chao1 and ACE indexes.

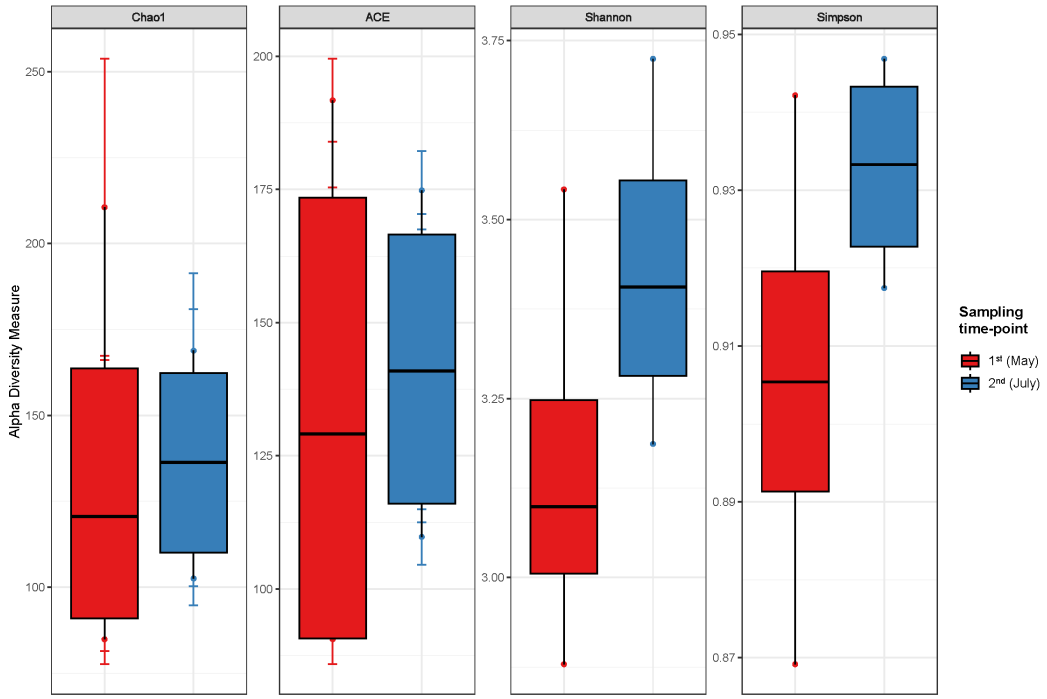

Figure S4.3 - Alpha-diversity of fungal communities during the two time-points: first time-point in red (corresponded to kiwifruit flowering stage) and second time-point in blue (corresponded to kiwifruit fruit set stage). No statistically significant differences were observed for any of the indexes.

Table S4.1 - Physical and chemical soil analysis

Parameter	***Value (%)***
Sand	52
Silt	24
Clay	24
Texture	Sandy

Parameter	***Value***
pH	6.8 (neutral)
Electrical conductivity	0.13 dS/m
Limestone	absent
Organic matter	1.94 % (regular)

Table S4.2 - Analysis of soil elements

Parameter	***Value***
Total nitrogen	0.13 % (high)
Phosphorus abs.	304 ppm (very high)
Ca	4000 ppm (high)
Mg	500 ppm (high)
Cu	18 ppm (very high)
Zn	19 ppm (very high)

Table S4.3 - Average of quality metrics and percentage of reads

Species	Sample type	Time point	Input	Filtered	% of input passed filter	Denoised	Non-chimeric	% of input non-chimeric	ASVs
Ficus carica	Roots	Flowering	656.630	582.672	88,74	580.765	503.249	76.64	439
Ficus carica	Roots	Fruit set	742.534	703.400	94,73	701.379	589.925	79.45	1.410
Ficus carica	Soil	Flowering	719.237	618.305	85,97	614.259	513.421	71.38	433
Ficus carica	Soil	Fruit set	518.214	484.580	93,51	481.690	414.781	80.04	906
Actinidia chinensis	Roots	Flowering	602.286	527.964	87,66	526.136	454.646	75.49	413
Actinidia chinensis	Roots	Fruit set	543.064	481.079	88,59	479.430	434.108	79.94	982
Actinidia chinensis	Soil	Flowering	548.999	448.069	81,62	444.349	363.051	66.13	464
Actinidia chinensis	Soil	Fruit set	475.061	382.281	80,47	379.592	318.202	66.98	1.033

Table S4.4 - PERMANOVA results of fungal communities' composition indicating the partitioning of variation and tests for species (*Actinidia chinensis* and *Ficus carica*), sample type (roots and soil) and sampling time-point (May and July)

	Df	***Sum of Sqs***	***R^2***	***F***	***P(>F)***
GROUP	1	0.67213	0.42342	5.5886	0.002 **
SAMPLE TYPE	1	0.17330	0.10918	1.4410	0.214
PHENOLOGICAL STAGE	1	0.26086	0.16434	2.1690	0.047 *
RESIDUAL	4	0.48107	0.30306		

*Signif. codes: 0 '***' 0.001 '**' 0.01 '*' 0.05 '.' 0.1 ' ' 1*

Conclusions

This study provides a comprehensive investigation into the microbial, physiological, and ecological factors influencing Kiwifruit Vine Decline Syndrome (KVDS), a devastating disease that poses a significant threat to kiwifruit Italian orchards. By integrating high-throughput sequencing, immunity gene expression profiling, and hormonal quantification across different phenological stages, it has been demonstrated that KVDS is characterised by significant shifts in microbial communities, altered plant defence responses, and complex plant-environment interactions that contribute to disease progression. These findings emphasise the multifactorial nature of KVDS and provide novel insights that can support the development of more targeted disease management strategies.

Microbiome analysis revealed that KVDS-affected plants undergo significant compositional changes in their root and rhizosphere microbial communities when compared to asymptomatic plants. The most prevalent bacterial genera identified in the root microbiota were *Ralstonia, Pseudomonas,* and *Bacillus*, each displaying distinctive patterns of abundance and functional roles. Of particular interest was the finding that *Ralstonia* exhibited a marked increase in plants affected by KVDS, particularly during the process of vegetative renewal, which suggests a potential role in the progression of the disease. While *Pseudomonas* species were found in both symptomatic and asymptomatic roots, their dual role as both pathogens (*P. syringae, P. viridiflava*) and plant growth promoters (*P. fluorescens, P. stutzeri*) highlights the complexity of plant-microbe interactions. *Bacillus*, known for its biocontrol and plant growth-promoting properties, exhibited a higher prevalence in asymptomatic roots during the flowering and fruit set stages, indicating a potential protective role against KVDS-associated pathogens.

Significant alterations in the composition of fungal and oomycete communities were also observed, with *Fusarium* emerging as the predominant genus in KVDS-affected roots. Furthermore, the presence of *Ilyonectria, Thelonectria*, and *Plectosphaerella* in both soil and root samples suggest that fungal dysbiosis plays a critical role in disease establishment. Furthermore, the predominance of *Phytophthora* and *Globisporangium* in KVDS-affected samples aligns with previous studies identifying

oomycetes as key contributors to kiwifruit decline. The detection of *Globisporangium intermedium* in *Actinidia* genotypes resistant to KVDS suggests the possibility that specific microbial interactions could influence disease susceptibility and plant resilience.

At the physiological and molecular levels, the analysis of immune-related gene expression and hormonal regulation provided further evidence of KVDS-induced stress responses. Genes involved in pathogen recognition (*AcCERK1*), chitin degradation (*AcCHI*), and reactive oxygen species (ROS) detoxification (*AcCAT, AcAPX, AcSOD*) exhibited dynamic expression patterns, indicating that KVDS-affected plants activate multiple defence pathways in response to infection. The hormonal quantification revealed significant differences in key phytohormones, with asymptomatic plants maintaining higher levels of salicylic acid (SA), jasmonic acid (JA), and gibberellic acid (GA3) during early infection stages. Conversely, plants affected by KVDS exhibited a delayed defense response, with increased SA, JA, and 6-BA levels during fruit set, possibly as a compensatory mechanism to counteract pathogen invasion. The absence of detectable abscisic acid (ABA) despite the upregulation of ABA-related genes suggests a post-transcriptional regulatory mechanism that may influence disease progression. The results of this study highlight the intricate nature of plant hormonal signalling in KVDS and suggest that hormonal imbalances may contribute to disease susceptibility.

A particularly novel aspect of this study was the comparative analysis of the rhizosphere microbiome between kiwifruit and fig trees cultivated in former kiwifruit orchards affected by KVDS. While *Fusarium* remained dominant in both species, fig trees exhibited a higher prevalence of beneficial microbial genera, including *Humicola, Plectosphaerella*, and *Chaetomium*. The presence of *Humicola*, a microbe known for its biocontrol potential, suggests that fig trees may actively recruit beneficial microbes that contribute to disease suppression. Furthermore, the lower water demand of fig trees, in comparison to kiwifruit, reduces the risk of excessive soil moisture, a key factor favouring pathogen proliferation. These findings underscore the potential of fig trees as a resilient alternative crop in KVDS-affected orchards, offering a sustainable strategy for microbiome restoration and disease mitigation.

The present study suggests that KVDS is linked to microbial dysbiosis, altered plant defence responses, and complex interactions between plant physiology and environmental factors. The observed shifts in microbiome composition throughout the vegetative season indicate that plant-microbe interactions are highly dynamic and influenced by host phenology and external stressors, including soil conditions and climate factors. While microbial imbalances appear to contribute to KVDS progression, the relative influence of deterministic versus stochastic processes in microbiome assembly remains inconclusive. Recent studies have produced conflicting results, with some suggesting that stochastic processes predominantly shape the rhizosphere microbial communities, while others highlight the role of deterministic factors in structuring bacterial and fungal populations. Future research should explore whether KVDS-induced dysbiosis is a causal factor or a consequence of disease progression.

Furthermore, the role of soil suppressiveness in modulating pathogen proliferation warrants further investigation. It is acknowledged that certain soils naturally inhibit pathogen establishment through microbial competition, antagonism, or induced resistance. A deeper understanding of the mechanisms underlying soil suppressiveness could lead to the development of soil-based disease management strategies, reducing the need for chemical treatments and enhancing soil health. Finally, targeted microbiome interventions, such as probiotic bacterial inoculants, organic amendments, and precision agricultural techniques, could help restore beneficial microbial communities and mitigate the effects of KVDS. From an applied perspective, this study underscores the importance of a multi-omics approach in unravelling complex plant diseases and guiding the development of sustainable disease management strategies. The integration of microbiome profiling, molecular diagnostics, and ecological assessments provides a powerful framework for identifying key biomarkers and potential targets for intervention. Future studies should focus on long-term field experiments to validate microbiome-based disease mitigation strategies and explore the potential for breeding kiwifruit varieties with enhanced microbial recruitment capabilities. By combining ecological, molecular, and microbiological approaches, this research contributes to a deeper understanding of plant disease dynamics and could contribute to the development of sustainable disease management strategies.

Acknowledgements

This research was co-funded by Lazio Region, DIREZIONE REGIONALE AGRICOLTURA, PROMOZIONE DELLA FILIERA E CULTURA DEL CIBO, CACCIA E PESCA, FORESTE (Det. n. G15953, 22/12/20).